Study on thermotolerant mechanisms of thermotolerant acetic acid bacteria by experimental evolution

(耐熱化育種酢酸菌の耐熱化機構に関する研究)

Nami Matsumoto

Graduate School of Sciences and Technology for Innovation
Yamaguchi University

June 2021

CONTENTS

LIST OF FIGURES

CHAPTER 2

CHAPTER 3

LIST OF TABLES

LIST OF ABBREVIATION

AAB	Acetic acid bacteria
Ap	Ampicillin
Cm	Chloramphenicol
DHA	Dihydroxyacetone
G6P	Glucose-6-phosphate
GLDH	Glycerol dehydrogenase
Km	Kanamycin
5KGA	5-Keto-D-gluconate
NADH	Nicotinamide adenine dinucleotide
NADPH	Nicotinamide adenine dinucleotide phosphate
6PG	6-Phosphogluconate
KPB	Potassium phosphate buffer
ROS	Reactive oxygen species
rpm	Round per minute
HPLC	High-performance liquid chromatography
ORFs	Open reading frames
PPP	Pentose phosphate pathway
SDH	Sorbitol dehydrogenase
SR	Sorbose reductase
vvm	Volume per volume per minute

SUMARRY

Study on thermotolerant mechanisms of thermotolerant acetic acid bacteria by experimental evolution

Acetic acid bacteria (AAB) are obligate aerobic bacteria and inhabit flowers and fruits in the nature. AAB have a capacity of oxidizing sugar, alcohol, or sugar alcohol, and such the oxidative fermentations are carried out by membrane-bound dehydrogenases linked to the respiratory chain. Of these fermentations, acetic acid fermentation (vinegar production) and sorbose fermentation (Vitamin C production) are industrially performed with AAB. These fermentations are generally carried out at around 25-30°C, but the submerged large-scale fermentation is limited by the heat generated from the fermentation reaction and/or mechanical agitation. Thermotolerant microorganisms are beneficial to the fermentation industry because of a capability to reduce cooling expense and other operational risks. This study objective is to obtain strains that have an ability of practical fermentation at high temperature condition and to elucidate the thermotolerant mechanism of the thermally adapted strains.

In CHAPTER 1, the analysis of thermotolerant mechanism in thermally adapted strain was carried out with a sorbose fermentation strain *Gluconobacter frateurii* CHM43. It was found in the adapted strain that only a single G insertion, which causes a frameshift mutation, occurred in a gene encoding a putative drug transporter. A mutant derivative strain with the single G insertion in the transporter gene (Wild-G) was constructed from the wild-type strain, and it was confirmed for the artificial mutant to increase its thermotolerance. It was also found that the thermotolerant strains substantially accumulated intracellular trehalose and caused a defect in sorbose assimilation, suggesting that the transporter is partly involved in trehalose efflux and sorbose uptake. As the accumulation of trehalose was expected to induce thermotolerance, a strain Δ*otsAB* was constructed by elimination of trehalose synthesis genes in the wild type. However, unexpectedly the Δ*otsAB* strain exhibited much better growth than the adapted strain at high temperatures, despite of no trehalose production. Since the Δ*otsAB* mutant produced more acetate as the final metabolite than the wild-type strain, it was hypothesized that trehalose does not contribute to the thermotolerance directly, rather induce a metabolic change to cause an increased carbon flux to the pentose phosphate pathway. This notion was supported by the increased NADPH/$NADP^+$ ratio in strain Wild-G and much higher in strain Δ*otsAB*. Reactive oxygen species (ROS) level was also shown to be decreased in the thermotolerant strains, concomitant with the increased NADPH/$NADP^+$ ratio. Thus,

it was proposed that the defect of the transporter causes metabolic flux change to generate more NADPH, which contributes to enhance the thermotolerance of *G. frateurii* via a reduction of ROS.

Next, in CHAPTER 2, thermal adaptation of *Acetobacter pasteurianus* IFO 3283-32 was performed by experimental evolution approach from 37ºC to 40ºC under acetic acid fermentation conditions. The adapted strains exhibited an increased growth and acetic acid fermentation ability at high temperatures, while the trade-off response was observed exhibiting the opposite phenotype at lower temperatures. Genome analysis followed by PCR sequencing showed that the adapted strain had 11 mutations, a single 64-kb large deletion, and a single plasmid loss. Comparative phenotypic analysis suggested that at least the large deletion (containing many ribosomal RNAs and tRNAs genes) and a mutation of DNA polymerase (one of the 11 mutations) critically contributed to this thermotolerance. The relationship between the phenotypic changes and the gene mutations are discussed, comparing with another thermally adapted *A. pasteurianus* strains obtained previously.

Several thermally adapted strains had been previously obtained from *A. pasteurianus* in an experimental culture conditions with nutrient-rich medium. However, these adapted strains could not grow well at high temperature in the nutrient-poor practical culture medium, ‘rice moromi’. In CHAPTER 3, *A. pasteurianus* K-1034 originally capable of performing acetic acid fermentation in rice moromi, was thermally adapted by experimental evolution using a ‘pseudo’ rice moromi culture. The adapted strains thus obtained were confirmed to grow well in such the nutrient-poor media in flask culture or jar-fermentor culture up to 40ºC or 39ºC, respectively. The high-temperature fermentation ability was also shown to be comparable with a low-nutrient adapted strain of the thermally adapted strain previously obtained. Using the practical high-aeration fermentation system, ‘Acetofermenter’, acetic acid production was compared in the moromi culture with the thermally adapted strains in this study together with the low-nutrient adapted thermotolerant strain. These adapted strains were shown to efficiently perform practical vinegar production under high-temperature conditions.

GENERAL INTRODUCTION

Experimental evolution is an efficient approach to obtain mutants that are highly tolerant to stressors and thus could grow at higher rates with high productivity even under stressful condition (Sandberg et al., 2019). Such an experimental adaptation is an elegant approach to search the adaptation mechanism because whole-genome analysis could be performed easily today (Azuma et al., 2009; Sjödin et al., 2010). Experimental adaptation, especially to lethal high temperatures, has been tried in several microorganisms including not only *Escherichia coli* (Rudolph et al., 2010; Rodriguez-Verdugo et al., 2014) as a model strain but also practical fermentative microbes such as *Saccharomyces cerevisiae* (Wallace-Salinas and Gorwa-Grauslund 2013; Caspeta et al., 2014; Satomura et al., 2016) and *Acetobacter pasteurianus* (Azuma et al., 2009; Matsutani et al., 2013) for ethanol and acetic acid fermentation, respectively, as well as *Gluconobacter frateurii* CHM43 (Hattori et al., 2012).

Large-scale fermentation with usual mesophilic strains is limited by the heat generated from the fermentation reaction and/or mechanical agitation. Additionally, the natural atmospheric temperature is currently on the rise as a result of global warming. Therefore, stable fermentation needs to be carried out by a strict temperature control using cooling system, which expenses a lot of energy such as electricity or water supply. While, thermotolerant microorganisms have a potential to release the industry from these cooling expense, because they could be used for stable fermentation at high temperatures with less or even without use of the expensive cooling system (Matsushita et al., 2016; Hattori et al, 2012). Our research group have succeeded in obtaining many strains adapted to higher temperatures from several fermentative bacteria, including both mesophilic and thermotolerant species; all these thermally adapted strains have been shown to acquire 2–3°C higher growth temperatures (Matsushita et al., 2016).

Acetic acid bacteria (AAB) are obligate aerobic bacteria that are well known for their ability to oxidize ethanol, sugars, or sugar alcohols, subsequently releasing a large amount of partially oxidized products into the culture medium. These oxidation reactions, called as oxidative fermentation, are carried out by membrane-bound dehydrogenases linked to the respiratory chain (Matsushita et al., 1994). In particular, the *Gluconobacter* genus catalyzes many oxidative fermentation reactions of sugars or sugar alcohols, resulting in valuable products such as L-sorbose, dihydroxyacetone (DHA), D-gluconate, 2-keto-D-gluconate, or 5-keto-D-gluconate (5KGA). Of these fermentation products, L-sorbose, DHA, or 5KGA is produced by quinoprotein glycerol dehydrogenase (GLDH) (Matsushita et al., 2003). In particular, L-sorbose produced from D-sorbitol serves as an

intermediate in the commercial production of vitamin C (ascorbic acid). *Gluconobacter frateurii* CHM43 is a thermotolerant *Gluconobacter* strain able to grow even at 37°C, isolated in Thailand (Moonmangmee et al., 2000), and has a strong capacity for L-sorbose fermentation even at high growth temperatures (Hattori et al., 2012). While, the *Acetobacter* genus is characterized by their ability to ferment acetic acid, whereby a high concentration of acetic acid is produced from ethanol. The oxidative reaction is carried out by two membrane-bound enzymes, alcohol and aldehyde dehydrogenases, linking to the terminal oxidases via ubiquinone (Yakushi and Matsushita, 2010). AAB undergo diauxic growth during acetic acid fermentation (Kanchanarach et al., 2010); the first growth stage is comprised by an ethanol oxidation step (acetic acid-producing phase) followed by a period similar to a stationary phase (acetic acid-resistant phase), and the second growth stage occurs by assimilating the accumulated acetic acid (acetic acid overoxidation phase) that is unfavorable for industrial vinegar fermentation. Currently, industrial acetic acid fermentation is carried out in fermentation tanks with a culture temperature that is maintained at around 25–30ºC via a cooling system. This protects the cell growth and acetic acid production from the heat generated by fermentation. Therefore, thermotolerant AAB could be useful for a stable and cost-effective fermentation by sparing any cooling expenses.

This study objective is to obtain strains that have an ability of practical fermentation at high temperature condition from AAB, and to elucidate the thermotolerant mechanism of the thermally adapted strains. In CHAPTER 1, thermotolerant mechanism was examined in a thermally adapted strain obtained from sorbose fermentation strain *G. frateurii* CHM43. The adapted strain has only one mutation (in a gene encoding a putative drug transporter), and thus the same transporter mutation (Wild-G) was artificially created. The Wild-G strain showed that this transporter mutation increases thermotolerance, and further causes trehalose accumulation inside the cells. The following experiments suggested that the metabolic flux change induced by this mutation increases NADPH/$NADP^+$ ratio and then decreases ROS levels, thereby conferring thermotolerance on the bacterium.

In the following CHAPTER 2, the thermal adaptation of *A. pasteurianus* IFO 3283-32, a derivative of NBRC 3283, was conducted under acetic acid fermentation conditions. The adapted strain thus obtained had a total 12 mutations including a large gene deletion of 64-kbp, and exhibited a higher growth and fermentation ability at 40ºC while did a decreased ability at lower temperatures. This phenotypic change of the adapted strain is discussed by comparing several different thermally-adapted strains obtained in previous studies.

Furthermore, in order to achieve practical high-temperature acetic acid fermentation (vinegar production) in ‘rice moromi’, in CHAPTER 3, the thermal adaptation of *Acetobacter pasteurianus* K-1034, a practical strain originally adapted to moromi, was performed. By experimental evolution under nutrient-poor conditions, two thermally adapted strains were obtained. These adapted strains exhibited high-temperature fermentation ability, in flask culture up to 40ºC, in jar-fermentor culture up to 39ºC, and in the practical culture with a high-aeration fermentation system, ‘Acetofermenter’ up to 37ºC.

CHAPTER 1

A single-nucleotide insertion in a drug transporter gene induces a thermotolerant phenotype of *Gluconobacter frateurii* by increasing the NADPH/NADP$^+$ ratio via metabolic change

ABSTRACT

Thermotolerant microorganisms are beneficial to the fermentation industry because of a reduction in cooling efforts and other operational risks. Previously, a thermally adapted *Gluconobacter frateurii* strain have obtained by experimental evolution. In the present study, it was found that adapted strain has only a single G insertion in the genome, which causes a frameshift in a gene encoding a putative drug transporter. A mutant derivative strain with the single G insertion in the transporter gene (Wild-G) was constructed from the wild-type strain and showed increased thermotolerance. I found that the thermotolerant strains substantially accumulated intracellular trehalose and manifested a defect in sorbose assimilation, suggesting that the transporter is partly involved in the trehalose efflux and in sorbose uptake, and that the defect in the transporter can improve thermotolerance. Strain Δ*otsAB* constructed by elimination of the trehalose synthesis gene in the wild type showed no trehalose production but unexpectedly much better growth than the adapted strain at high temperatures. The Δ*otsAB* mutant produced more acetate as the final metabolite than the wild-type strain did. I hypothesized that trehalose does not contribute to the thermotolerance directly; rather a metabolic change including increased carbon flux to the pentose phosphate pathway may be the key factor. The NADPH/NADP$^+$ ratio was higher in strain Wild-G and much higher in strain Δ*otsAB* than in the wild-type strain. Reactive oxygen species levels in the thermotolerant strains decreased. It is proposed that the defect of the transporter causes metabolic flux to generate more NADPH, which may enhance thermotolerance in *G. frateurii*.

1.1 INTRODUCTION

Large-scale fermentation with usual mesophilic strains is limited by the heat generated by the fermentation reaction and/or mechanical agitation. Therefore, we have

tried to create several bacterial strains useful for fermentation by repeated cultivation at their limited growth temperatures until they acquired a reasonably high growth rate at the high temperatures. A thermally adapted strain could grow at higher temperatures than the wild-type strain could, and thus, was useful for fermentation at high temperatures and/or without temperature control (Matsushita et al., 2016). Such an experimental adaptation is an elegant approach to obtaining useful mutated strains whose whole-genome analysis could be performed easily today (Azuma et al., 2009; Sjödin et al., 2010). Experimental adaptation, especially to lethal high temperatures, has been tried in several microorganisms including not only *Escherichia coli* (Rudolph et al., 2010; Rodriguez-Verdugo et al., 2014) as a model strain but also practical fermentative microbes such as *Saccharomyces cerevisiae* (Wallace-Salinas and Gorwa-Grauslund 2013; Caspeta et al., 2014; Satomura et al., 2016) and *Acetobacter pasteurianus* (Azuma et al., 2009; Matsutani et al., 2013) for ethanol and acetic acid fermentation, respectively, as well as *Gluconobacter frateurii* CHM43 (Hattori et al., 2012).

Acetic acid bacteria are obligate aerobic bacteria that are well known for their ability to oxidize ethanol, sugars, or sugar alcohols, subsequently releasing a large amount of partially oxidized products into the culture medium. These oxidation reactions are carried out by membrane-bound dehydrogenases linked to the respiratory chain (Matsushita et al., 1994). In particular, the *Gluconobacter* genus catalyzes many membrane-bound-dehydrogenase–dependent oxidative fermentation reactions resulting in valuable products, such as L-sorbose, dihydroxyacetone, D-gluconate, and 2- or 5-keto-D-gluconate. The synthesis of many of these fermentation products is catalyzed by quinoprotein glycerol dehydrogenase (GLDH) (Matsushita et al., 2003). For example, L-sorbose is produced from D-sorbitol in a reaction catalyzed by GLDH and serves as an intermediate in the commercial production of vitamin C (ascorbic acid). *G. frateurii* CHM43 is a thermotolerant *Gluconobacter* strain able to grow even at 37°C, isolated in Thailand (Moonmangmee et al., 2000), and has strong capacity for L-sorbose fermentation even at high growth temperatures (Hattori et al., 2012). We have previously used thermotolerant *G. frateurii* CHM43 for the thermal adaptation and successfully derived a thermally adapted strain, CHM43AD. This strain was uniquely obtained within a relatively short adaptation period, even though thermal adaptation used to take a long time to yield desirable mutants (Matsutani et al., 2013). The thermally adapted strain can grow at higher temperatures relative to the wild-type strain and thus is useful for sorbose fermentation at high temperatures and/or without temperature control (Hattori et al., 2012).

Aerobic organisms generate reactive oxygen species (ROS) causing cell damage,

which has been shown to increase when microbes are grown at a lethal high temperature (Davidson et al., 1996; Chang et al., 2017) or after heat treatment in plants (Lee et al., 2015; Zang et al., 2017). ROS are generated in the respiratory chain, mainly by flavoproteins, especially NADH dehydrogenase, as demonstrated in many microbes, such as yeast (Davidson and Schiestl, 2001), *E. coli* (Messner and Imlay, 1999; Messner and Imlay, 2002), and *Corynebacterium glutamicum* (Matsushita et al., 1998; Nantapong et al., 2005). Under certain conditions, these flavoproteins can react directly with oxygen to generate superoxide or hydrogen peroxide, which could be detoxified by superoxide dismutase, catalase, and/or several different types of peroxidase. Some peroxidases, e.g., thioredoxin peroxidase or glutathione peroxidase, detoxify hydrogen peroxide by means of NADPH as a reducing agent (Thelander, 1967; Carlberg and Mannervik, 1975). It has been reported that increased intracellular NADPH content alleviates oxidative stress in yeast (Bankapalli et al., 2015), and that activation of some ROS-scavenging enzymes including glutathione reductase or thioredoxin reductase is associated with enhanced thermotolerance in plants and microbes (Lee et al., 2015; Sánchez-Riego et al., 2016). Furthermore, *E. coli* strains with mutations in thermotolerance genes are known to become sensitive to oxidative stress, suggesting that the thermotolerance mechanism overlaps with oxidative-stress resistance (Murata et al., 2011). Thus, although the reason why high temperature induces high ROS levels is not well understood, thermotolerant or thermally adapted strains may reduce such excess ROS caused by high temperatures by diminishing the ROS generation itself or by activating ROS-scavenging enzymes.

In the present study, we conducted whole-genome mapping analysis of strains CHM43 and CHM43AD to identify and characterize the mutated sites in CHM43AD. We found that the adapted strain has only one mutation (in a gene encoding a putative drug transporter) and showed that this mutation increases thermotolerance. In addition, the mutation in the transporter causes trehalose accumulation inside the cells, and this alteration changes metabolic flux to generate a larger NADPH amount and decreases ROS levels, thereby conferring thermotolerance on the bacterium.

1.2 MATERIALS AND METHODS

1.2.1 Culture media and growth conditions

Gluconobacter frateurii CHM43 (NBRC 101659; BCC 36198), its adapted strain, CHM43AD (Hattori et al., 2012), and several mutated strains were used in this study (Table 1.1). Cells were grown in 10% (w/v) sorbitol medium consisting of 100 g/L D-sorbitol, 3 g/L yeast extract (Oriental Yeast, Tokyo, Japan), and 3 g/L polypeptone

(Nihon Pharmaceuticals Co. Ltd., Osaka, Japan). The precultures were cultivated in 5 mL of 5% (w/v) sorbitol medium at 30°C, and transferred to 50 mL of 10% (w/v) sorbitol medium in 500 mL baffled flasks. The cultures were grown with rotary shaking at 200 rpm at different temperatures in an air incubator as described previously (Hattori et al., 2012). The carbon source (10% sorbitol) was exchanged with 10% (w/v) mannitol or 5% (w/v) glycerol in some experiments. And also, for the assimilation of sorbose, cells were cultivated in 50 mL of 0.1-10% (w/v) sorbose medium in baffled flasks at 30°C.

Table 1.1. Summary of the draft genome assembly of Illumina sequence reads for *G. frateurii* CHM43.

G. frateurii CHM43	Updated genome data in this study	Previous genome data (Hattori et al., 2012)
Total length of contigs (bp)	3,157,471	3,148,763
Number of contigs	44	145
GC content (%)	55.73	55.73
Number of open reading frames	2,928	-
N50 length (bp)	400,768	164,017
Max contig length (bp)	670,742	383,535
Number of tRNAs	49	-
Number of tmRNAs	1	-
Number of rRNAs	3	-

The updated version sequence (BADZ02000001-BADZ02000044) was compared with the original version (BADZ01000001-BADZ01000145).

1.2.2 Isolation of thermotolerant mutants by ultraviolet (UV) irradiation

CHM43 cells were cultivated in 5 mL of 5% (w/v) sorbitol medium at 30°C with shaking at 200 rpm for 2 d. Then, 50 µL of the preculture was transferred to 5 mL of 5% (w/v) sorbitol medium, and cultivated for 6–7 h at 30°C with shaking at 200 rpm. Cells were harvested by centrifugation at 8,000 x g for 3 min, and washed with 5 mL of sterilized tap water. The cell pellets were resuspended in 30 mL of 50 mM sodium phosphate buffer (pH 7.0). The cell suspension (3 mL) was transferred to a glass plate (diameter 4.3 cm) and irradiated with ultraviolet light-C (UV-C, 235.7 nm) for 90 s. The irradiation distance between the UV lamp (TUV 15W G15T8 UV-C, Philips, USA) and the glass plate was 45 cm. After irradiation, 200 µL of the irradiated samples were spread

on 5% (w/v) sorbitol agar plates and incubated for 4 h at 30°C under darkness to fix the mutation. Then, the incubation temperature was changed to 39°C, and the plates were further cultivated for 5 d. Relatively large colonies were isolated, and cultivated in 5 mL sorbitol medium at 38°C for 48 h. The cultures (300 μL) were transferred to fresh medium and cultivated for another 48 h. The cultivation was repeated three times, the culture media were spread on 5% (w/v) sorbitol agar plates, and incubated at 30°C. Few colonies were isolated and cultivated in 5 mL 5% (w/v) sorbitol medium at 38°C, and strains showing higher growth than the wild-type strain were identified as UV mutant strains.

1.2.3 Construction of transporter-defective mutants

The *steP* gene (locus tag GLF_2756) was amplified from the chromosomal DNA of strain CHM43 using primers GLF2755 Xba-F and GLF2755 Sac-R (Table 1.2) and was cloned into the pGEM-T Easy vector (Promega Corporation, USA). The resultant plasmid, pTWsH, was digested with *Xba*I and *Sac*I, and the DNA fragment was inserted into the respective sites of the pBAD33 vector. The resultant plasmid, pBWsH, was digested with *Pvu*I, blunt-ended using Blunting High (Toyobo, Osaka, Japan), and ligated with an *Eco*RV fragment containing the kanamycin resistance (Km^r) cassette from pT Km (Yoshida et al., 2003). The disruption plasmid thus obtained, pBDsKmH, was introduced into wild-type strain CHM43 and strain AD-G by electroporation to construct the CDWsH (CHM43 Δ*steP*::Km^r) (Wild Δ*steP*) and CDGsH (CHM43 AD-G Δ*steP*::Km^r) (AD-G Δ*steP*) strains, respectively (Table 1.2).

1.2.4 Construction of G inserted mutant, Wild-G

The mutated *steP* gene (locus tag GLF_2756) was amplified from the chromosomal DNA of the CHM43 AD-G strain using the same primers as those described above and was cloned into the pGEM-T Easy vector (Promega Corporation, USA). The resultant plasmid, pTGsH, was digested with *Xba*I and *Pst*I, and the resulting fragment was inserted into the corresponding sites of pK19mobGII, which carries the β-glucuronidase (*gusA*) and Km^r genes (55), to construct pKGsH (Table 2). This recombinant plasmid was introduced into the wild-type CHM43 strain by electroporation. The transformed cells were screened for β-glucuronidase (GUS)-positive and kanamycin-resistant phenotypes. The selected colonies were grown at 37°C, and recombinant strains with GUS-negative and kanamycin-sensitive phenotypes were selected. The G insertion mutation was verified by sequencing.

Table 1.2. Bacterial strains and plasmids used in this study.

Bacterial strains or plasmid	Relevant properties	Source (reference)
Strains		
Gluconobacter frateurii		
CHM43	Wild type (NBRC101659; BCC 36198)	Moonmangmee et al., 2000
CHM43AD	Adapted strain of CHM43	Hattori et al., 2012
CHM43 AD-G	G-inserted strain isolated from CHM43AD	This study
CHM43 AD-T	T-inserted strain isolated from CHM43AD	This study
CDWsH	CHM43 Δ*steP*::Km^r	This study
CDGsH	CHM43 AD-G Δ *steP*::Km^r	This study
Wild-G	CHM43 mutant with insertion of G in the *steP* gene	This study
CNM-1	CHM43 Δ*otsAB* gene	This study
CNM-2	Wild-G Δ*otsAB* gene	This study
UVA10	UV irradiation mutant grown on 5% sorbitol medium at 38˚C	This study
UVB1	UV irradiation mutant grown on 5% sorbitol medium at 38˚C	This study
E. coli DH5α	F$^-$*endA1 hsdR17* (r_k^-, m_k^+) *supE44 thi-1* λ^-*recAl gyrA96 relA1 deoR* Δ(*lacZYA-argF*)U169 ϕ80d*lacZ*ΔM15	Grant et al., 1990
Plasmids		
pGEM-T Easy	Ap^r; *lacZ* promoter	Promega
pTGsH	pGEM-T Easy with the *steP* gene from CHM43 AD-G	This study
pK19mobGII	*gusA* gene; Km^r; *lacZ* promoter	Katzen et al., 1999
pKGsH	pK19mobGII with a *Xba*I and *Pts*I fragment from pTGsH	This study
pTWsH	pGEM-T Easy *steP*	This study
pBAD33	Cm^r, *araBAD* promoter	Guzman et al., 1995
pBWsH	pBAD33 with a *Xba*I and *Sac*I fragment from pTWsH	This study
pT Km	pT7Blue T-vector with 0.9-kb *Eco*RV fragment containing nonpolar Km^r cassette	Yoshida et al., 2003
pBDsKmH	pBAD33 Δ*steP*::Km^r	This study
pBBR1MCS-4	Ap^r; *lacZ* promoter	Kovach et al., 1995
pMWsH	pBBR1MCS-4 with the *steP* gene under transcriptional control of *lacZ* promoter	This study
pT7Blue	Ap^r; *lacZ* promoter	Novagen
pCNM1	pT7Blue with a *Xba*I and *Sac*I fragment from pTWsH	This study
pCNM2	pBBR1MCS-4 with the *steP* gene without artifical promoter	This study

pKOS6b	*codBA* gene; Km^r; 5-fluorocutosine sensitive; *lacZ* promoter	Kostner et al., 2013
pCNM3	pT7Blue T-vector *otsAB*	This study
pCNM4	pKOS6b with Δ*otsAB*	This study

Table 1.3. Primers used in this study.

Function of plasmid constricted	Primer
Expression of Wild-type *steP* and G-inserted *steP*	GLF2755 Xba-F: 5' TCTAGACGGCCTTCGCATTTGCGACC 3'
	GLF2755 Sac-R: 5' GAGCTCCTGACCTTCCTCGAAGTCTC 3'
Disruption of *otsAB*	GLF0036-XhoI-F: 5' CTCGAGCGGGGATAATCCTGAC 3'
	GLF0035-KpnI-R: 5' GGTACCGGAACAACCGTACG 3'

1.2.5 Construction of expression plasmids for the transporter and hypothetical protein genes

The pBBR1MCS-4 plasmid, carrying the ampicillin resistance (Ap^r) gene, was used as the expression plasmid (Table 1.2). The target gene was amplified by PCR from the CHM43 genome. The primer pair GLF2755 Xba-F/GLF2755 Sac-R was used for amplifying the *steP* gene (Table 1.3). The PCR products were purified using the MagExtractor gel extraction kit (Toyobo, Osaka, Japan) and were ligated into the pGEM-T Easy vector (Promega Corporation, USA) to yield pTWsH. Plasmid pTWsH was digested with *Xba*I and *Sac*I, and the DNA fragment was inserted into the respective sites of pBBR1MCS-4. The constructed plasmid, pMWsH, was transformed into CHM43 AD-G by electroporation. The growth of CHM43 AD-G harboring pMWsH ($steP^+$) was very weak, probably owing to the intense promoter (*lac* promoter) activity of pBBR1MCS-4. Therefore, we reconstructed a plasmid with the *steP* gene in the opposite direction. For this purpose, pMWsH was digested with *Xba*I and *Sac*I, and the resulting fragment was inserted into the respective sites of the pT7Blue vector. The resultant plasmid, pCNM1, was cut with *Eco*RI and was ligated into pBBR1MCS-4 at the *Eco*RI site. The direction of the insert was confirmed by transforming the plasmid into *E. coli* DH5α, followed by sequencing. Finally, the plasmid thus obtained, pCNM2, was transformed into Wild-G or Wild Δ*steP* by electroporation.

1.2.6 Construction of trehalose synthesis gene-defective mutants

Trehalose synthesis is performed by α,α-trehalose phosphate synthase, encoded by *otsA* (locus tag GLF_0035), and trehalose phosphatase, encoded by *otsB* (locus tag GLF_0036). In order to construct an *otsAB* disruptant, we used the markerless deletion system of plasmid pKOS6b (Kostner et al., 2013). The *otsAB* genes were amplified from the CHM43 genome by primers GLF0036-XhoI-F and GLF0035-KpnI-R (Table 3) and were then cloned into pT7Blue. The resultant plasmid, pCNM3 (Table 2), was digested by two sets of restriction enzymes: *Xho*I and *Bgl*II (fragment size, 0.7 kbp) and *Bam*HI and *Kpn*I (fragment size, 0.7 kbp). These fragments were inserted into the *Sal*I and *Kpn*I sites of the pKOS6b vector. The resultant plasmid, pCNM4 (Table 1.2), was introduced into the CHM43 and Wild-G strains by electroporation. Colonies grown on 5% (w/v) sorbitol medium containing 50 μg/mL kanamycin were isolated as the first recombinant strains and were confirmed by PCR using primers GLF0036-XhoI-F and GLF0035-KpnI-R to have a wild-type *otsAB* DNA band (3.2 kbp) or a disrupted *otsAB* DNA band (1.5 kbp). Next, the first recombinant strains were spread on a plate of 5% (w/v) sorbitol medium containing 120 μg/mL 5-fluorocytosine, which was used as a negative selection marker because pKOS6b contains the *codAB* genes (Kostner et al., 2013). For colony isolation, several colonies grown on this plate were confirmed not to grow on a plate of 5% (w/v) sorbitol medium containing 50 μg/mL kanamycin. Finally, by confirmation of the disrupted *otsAB* DNA band (1.5 kbp), the CNM-1 strain (CHM43 Δ*otsAB*) (Wild Δ*otsAB*) and the CNM-2 strain (Wild-G Δ*otsAB*) were obtained.

1.2.7 Extracellular and intracellular sugars and acetic acid measurement using HPLC

The wild-type strain CHM43, the adapted strain CHM43AD-G, and the mutant strains, Wild-G, Wild Δ*otsAB*, and Wild-G Δ*otsAB*, were cultivated in 50 mL of 10% (w/v) sorbitol medium in 500 mL Erlenmeyer baffled flasks at 30, 37, and 38.5°C. The cultures were centrifuged at 13,000 x g for 5 min to separate the supernatants and the cell pellets. The supernatants were applied directly to the HPLC column, for extracellular sugar analysis. For analysis of intracellular sugars, the cell pellets were washed twice with 10 mM potassium phosphate buffer (KPB, pH 7.0), and aliquoted into three microtubes (~5 mg dry cell weight each). The cells were suspended in 500 μL of Bligh and Dyer mixture (methanol:chloroform:water, 10:5:4) (Bligh and Dyer, 1959), and vortexed for 5 min at 25ºC. Then, 130 μL each of distilled water and chloroform were added to the mixture. The mixture was vortexed again for 5 min and centrifuged at 13,000

x g for 5 min. The upper layer (methanol and water layer) of the two-layered sample was separated and desiccated until methanol was evaporated, while the lower chloroform layer was also dried. The upper and lower layers were used for HPLC and protein analysis, respectively. For protein analysis, the lower layer was dissolved in 10 mM NaOH and the protein content was measured by modified Lowry method (Dulley and Grieve, 1975). For HPLC analysis, the upper layer was filtered and applied to the HPLC column, and HPLC was carried out by two different columns, RSpak KC-811 (8×300 mm, Shodex; Showa Denko K.K., Japan) and Sugar SP0810 (8×300 mm, Shodex; Showa Denko K.K., Japan). In the former column, elution was performed using 0.1% (v/v) phosphoric acid at 60°C at a flow rate of 0.4 mL/min, and monitored by the reflection index. Acetic acid, L-sorbose, and D-sorbitol were detected at 15.2, 19.85, and 20.95 min, respectively. While the latter column was eluted with Milli-Q water at 80°C at a flow rate of 0.5 mL/min, and the elution was monitored by the refractive index. Trehalose, L-sorbose, fructose, and D-sorbitol were detected at 17.1, 21.9, 24.8 and 48.5 min, respectively.

1.2.8 Intracellular trehalose measurement with enzymatic method

Intracellular trehalose content was also measured by an enzymatic method. The cell pellet was washed twice with 10 mM KPB (pH 7.0), and finally resuspended in KPB at 4 mL/g wet cells. The resuspended cells were disrupted twice using a French pressure cell press (American Instrument Co., Silver Spring, MD, USA) at 16,000 psi, followed by centrifugation at 8,000 x g for 10 min to remove intact cells. The supernatant was mixed with trichloroacetic acid at a final concentration of 5% (w/v), incubated for 30 min at 25ºC, and centrifuged at 13,000 x g for 5 min. After adjusting the pH of the supernatants to ~6.0 using NaOH, the samples (100 µL) were mixed with 92 µL of citric acid buffer (pH 5.7) and 8 µL of 1 U/mL trehalase (Sigma Aldrich), and incubated overnight at 37°C. The glucose concentrations in the samples were measured using the Glucose (GO) Assay Kit (Sigma Aldrich) to estimate the trehalose content.

1.2.9 Enzyme assay

CHM43, Wild-G and Wild Δ*otsAB* were cultivated in 50 mL of 10% (w/v) sorbitol medium in 500 mL-Erlenmeyer baffled flasks at 30, 37 and 38.5ºC for until late-log phase. Cells were harvested by centrifugation at 9,000 x g for 10 min and washed twice with 10 mM KPB (pH 7.0). The washed cells were resuspended in the same buffer at a concentration of 4 mL/g of wet cells, and passed twice through a Franch pressure cell press (American Instrument Co., Silver Spring, MD, USA) at 16,000 psi. After centrifugation at 9,000 x g for 10 min to remove intact cells, the supernatant was

ultracentifuged at 100,000 x g for 60 min to separate the soluble fractions from the membrane fractions. Using the soluble fractions, glucose-6-phosphate (G6P) dehydrogenase and 6-Phosphogluconate (6PG) dehydrogenase activities were measured spectrophotometrically by monitoring the absorbance at 340 nm due to the reduction of $NAD(P)^+$. The reaction mixture (1 mL) contained 10 mM G6P or 6PG, 10 mM $MgCl_2$, 0.5 mM $NAD(P)^+$, 50 mM glycine-NaOH buffer (pH 9.5) or 50 mM Tris-HCl buffer (pH 8.0), respectively. The activity was calculated by using a millimolar extinction coefficient of 6.2 mM^{-1} cm^{-1} and 6.3 mM^{-1} cm^{-1} for NADH and NADPH, respectively. One unit of enzyme activity was defined as the amount of enzyme catalyzing the formation of 1 μmol of NAD(P)H per min at 25ºC under the assay conditions.

1.2.10 Measurement of intracellular ROS level

Cells were grown in 50 mL of 10% (w/v) sorbitol medium containing 2 μM H_2DCFDA (dichlorodihydrofluorescein diacetate) as the fluorescence probe at 30, 37 and 38.5°C. Cells were harvested at late-log and/or stationary phases by centrifugation at 9,000 rpm for 5 min, at 4°C, and washed two times with 10 mM KPB (pH 7.0). The washed cells were resuspended in the same buffer at a concentration of 4 mL/g of wet cells, and passed twice through a French pressure cell press (American Instrument Co., Silver Spring, MD, USA) at 16,000 psi. After centrifugation at 9,000 x g for 10 min to remove intact cells, the supernatant was ultracentifuged at 100,000 x g for 30 min. Using the resultant supernatant, the fluorescence intensity was measured at 25ºC with excitation at 504 nm and emission at 524 nm. The fluorescence intensity was normalized by protein concentrations.

1.2.11 Measurement of intracellular $NADP^+$ and NADPH contents

Strains were cultivated in 50 mL of 10% (w/v) sorbitol medium at 37ºC for until late-log phase, then cells were harvested by centrifugation at 13,000 x g for 5 min and washed twice with 50 mM KPB (pH 7.0). Intracellular $NADP^+$ and NADPH were analyzed by Fluorescent NADP/ NADPH Detection Kit (Cell Technology Inc.), according to the supplier's protocol.

1.2.12 Genome sequencing

Previously, we have reported the draft genome sequence of *G. frateurii* CHM43; their genome-fragments consisted of 145 contigs and are available at DDBJ/ EMBL/GenBank accession numbers BADZ01000001 to BADZ01000145 (Hattori et al., 2012). In this study, we performed genome resequencing using the Illumina Hiseq 2000

platform to obtain a high-quality draft genome sequence. In addition, the previously obtained thermo-adapted strain, CHM43AD, was also sequenced to identify its mutation sites. Genome sequencing of both the strains, CHM43 and CHM43AD, were carried out as previously reported (Matsutani et al., 2014). Total sequence pairs of 100-bp paired-end nucleotide reads obtained for CHM43 and CHM43AD were 6,925,823 and 6,411,844, which yielded approximately 439× and 406× sequence coverage, respectively.

1.2.13 *De novo* sequence assembly and annotation

The draft genome sequencing data from the wild-type CHM43 strain was assembled using Velvet v1.2.08 with VelvetOptimiser v2.2.4 (Zerbino et al., 2008; Zerbino et al., 2009). The resulting contigs were ordered against the complete genome sequence of *G. oxydans* strain 621H using Mauve (Darling et al., 2010). The gene detection and annotation were performed using the autoannotation package, Prokka (Seemann, 2014). Protein-coding regions or open reading frames (ORFs) of the draft genome sequences were predicted using Prodigal v2.62 (Hyatt et al., 2010). tRNAs and rRNAs were predicted using ARAGORN v1.26 and Barrnap v0.6, respectively (Laslett and Canback, 2004). Functional assignments of the predicted ORFs were obtained using the basic local alignment search tool-protein (BLASTP) homology search against the National Center for Biotechnology Information (NCBI) nonredundant (NR) database, and then manually edited (Altschul et al., 1997). The resulting assembly was used for further comparative genome analysis.

1.2.14 Genome mapping of CHM43AD strain against CHM43 whole contigs

The Illumina sequencing reads for CHM43AD were aligned with the draft genome sequence of CHM43 using Bowtie 2 and the Burrows-Wheeler Aligner (BWA) (Langmead and Salzberg, 2012; Li and Durbin, 2009; Li and Durbin, 2010). To detect the sequencing or assembly error, sequencing data from the CHM43 strain was also mapped onto the draft genome assembly. The mutational sites were searched using the method described previously (Matsutani et al., 2015).

1.2.15 Sequence data deposition

The updated version of *G. frateurii* CHM43 draft genome sequence was deposited at DDBJ/EMBL/GenBank under the accession number BADZ00000000. The versions described here are the second versions, corresponding to the GenBank accession numbers BADZ02000001 to BADZ02000044. Illumina sequence reads of CHM43 and CHM43AD strains have been deposited in the DDBJ Sequence Read Archive (DRA)

under accession numbers DRA003758 and DRA003759, respectively. The BioProject ID of CHM43 and CHM43AD strains are PRJDB2 and PRJDB4049, respectively.

1.3 RESULTS

1.3.1 Mutational analysis of the thermally adapted strain, CHM43AD

We have previously obtained the thermally adapted strain, *G. frateurii* CHM43AD, through experimental evolution (Hattori et al., 2012). To identify the mutations in CHM43AD, we performed whole-genome mapping analysis of strains CHM43 and CHM43AD in the present study. The reference genome sequence of CHM43 was assembled from the Illumina reads. The characteristics of the *de novo* genome assembly for CHM43 are summarized and compared with the previous data in Table 1.1. The resulting assembly had 44 contigs, with the N_{50} length and maximum contig length of 400,768 and 670,742 bp, respectively. The results clearly showed that the sequence quality drastically improved as compared to the previously reported sequence (Hattori et al., 2012). Thus, 2,928 protein-coding genes, 49 tRNA genes, one transfer-messenger RNA (tmRNA) gene, and three rRNA genes were identified in the genome (Table 1.1).

Using the updated reference genome, we found two mutations in the same gene (locus_tag: GLF_2756 in the genome of CHM43AD) that encodes a putative drug transport transmembrane protein. Because two single-nucleotide insertions were found in the same gene, we reisolated several colonies and performed PCR analysis. We thus found that the original CHM43AD strain was a mixture of mutants with a G insertion or T insertion, which we named CHM43 AD-G and CHM43 AD-T, respectively (Fig. 1.1). The insertions were only 21 bp apart and both caused a frameshift mutation. We did not observe a significant difference in the growth of the strains at 38.5°C; accordingly, we selected the CHM43 AD-G strain for subsequent experiments. After colony isolation, we repeated the comparative genome analysis of strains CHM43 and CHM43 AD-G. Nevertheless, we did not detect any other mutations besides the G insertion in the transporter gene.

Matayoshi attempted to obtain other thermotolerant mutants of *G. frateurii* CHM43 by UV mutagenesis under the same culture conditions as in the experimental evolution. Two UV mutant strains, UVA10 and UVB1, were thus obtained (Matayoshi, master thesis 2018). The growth curves of these strains (Fig. 1.2A) were similar to that of CHM43 AD-G. Moreover, comparative genome analyses of CHM43 and the two UV mutants were conducted to identify the mutations (data not shown). The UVB1 strain was found to have the same G insertion as CHM43 AD-G does. The UVA10 strain had a

single-base substitution of cytosine (C) with T at position 334 in the same gene, GLF_2756, resulting in a missense mutation (substitution of arginine with cysteine, R112C).

Therefore, the thermally adapted strains obtained by either experimental evolution or UV mutagenesis had mutations in the same gene; each mutation conferred thermotolerance on these strains.

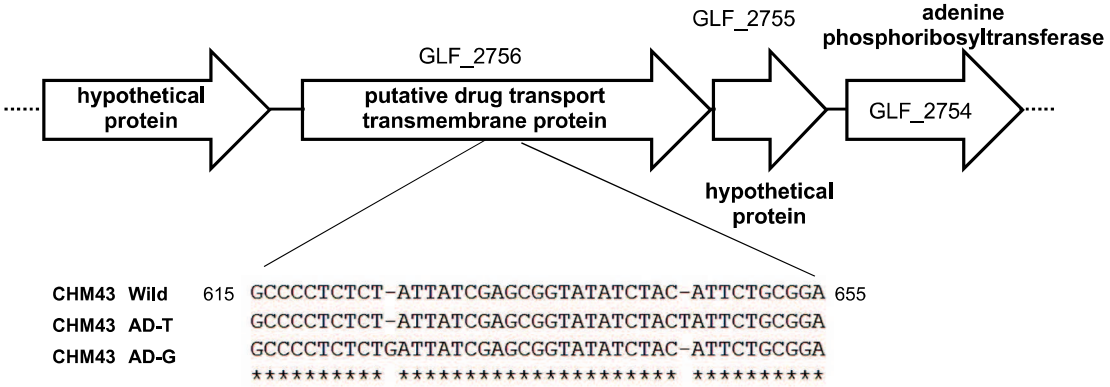

Fig. 1.1. (Top) Genomic organization of the transporter gene (locus_tag: GLF_2756) flanking regions. (Bottom) Sequence alignment showing the mutations in thermally adapted strains: CHM43 AD-T and CHM43 AD-G.

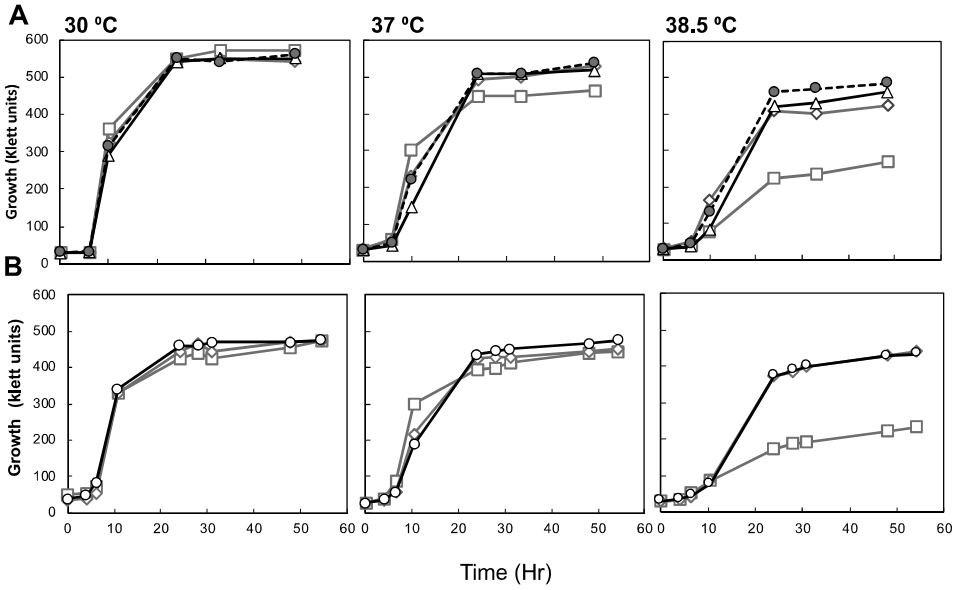

Fig 1.2. Comparison of growth characteristics of *G. frateurii* CHM43 parental and mutated strains at various temperatures. (A) Growth curves of the mutant strains obtained by UV mutagenesis [UVA10 (△: solid black line) and UVB1 (●: dashed black line)]; the parental strain, CHM43 (□: solid grey line); and the thermally adapted strain, CHM43 AD-G (◇: solid grey line). Cells were cultivated in 50 mL of a 10% (w/v) sorbitol medium at 30, 37, or 38.5°C. (B) Growth curves for the Wild-G (○: black line), parental (□: grey line), and CHM43 AD-G (◇: grey line) strains cultured under the same growth conditions as those described for panel A.

1.3.2 Construction of an artificial mutant with the G insertion

To determine whether the single G insertion was sufficient to enable CHM43 AD-G to grow at high temperatures, we constructed a mutant strain, designated Wild-G, with the same G insertion in the transporter gene (the *steP* gene, encoding *s*ugar-*t*ransporting/*e*xporting *p*ermease [SteP]) as that found in CHM43 AD-G. As shown in Fig. 1-2B, the Wild-G strain grew well at 38.5°C, with a growth curve similar to that of the CHM43 AD-G strain. The growth curves of these strains were different from that of the CHM43 wild-type strain, confirming that this single mutation accounts for the thermotolerant phenotype of the adapted strain.

1.3.3 Disruption and/or complementation of the transporter gene in *G. frateurii* CHM43 wild-type strain and Wild-G mutant strain

The CHM43 AD-G and Wild-G strains both carry a frameshift mutation approximately halfway through the gene of the transporter protein, which may comprise 12 transmembrane segments (TMSs). It is thus possible that the N-terminal half of the transporter (six TMSs) may retain some function, as reported for the *Lac* permease of *E. coli* (Wu et al., 1996). To test this hypothesis, the *steP* gene of the wild-type strain and of CHM43 AD-G was disrupted by the insertion of a kanamycin cassette into the wild type and CHM43AD-G to create Wild Δ*steP* and AD-G Δ*steP*, respectively. Strains Wild Δ*steP* and Wild-G were then complemented by means of a plasmid harboring the wild-type *steP* gene. The growth rates of these strains were compared at various temperatures (Fig. 1.3). As shown in the Fig. 1.3, similarly to strain CHM43 AD-G, strains Wild-G and Wild Δ*steP* (as well as strain CHM43 AD-G Δ*steP* (data not shown)) showed better growth than the parental strain at 38.5°C. In contrast, after complementation with the wild-type *steP* gene, the growth rate of both Wild-G and Wild Δ*steP* at 38.5°C decreased, and their growth profile was now similar to that of the wild-type strain. It should be noted that in this experiment, the complementation was successful only when performed with the plasmid having the promoter-less *steP* gene placed in the opposite orientation from the *lac* promoter. The Wild-G and Wild Δ*steP* transformants with plasmids carrying the *steP* gene under the control of the lac promoter or either of the two different promoters for the ribosomal protein genes (Kallnik et al., 2010) grew worse even at 30°C than those with the vector plasmid pBBR1MCS-4 (data not shown). Thus, we could not prepare cells overproducing the transporter.

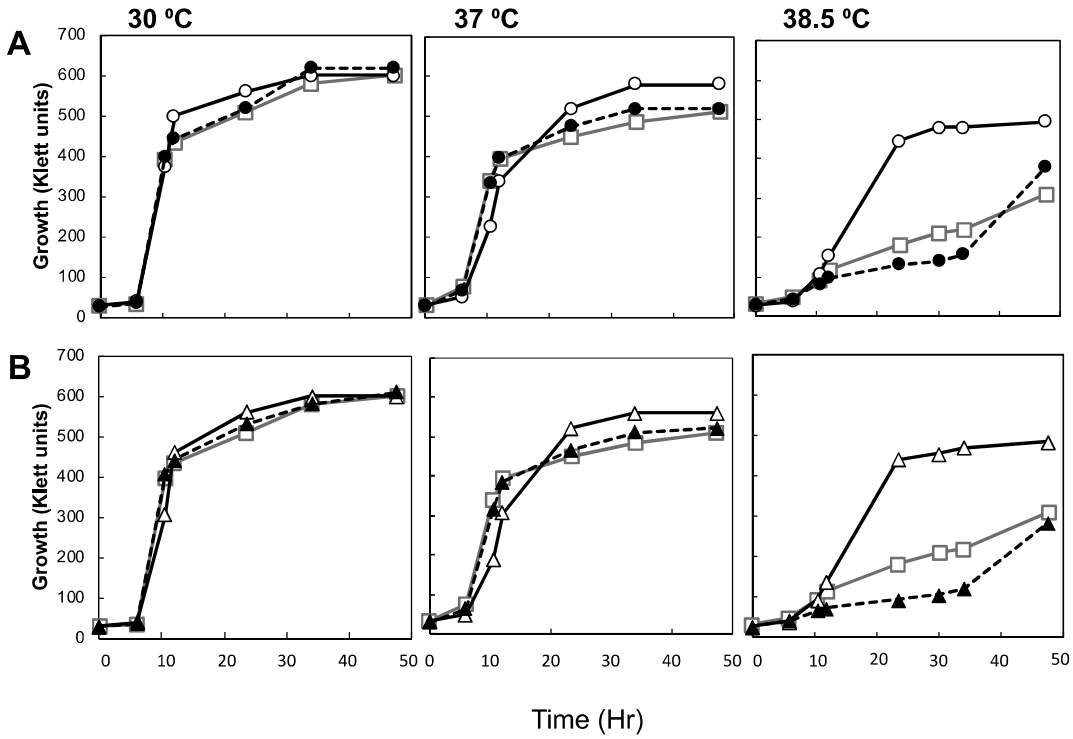

Fig. 1.3. Effects of disruption and complementation of the transporter gene on bacterial growth at various temperatures. The parental strain, CHM43, harboring pMCS4 (□: solid grey line), Wild-G harboring pBBR1MCS-4 (○: solid black line), Wild Δ*steP* harboring pBBR1MCS-4 (△: solid black line), Wild-G harboring pCNM2 (promoterless *steP*) (●: dashed black line), and Wild Δ*steP* harboring pCNM2 (promoterless *steP*) (▲: dashed black line) were cultured in 50 mL of a 10% (w/v) sorbitol medium containing 500 μg/mL ampicillin at 30, 37, or 38.5°C. (A) Growth curves of strains CHM43/pBBR1MCS-4, Wild-G/pBBR1MCS-4, and Wild-G/pCNM2 (promoterless *steP*). (B) Growth curves of strains CHM43/pBBR1MCS-4, Wild Δ*steP*/ pBBR1MCS-4, and Wild Δ*steP*/pCNM2 (promoterless *steP*).

1.3.4 Metabolic change in Wild-G and several mutant strains

To investigate the physiological properties of the thermotolerant strains, sorbose production and its assimilation were examined in the wild-type and adapted strains. Sorbitol consumption and sorbose accumulation in the culture medium were similar for the wild-type (CHM43) and CHM43 AD-G or Wild-G strains, although the wild-type strain had a slightly slower sorbose production rate at 38.5°C owing to reduced bacterial growth at this temperature (see Fig. 1.4). When we quantified several other metabolites by HPLC, besides high concentrations (~500 mM) of sorbose, relatively small amounts

of acetate (10–20 mM), fructose (~40 mM), and trehalose (1.0–4.5 mM) were detected in the culture medium, whose trehalose content with the wild-type strain clearly differed from that with mutant strains, Wild-G and Wild Δ*otsAB* (see below) (Fig. 1.4). To confirm the change in trehalose concentration in detail, both the extracellular and intracellular trehalose concentrations were measured by an enzymatic method (Fig. 1.5), together with HPLC analysis (Fig. 1.6), and compared among the wild-type and several mutant strains. The results clearly indicated that the extracellular trehalose production decreased in all the *steP* strains (AD-G, Wild-G, and Wild Δ*steP*). Concomitantly with the change in extracellular concentration, trehalose accumulated intracellularly in these mutant strains. Although relatively higher intracellular (or lower extracellular) accumulation of trehalose was observed in strains Wild-G and Wild Δ*steP* at 30°C (Figs. 1.5 and 1.6), this change could be explained by change in pentose phosphate pathway (PPP) flux (see below). The trehalose levels in the *steP* strains were recovered by complementation with the wild-type *steP* gene (Fig. 1.5).

Furthermore, to evaluate the assimilation of sorbose produced, the cells were grown at several concentrations of sorbose as a carbon source (Fig. 1.7). The Wild-G strain (Fig. 5), as well as the AD-G strain (data not shown), manifested slower growth than the wild-type strain, especially when the concentration of sorbose in the medium was <5%. Actually, with a lower concentration of sorbose in the medium, sorbose consumption was lower in the AD-G strain than in the CHM43 strain even in the stationary phase (e.g., 3.2 and 20.4 mM, respectively, in a 1.0% sorbose medium), but sorbose consumption by these strains did not differ much at a high concentration of sorbose (e.g., 21.5 and 18.6 mM, respectively, in a 10% sorbose medium). These results suggested that the *steP* strains have some defect in sorbose uptake at lower concentrations. Therefore, in the normal medium (10% sorbitol), the *steP* strains seemed to utilize sorbitol instead of sorbose, at least in the relatively early growth phase, when sorbose accumulation was not sufficient, in contrast to the wild-type cells, which were able to take up sorbose efficiently.

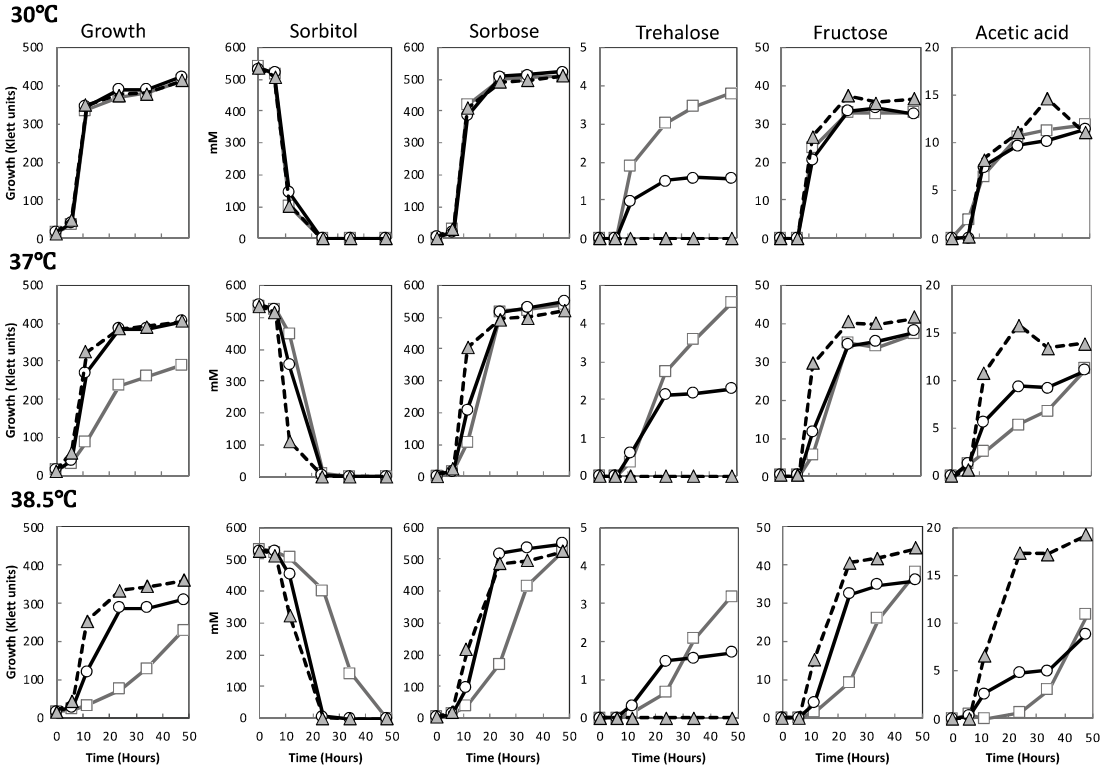

Fig. 1.4. Extracellular sugar concentrations in the wild-type strain, Wild-G strain, and a disruptant of trehalose synthesis genes (strain Wild Δ*otsAB*). Wild-type CHM43 (□: grey line), Wild-G (○: black line), and Wild Δ*otsAB* (▲: dashed line) were cultivated in a 10% (w/v) sorbitol medium at 30, 37, or 38.5°C. The supernatant concentrations of sorbitol, sorbose, trehalose, fructose, and acetic acid were measured by HPLC.

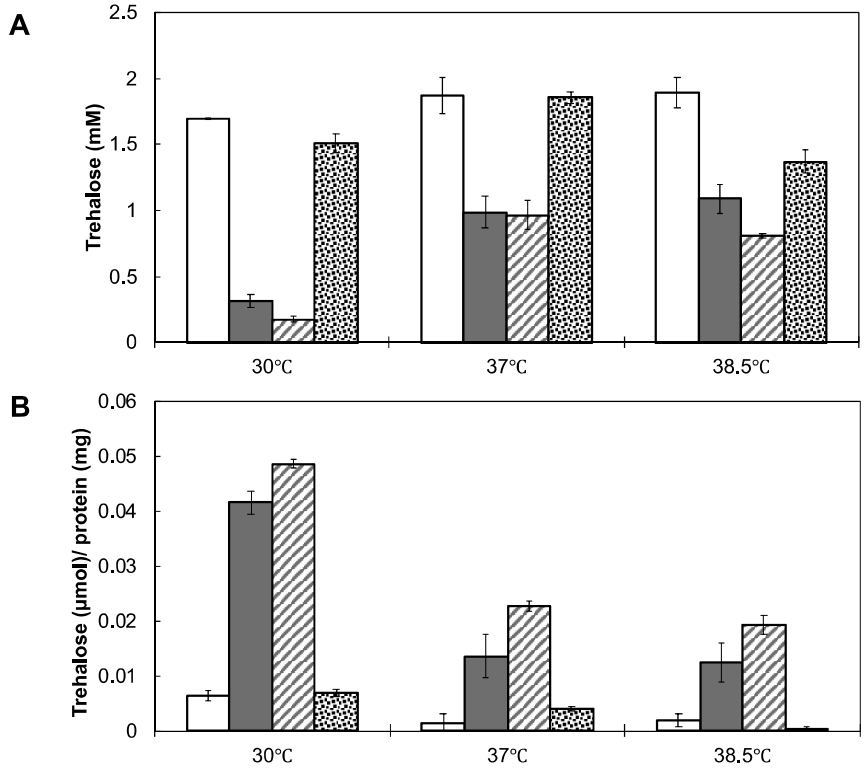

Fig. 1.5. Measurement of extracellular (A) and intracellular (B) trehalose concentrations by an enzymatic assay. Wild-type strain CHM43 harboring pBBR1MCS4 (white bars), strain Wild-G harboring pBBR1MCS4 (grey bars), Wild Δ*steP* harboring pBBR1MCS4 (hatched bars), and the Wild Δ*steP* strain harboring pCNM2 (promoterless *steP*) (stippled bars) were cultivated in a 10% (w/v) sorbitol medium containing 500 μg/mL ampicillin for 30 h (the stationary phase) at 30, 37, or 38.5°C. Trehalose concentrations in the samples were measured with the glucose oxidase (GO) assay kit after treatment with trehalase. Data are shown as mean ± standard deviation of three independent cultivation experiments.

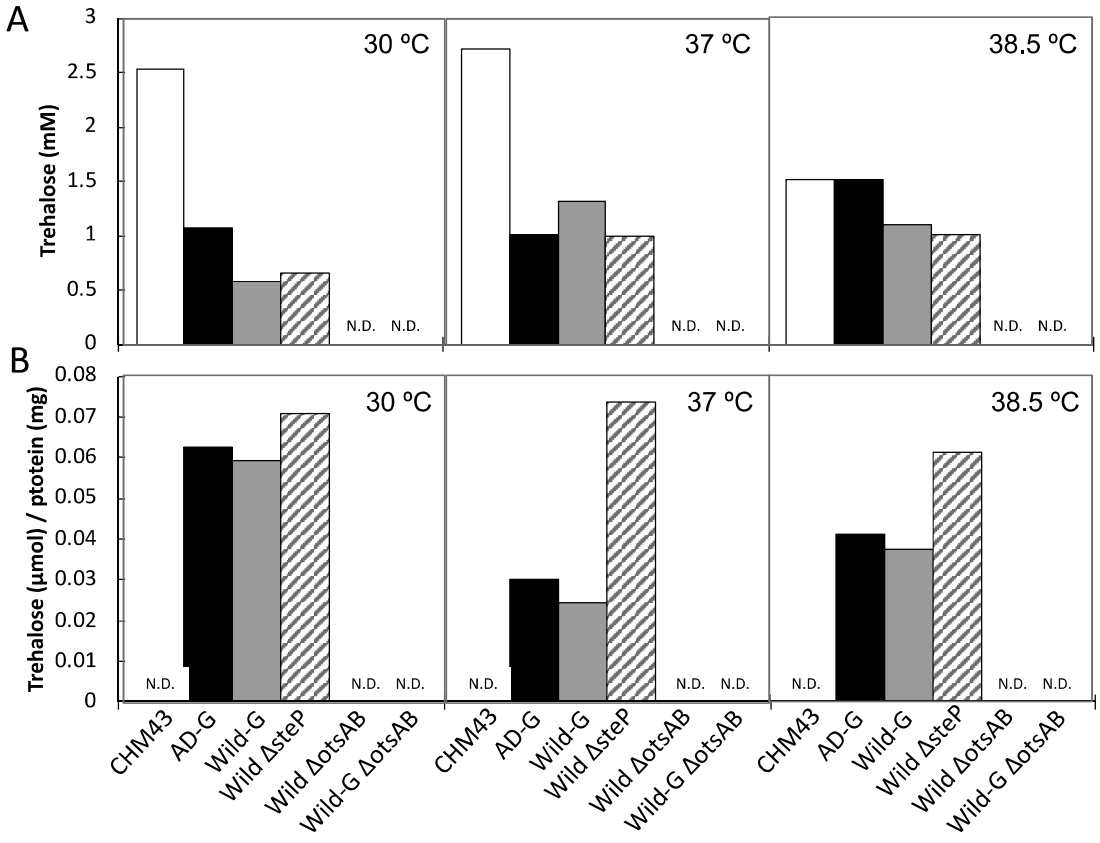

Fig. 1.6. Extracellular (A) and intracellular (B) trehalose concentrations in the wild-type, adapted CHM43 AD-G, Wild-G, Wild Δ*steP*, and in the *otsAB* disruptants: Wild Δ*otsAB* and Wild-G Δ*otsAB*. Wild-type CHM43, AD-G, Wild-G, Wild Δ*steP*, Wild Δ*otsAB*, and Wild-G Δ*otsAB* were cultivated in a 10% (w/v) sorbitol medium at 30, 37, or 38.5°C. The cells were harvested at 24–30 h (stationary phase), and the culture supernatant and the intracellular samples were prepared. In both types of samples, trehalose was quantified by HPLC on a sugar column (Sugar SP0810). N.D., not detected.

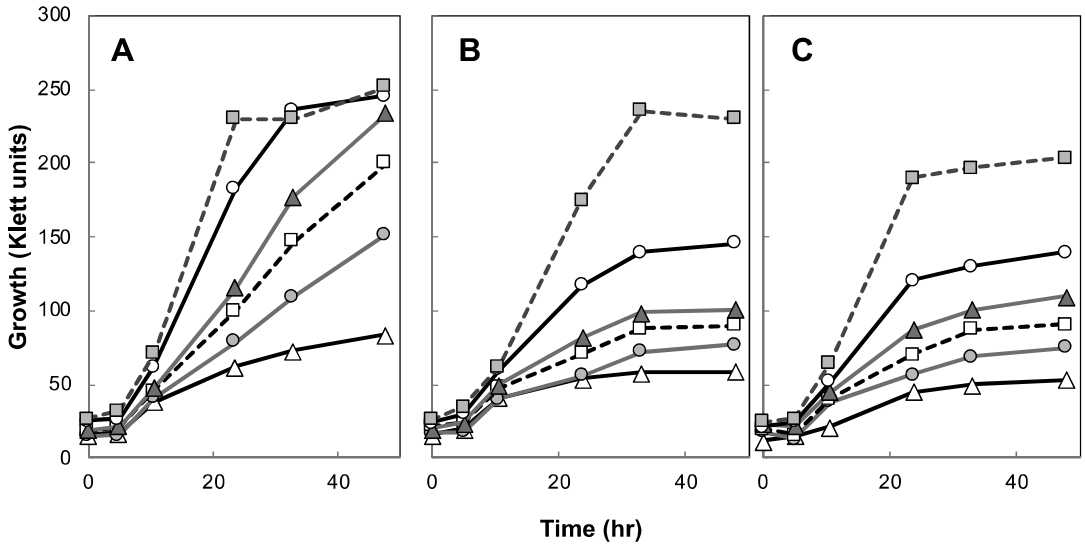

Fig. 1.7. Comparison of growth characteristics of *G. frateurii* CHM43 parental, Wild-G, and Wild Δ*otsAB* strains in a sorbose medium. Strains CHM43 (A), Wild-G (B), and Wild Δ*otsAB* (C) were cultivated in 50 mL of a 0.1–10% (w/v) sorbose medium at 30°C. The sorbose concentrations were 0.1% (△: solid line), 0.5% (●: grey line), 1.0% (□: dashed line), 2.0% (▲: grey line), 5.0% (○: solid line), and 10% (■: dashed line).

1.3.5 Increased trehalose synthesis is not directly responsible for thermotolerance

To elucidate this relation, trehalose synthesis enzymes, encoded by *otsA* (α,α-trehalose phosphate synthase, GLF_0035) and by *otsB* (trehalose 6-phosphate phosphatase, GLF_0036), were disrupted in wild-type and Wild-G strains in order to observe the effects on trehalose accumulation and thermotolerance. Although both intra- and extracellular trehalose disappeared for these disruptants of trehalose synthesis genes (Wild Δ*otsAB* and Wild-G Δ*otsAB*; Fig. 1.6), both mutants grew better than strains Wild-G and Wild Δ*steP* at 38.5 and 39°C and grew well even at 39.5°C (Fig. 1.8). Disruption of the *otsAB* gene did not have a synergistic effect on drug transporter mutant Wild-G, and thus, the growth of strain Wild-G Δ*otsAB* was similar to that of the Wild Δ*otsAB* strain. These results clearly indicated that trehalose itself did not directly contribute to the thermotolerance; instead, trehalose synthesis may be related to a flux change of central metabolism in these strains.

Gluconobacter strains including *G. frateurii* CHM43 have an incomplete TCA cycle and glycolysis because of defects in succinyl-coenzyme A synthetase, succinate dehydrogenase, and phosphofructokinase (Bringer and Bott, 2016) and consequently employ PPP instead of incomplete glycolysis for sugar metabolism. Sorbose is produced

directly from sorbitol by membrane-bound GLDH (Hattori et al., 2012) and is taken up into the cell, then converted to sorbitol by sorbose reductase (SR), and further metabolized to fructose by sorbitol dehydrogenase (SDH) in the cytoplasm (Soemphol et al., 2012). Glucose-6-phosphate (G6P) could be produced from fructose and further metabolized through PPP or to trehalose (Fig. 1.9). The Entner–Doudoroff pathway (EDP) is also present in CHM43 and may bypass G6P to pyruvate by means of two enzymes [phosphogluconate dehydratase (GLF_0494) and 2-keto-3-deoxy-6-phosphogluconate (KDPG) aldolase (GLF_0493)] without such oxidoreduction. Nevertheless, because their expression was 10-fold lower than that of the enzymes of PPP (data not shown), the EDP may not work well in CHM43 as in the case of *Gluconobacter oxydans* (Richhardt et al., 2012). Therefore, to confirm whether PPP reliably works or not, we first measured enzymatic activities of G6P dehydrogenase (G6PDH) and 6-phosphogulconate (6PG) dehydrogenase (6PGDH) (working in PPP) in strains wild-type CHM43, Wild-G, and Wild Δ*otsAB* (Fig. 1.10). In *G. oxydans*, both enzymes have been shown to use $NADP^+$ and NAD^+, respectively, as a coenzyme (Tonouchi et al., 2003). In *G. frateurii* CHM43, G6PDH was found to preferentially utilize $NADP^+$, whereas 6PGDH mainly uses NAD^+ but with some $NADP^+$. G6PDH activity (NADP-dependent) increased with the increasing temperature, while NAD-dependent activity of 6PGDH decreased at 38.5°C, but the NADP-dependent activity increased. Nonetheless, no striking difference was observed among these strains. Thus, both enzymatic activities seemed to be high enough to stimulate G6P oxidation, at least at high temperatures. Actually, simultaneously with the decreased trehalose accumulation, the Wild Δ*otsAB* strain excreted more acetic acid into the culture medium than the wild-type strain did at least at high temperatures (Fig. 1.4), suggesting that G6P was oxidized via PPP to pyruvate and then to acetic acid.

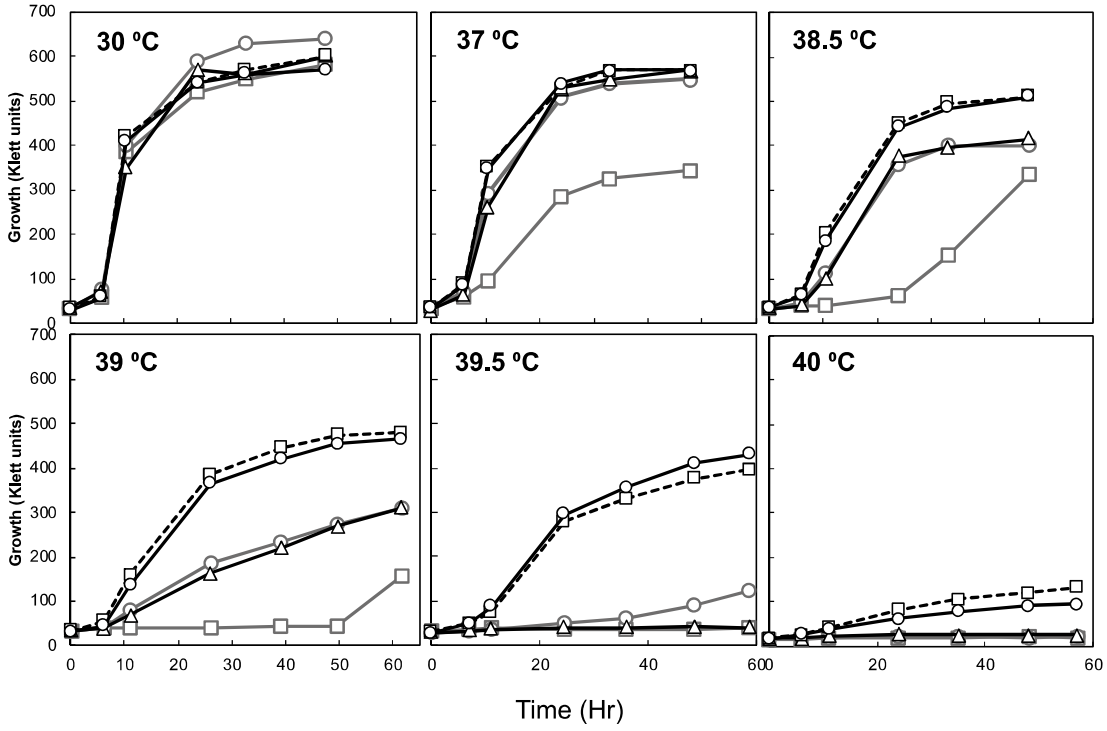

Fig. 1.8. Comparison of growth characteristics of *G. frateurii* CHM43 parental, Wild-G, and mutated strains at various temperatures. Strains CHM43 (□: solid grey line), Wild-G (○: solid grey line), Wild Δ*steP* (△: solid black line), Wild Δ*otsAB* (□: dashed brack line), and Wild-G Δ*otsAB* (○: solid black line) were cultivated in 50 mL of a 10% (w/v) sorbitol medium at various temperatures.

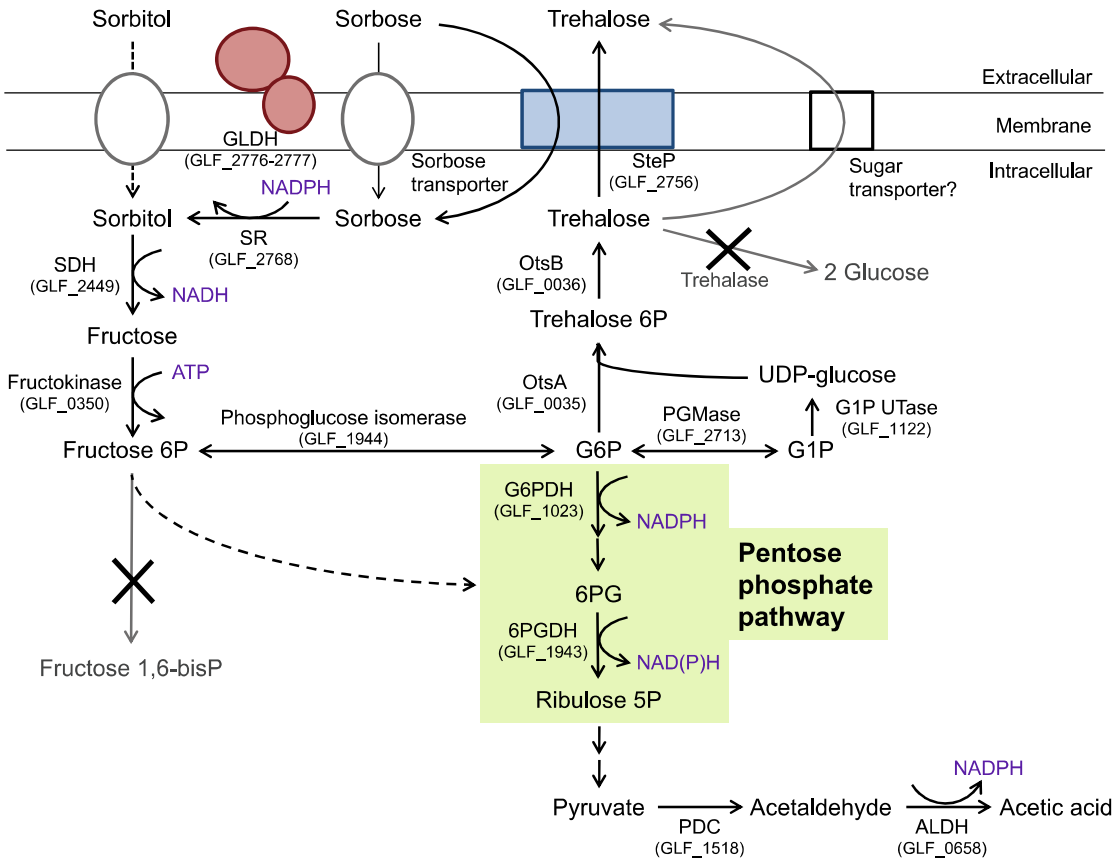

Fig. 1.9. Sugar metabolism related to sorbose utilization and trehalose production in *G. frateurii* CHM43. Fructose 6P, fructose 6-phosphate; fructose 1,6-bisP, fructose 1,6-bisphosphate; G6P, glucose 6-phosphate; G1P, glucose 1-phosphate; 6PG, 6-phospho-gluconate; ribulose 5P, ribulose 5-phosphate; trehalose 6P, trehalose 6-phosphate; GLDH, glycerol dehydrogenase (GLF_2776–2777); SR, sorbose reductase (GLF_2768); SDH, sorbitol dehydrogenase (GLF_2449); PGMase, phosphoglucomutase (GLF_2713); G1P UTase, G1P uridylyltransferase (GLF_1122); OtsA, α, α -trehalose phosphate synthase (GLF_0035); OtsB, trehalose 6-phosphatase (GLF_0036); SteP, sugar-transporting/exporting permease (GLF_2756); G6PDH, G6P dehydrogenase (GLF_1023); 6PGDH, 6PG dehydrogenase (GLF_1943); PDC, pyruvate decarboxylase (GLF_1518); ALDH, aldehyde dehydrogenase (GLF_0658). G. *frateurii* CHM43 possesses neither phosphofructokinase nor trehalase.

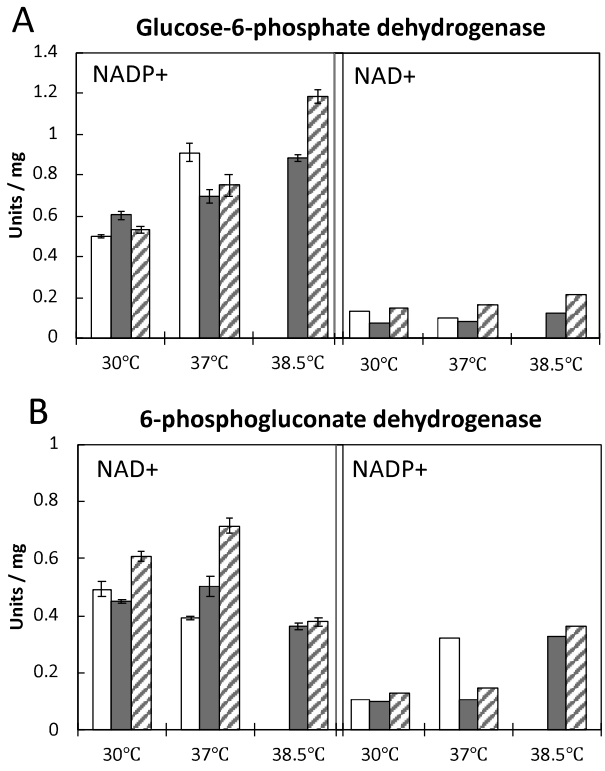

Fig. 1.10. A comparison of activity of glucose-6-phosphate dehydrogenase and 6-phosphogluconate dehydrogenase among strains CHM43, Wild-G, and Wild Δ*otsAB*. Wild-type CHM43 cells (white bars) were cultured in a 10% (w/v) sorbitol medium until the late log phase at 30 or 37°C. Strains Wild-G (gray bars) and Wild Δ*otsAB* (hatched bars) were cultivated on a 10% (w/v) sorbitol medium at 30, 37, or 38.5°C. The data represent the cytosolic fraction extracted from late- log-phase cells. The enzymatic activity was measured as described in Methods. Data are shown as mean ± standard deviation of triplicate measurements (same sample three times).

1.3.6 Relation between metabolic change and thermotolerance

Given that intense PPP flux has been reported to increase NADPH content of the cell (Lim et al., 2002; Lee et al., 2003), we directly measured the intracellular NADPH/$NADP^+$ ratio in strains CHM43, Wild-G, and Wild Δ*otsAB* at 37°C (Fig. 1.11A). The NADPH/$NADP^+$ ratio significantly increased in the Wild-G strain, and even more so in the Wild Δ*otsAB* strain, indicating that these strains may have greater PPP flux than wild type. The NADPH/$NADP^+$ ratio was lower in all strains grown at 30°C than at 37°C (data not shown), suggesting that the metabolic flux to PPP may be lower at 30°C than at 37°C. In case of the Wild-G strain, however, acetic acid production did not increase much, as compared with the Wild Δ*otsAB* strain (Fig. 1.4). Therefore, the Wild-G strain may have some other way to generate NADPH. When the cell growth of the wild type and

AD-G strains was compared on different polyol substrates, the cell growth was better with mannitol than with sorbitol, especially at a higher temperature (Fig. 1.12). Mannitol is oxidized to fructose by GLDH, which also oxidizes sorbitol to sorbose (Matsushita et al., 2003); fructose is then metabolized intracellularly via direct conversion to fructose-6 phosphate, where there is no need for an oxidoreduction step, in contrast to the processing of sorbose, which is reduced to sorbitol (and further to fructose) by consuming NADPH (see Fig. 1.9). Thus, when grown with mannitol, cells may keep surplus NADPH, which could be used for the thermotolerance. Given that the *steP* mutants (including Wild-G strain) have some defect in sorbose assimilation (Fig. 1.7), they seem to utilize sorbitol directly without sorbose uptake in some growth phase. This metabolic pattern may contribute to a higher NADPH/$NADP^+$ ratio as discussed below. Incidentally, the finding that cells could not be grown at a high temperature in a glycerol medium (Fig. 1.12) supported the notion that PPP is important for thermotolerance because glycerol is metabolized without passing through PPP.

Such an increased NADPH level, derived from the increased metabolic flux change, was expected to contribute to protection from thermal stress. As described in the INTRODUCTION, although the level of ROS generation is increased by several stressors including thermal stress (Davidson et al., 1996; Chang et al., 2017; Lee et al., 2015; Zang et al., 2017), it is expected to be lowered in the stress-resistant strains where ROS-scavenging activity is often high (Lee et al., 2015; Sánchez-Riegog et al., 2016). Because some ROS-scavenging enzymes require NADPH (Thelander, 1967; Carlberg and Mannervik, 1975), the increase of intracellular NADPH concentration may support the stress resistance of the cells (Bankapalli et al., 2015). Actually, in *G. frateurii* CHM43, intracellular ROS concentration increased with the increasing growth temperature, and the ROS level was lower in the adapted strain than in the wild-type strain (Fig. 1.13). Accordingly, to determine the relation between the NADPH and ROS levels, intracellular ROS concentrations of strains CHM43, Wild-G, and Wild Δ*otsAB* were measured (Fig. 1.11B). Reduction of ROS, in parallel with the increased NADPH level, was observed; the Wild Δ*otsAB* strain had the lowest ROS content, whereas strain CHM43 had the highest. Although osmotolerance data are not shown, the Wild-G and Wild Δ*otsAB* strains also showed some osmotolerance (against high concentrations [20%] of sorbitol), which has been reported to be related to ROS scavenging (Zang et al., 2017).

These results suggested that trehalose accumulation itself did not directly contribute to thermotolerance; instead, it induced a change in metabolic flux that may have contributed to the thermotolerance.

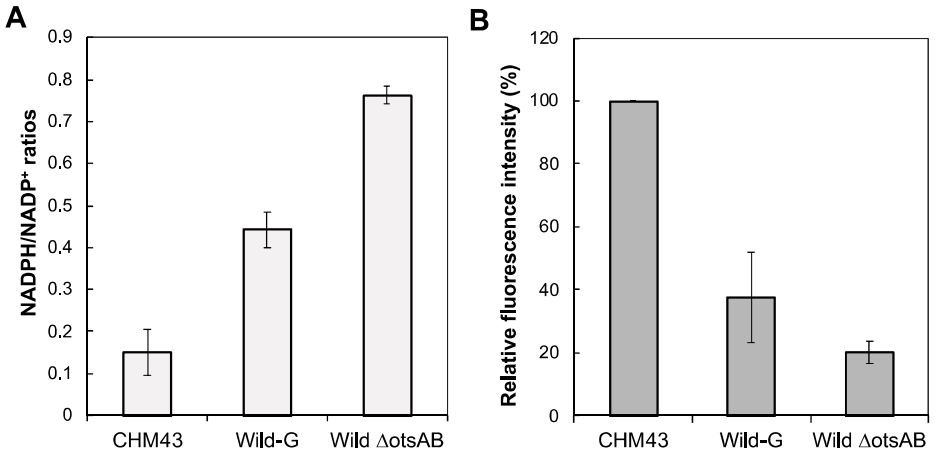

Fig. 1.11. Intracellular NADPH/NADP$^+$ ratios (A) and intracellular ROS levels (B) in strains CHM43, Wild-G, and Wild Δ*otsAB*. The cells were cultivated on a 10% (w/v) sorbitol medium at 37°C until the late log phase (12–13 h). NADP$^+$ and NADPH contents and ROS levels were measured as described in Materials and Methods. Data are shown as mean ± standard deviation of three independent cultivation experiments.

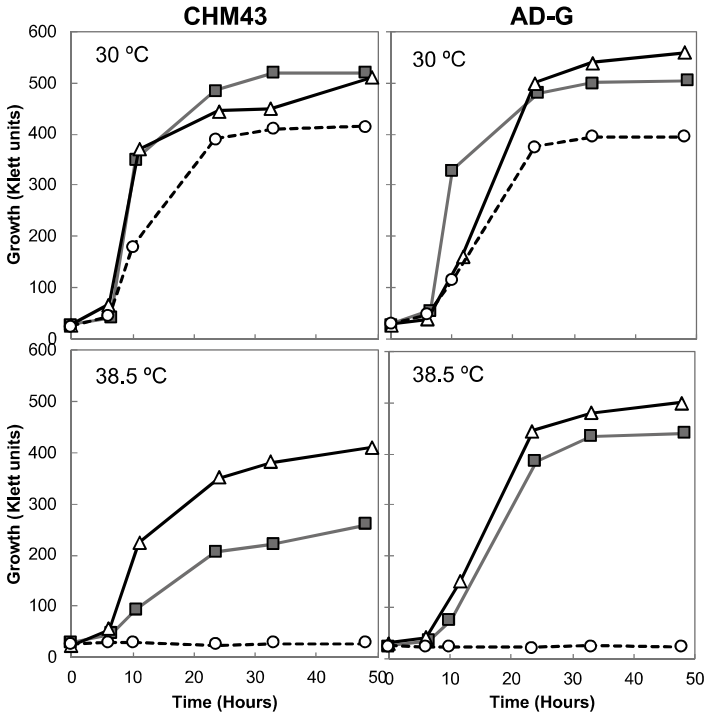

Fig. 1.12. Comparison of growth characteristics of *G. frateurii* CHM43 parental and adapted AD-G strains in various culture media. Strains CHM43 and AD-G were cultivated in 50 mL of a 10% (w/v) sorbitol medium (□: grey line), 10% (w/v) mannitol medium (△: solid line), or 5% (w/v) glycerol medium (○: dashed line) at 30 or 38.5°C.

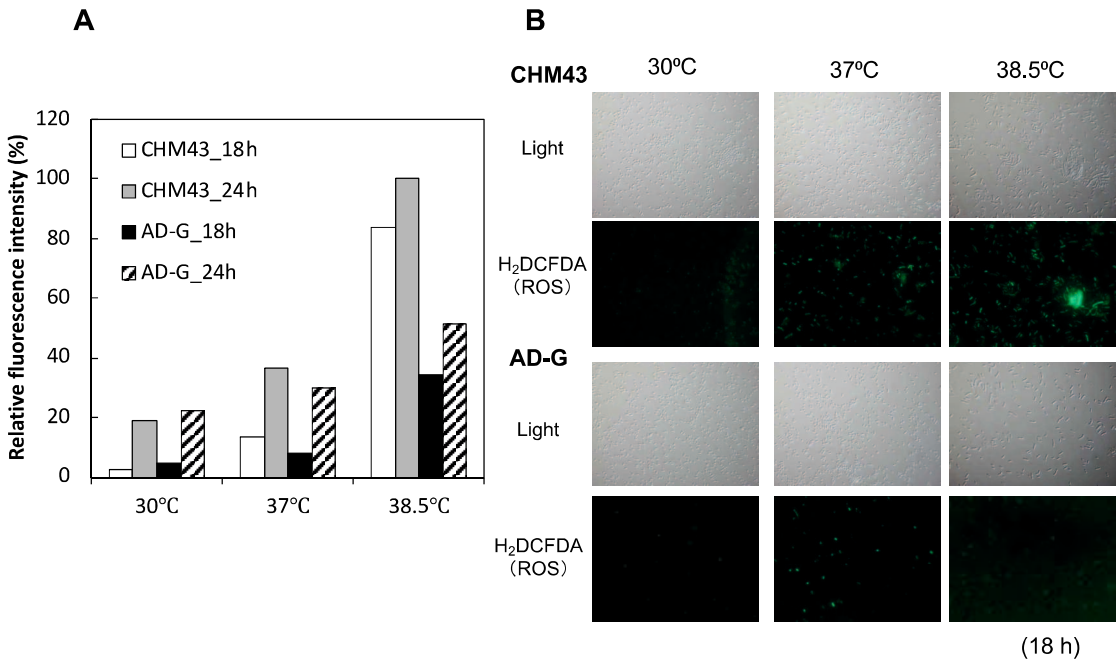

Fig. 1.13. Intracellular ROS levels. (A) Wild-type CHM43 and strain AD-G were cultivated in a 5% (w/v) sorbitol medium containing 10 μM H_2DCFDA at 30, 37, or 38.5°C. The cells cultivated for 18 or 24 h were disrupted, and intracellular ROS levels were measured via fluorescence intensity with excitation at 504 nm and emission at 524 nm. (B) Microscopic examination of cells cultivated for 18 h.

DISCUSSION

Previously, we have obtained a thermally adapted strain, TH-3, from *A. pasteurianus* SKU1108 (Matsutani et al., 2013) and found 11 mutations in this strain by Illumina genome sequencing. Because these mutations may affect thermotolerance to various degrees, it is challenging to delineate the contribution of each mutation to thermotolerance (Matsutani et al., 2013). In contrast, in the present study, only a single-nucleotide insertion (G or T) in the *steP* gene was detected in the CHM43AD strain. Although TH-3 was obtained by long-term thermal adaptation (40 serial subcultures, cultivation time ~2500 h), the CHM43AD strain was obtained by short-term thermal adaptation (seven serial subcultures, cultivation time ~250 h) (Hattori et al., 2012). In addition to the short-term adaptation, UV mutagenesis followed by selection under thermal stress caused mutations in the same *steP* gene, including exactly the same mutation in strain CHM43. The phenotype confirmed by this mutant was confirmed by constructing mutants with either a single G insertion (Wild-G) or disruption of the *steP*

gene (Wild Δ*steP*), both of which manifested the same growth phenotype at higher temperatures as the CHM43AD strain (Fig. 1.2 and 1.3). These results suggested that the mutation in CHM43AD could be specific, at least when growth was performed in a medium containing sorbose or sorbitol at high temperatures (38 to 39°C), and thus, we speculated that this mutation was critical for the growth of CHM43 under these conditions. Therefore, we could directly examine the thermotolerance mechanism in CHM43AD by characterizing only one gene mutated in response to thermal adaptation: the gene encoding the putative drug transporter.

By means of a BLASTP homology search (Altschul et al., 1997), the SteP protein was found to belong to the major facilitator superfamily (MFS) and was predicted to belong to the Bcr/CflA family of drug resistance efflux transporter proteins, which includes the bicyclomycin resistance (Bcr) protein of *E. coli*, the chloramphenicol resistance protein (CmlA) of a *Pseudomonas* sp., and an arabinose efflux permease. The single G or T insertion in the adapted strain resulted in a frameshift mutation halfway through the 12-TMS protein, which may generate either a completely dysfunctional protein or a 6-TMS transporter protein retaining some transporter activity. Nonetheless, the Wild Δ*steP* (complete deletion) mutant showed a phenotype similar to that of the Wild-G (G insertion) mutant, indicating that the mutated transporter with a single-nucleotide insertion is nonfunctional.

According to the gene annotation, the transporter protein was expected to be involved in sugar efflux. Therefore, we examined the mechanism of thermotolerance in the mutant by measuring the concentrations of metabolites related to sorbitol and sorbose metabolism. Of note, a small but significant amount of trehalose was detected both in the culture medium and inside the cells, and the extracellular trehalose level decreased, while the intracellular trehalose increased, in the *steP* mutants: AD-G, Wild-G, and Wild Δ*steP* (Figs. 1.4 and 1.5). At the same time, the *steP* mutants seemed not to take up lower concentrations of sorbose effectively (Fig. 1.7). These findings suggest that the drug transporter is involved, at least partly, in the efflux of trehalose as well as in the uptake of sorbose.

The trehalose pumped out by the transporter could be synthesized from sorbose taken up by the cells, where the transporter may also be involved. The genes for SR (locus tag GLF_2768) and SDH (GLF_2449) participate in fructose production from sorbose, and the genes for fructokinase (GLF_0350) and phosphoglucose isomerase (GLF_1944) produce G6P from fructose (Fig. 1.9). Finally, trehalose is produced from G6P and UDP-glucose by OtsA and OtsB. Accordingly, it is conceivable that the decreased efflux of trehalose in these cells underlies the thermotolerance ability of the adapted strain. A

relation between thermotolerance and trehalose metabolism or accumulation in thermally adapted strains has been reported previously. In a yeast thermal adaptation experiment, the relative trehalose concentration in an adapted strain increased over that in the parent strain (Satomura et al., 2013). Thermally adapted *C. glutamicum* has an *otsA* mutation that has been shown to be responsible for thermotolerance (Oide et al., 2015). Although these data do not offer any quantitative information about the intracellular trehalose concentration or about the role of trehalose in thermotolerance, there are many reports that trehalose accumulation occurs in yeast and bacteria in response to some stressful conditions, such as thermal stress (De Virgilio et al., 1994; Hottiger et al., 1994), heat shock stress (Benaroudj et al., 2001), osmotic stress (Wolf et al., 2003; Purvis et al., 2005), desiccation (Tapia et al., 2015), and antibiotics (Kuczyńska-Wiśnik et al., 2015). Some of these results suggest that a relatively high concentration of trehalose (>1 μmol per mg of protein) prevents denaturation or aggregation of denatured proteins (Hottiger et al., 1994) or oxidative damage to proteins (Benaroudj et al., 2001), according to theoretical analysis of the interaction between such osmolytes and proteins (Auton and Bolen, 2004; Street et al, 2006). Some other studies, however, have indicated that in yeast, trehalose 6-phosphate synthase (Tps1) itself, but not trehalose, may participate in thermotolerance through modulation of glycolysis, or the trehalose pathway itself might be involved through some other metabolic function, including a metabolic flux change (Thevelein and Hohmann, 1995; Gibney et al., 2015).

In case of *Gluconobacter* strains, although there was no information on trehalose accumulation, *G. oxydans* has been reported to intracellularly accumulate mannitol as a compatible solute when the strain is exposed to osmic stress (Zahid et al., 2015). The amount of mannitol is approximately 2.5 μmol/(mg protein) when the microbe is cultivated in the yeast extract-peptone-glycerol (YPG) medium containing 450–600 mM sucrose. In the present study, *G. frateurii* wild-type and mutant strains were cultivated in a 10% (w/v; 549 mM) sorbitol medium, but accumulated only small amounts of trehalose (0.03–0.07 μmol/[mg protein]; Figs. 1.4 and 1.5). Therefore, it is hard to imagine that trehalose that accumulated in the thermotolerant strains works as such a compatible solute for thermotolerance. Actually, disruptants of the trehalose synthesis gene, Wild Δ*otsAB* and Wild-G Δ*otsAB*, were found to grow well at high temperatures, better than the transporter-deficient mutant strains, Wild-G and Wild Δ*steP* (Fig. 1.8), even though no accumulation of trehalose was observed inside the cells (Fig. 1.6).

Thus, we expected that the defect in trehalose synthesis would modify sugar metabolism in *G. frateurii* although this situation is opposite to the case of yeast (Zahid et al., 2015), where Tps1 is required for thermotolerance, and thus deletion of this gene

makes yeast hypersensitive to heat stress. In *G. frateurii*, in contrast to yeast, the PPP may work preferentially because of the defect in the EMP pathway, and no glucose is generated from trehalose because of the defect in trehalase (Fig. 1.9). Such an atypical sugar metabolic pathway in CHM43 seems to represent a unique metabolic flux system; PPP flux is bypassed to the trehalose synthesis and excretion, and the trehalose bypass might mitigate excessive accumulation of energy or of reduced cofactors in the cell. Therefore, it is likely that in *G. frateurii*, the *otsAB* disruption (the Wild Δ*otsAB*) strain alters metabolic flux from trehalose synthesis to PPP directly. The increased PPP flux was actually demonstrated in the mutant strain by means of acetic acid accumulation concomitant with reduced trehalose production (Figs. 1.4, and 1.6), where acetic acid could be produced from pyruvate via pyruvate decarboxylase and then $NADP^+$-dependent aldehyde dehydrogenase (Fig. 1.9). Consequently, NADPH could be produced mainly via the activities of G6PDH and aldehyde dehydrogenase, and NADPH eventually contributed to ROS reduction via NADPH-dependent ROS-scavenging enzymes (Fig. 1.11). Although the *steP* mutants, AD-G, Wild-G, and Wild Δ*steP*, are also expected to acquire (partial) thermotolerance by changing the metabolic flux to the PPP: increasing the metabolic flux via G6P to the PPP, probably because of feedback inhibition of OtsA, with trehalose accumulating inside the cells, as seen in other organisms (Murphy and Wyatt, 1965; Oide and Inui, 2017). In addition, because the *steP* mutants were found to have some defect in sorbose assimilation, sorbitol seems to be directly utilized instead of sorbose in these cells. If this is the case, then some NADPH consumption will be prevented by escaping the reduction step from sorbose to sorbitol (Fig. 1.9), as in mannitol metabolism, where fructose converted from mannitol outside is metabolized directly via the PPP. Thus, the *steP* mutants (including Wild-G) may increase the $NADPH/NADP^+$ ratio by decreasing NADPH utilization, besides increasing the NADPH level via the PPP flux.

Additionally, we found that even Wild Δ*otsAB* (Fig. 1.7) and Wild-G Δ*otsAB* (data not shown) have a defect of sorbose assimilation just as the *steP* mutants do, indicating that similar sorbitol utilization may occur in these strains and may contribute to the increased $NADPH/NADP^+$ ratio. Meanwhile, the findings suggest how the drug transporter works simultaneously in trehalose efflux and in sorbose uptake. The transporter of the Wild Δ*otsAB* strain should be active, but like the transporter-deficient Wild-G and Wild-G Δ*otsAB* strains, the Wild Δ*otsAB* strain does not take up sorbose well, possibly because of the absence of trehalose as the driving force. This notion needs to be examined biochemically or confirmed more carefully in the future.

As described above, ROS could be released mainly by flavoproteins linked to

the respiratory chain. Thus, ROS levels may be increased by a structural change of such redox enzymes via a membrane fluidity change and/or via direct thermal denaturation when strains are grown at higher temperatures. Nevertheless, the level of ROS generation could be lowered in cells producing a higher level of ROS-scavenging enzymes. Accordingly, the level of ROS generation may be low in the Wild-G or Wild Δ*otsAB* strain, which may have a higher ROS-scavenging activity due to higher NADPH production.

Therefore, this study indicates that a metabolic change due to the defect in the transporter inside the cells of *G. frateurii* CHM43, including the accumulation of trehalose and the fluctuation between sorbose and sorbitol utilization, causes the thermotolerant phenotype by reduction of ROS via increased generation of NADPH.

CHAPTER 2

In vitro thermal adaptation of mesophilic *Acetobacter pasteurianus* NBRC 3283 generates thermotolerant strains with evolutionary trade-offs

ABSTRACT

Thermotolerant strains are critical for low-cost high temperature fermentation. In this study, we carried out the thermal adaptation of *A. pasteurianus* IFO 3283-32 under acetic acid fermentation conditions using an experimental evolution approach from 37ºC to 40ºC. The adapted strain exhibited an increased growth and acetic acid fermentation ability at high temperatures, however, with the trade-off response of the opposite phenotype at low temperatures. Genome analysis followed by PCR sequencing showed that the most adapted strain had 11 mutations, a single 64-kb large deletion, and a single plasmid loss. Comparative phenotypic analysis showed that at least the large deletion (containing many ribosomal RNAs and tRNAs genes) and a mutation of DNA polymerase (one of the 11 mutations) critically contributed to this thermotolerance. The relationship between the phenotypic changes and the gene mutations are discussed, comparing with another thermally adapted *A. pasteurianus* strains obtained previously.

2.1 INTRODUCTION

The industrial fermentation of microorganisms involves heat stress, whereby mechanical and fermentation heat is generated in large-scale fermentors. Additionally, the natural atmospheric temperature is currently on the rise as a result of global warming. Therefore, a stricter control of temperatures using cooling systems is needed to carry out stable fermentation reactions. However, thermotolerant microorganisms have the potential to spare the industry these cooling and energy costs, and could be used for stable fermentation at high temperatures with less, or even without, temperature control (Matsushita et al., 2016; Hattori et al, 2012). Experimental evolution is one of the methods used to obtain more thermotolerant microorganisms. Thermal adaptation has been previously performed using various microorganisms, including *Escherichia coli* (Rudolph et al., 2010; Tenaillon et al, 2012), *Saccharomyces cerevisiae* (Caspeta et al., 2015), *Acetobacter pasteurianus* (Azuma et al., 2009; Matsutani et al, 2013), and *Gluconobacter frateurii* (Hattori et al, 2012; CHAPTER 1). Furthermore, the analysis of

the thermotolerant mechanism has also been performed using these strains.

Acetic acid bacteria (AAB) are Gram-negative strictly aerobic bacteria and are known to have the ability to oxidize ethanol, sugars, or sugar alcohols to produce the corresponding acids and ketones. They are also characterized by their ability to ferment acetic acid, whereby a high concentration of acetic acid is produced from ethanol by aerobic respiration, in a reaction consisting of two membrane-bound enzymes, alcohol and aldehyde dehydrogenases, and terminal oxidases (Yakushi and Matushita, 2010). AAB undergo diauxic growth during acetic acid fermentation (Kanchanarach et al., 2010); the first growth stage is comprised by an ethanol oxidation step (acetic acid-producing phase), and is followed by a period similar to a stationary phase (acetic acid-resistant phase). Finally, the second growth stage occurs by assimilating the acetic acid (acetic acid overoxidation phase) that is unfavorable for industrial vinegar fermentation. Currently, industrial acetic acid fermentation is carried out in fermentation tanks, with a culture temperature that is maintained at around 25–30ºC via a cooling system. This protects the cell growth and acetic acid from the heat generated by fermentation. Therefore, thermotolerant AAB could be useful for a simultaneously stable and cost-effective fermentation by sparing any cooling expenses.

Previously, the thermal adaptation of *A. pasteurianus* has been performed using two different strains: *Acetobacter pasteurianus* NBRC 3283 (Azuma et al., 2009) and *Acetobacter pasteurianus* SKU1108 (Matsutani et al., 2013). The former is a mesophilic but relatively thermotolerant stain that was isolated in Japan, while the latter is a thermotolerant strain isolated in Thailand. Adaptation was first carried out with *A. pasteurianus* IFO 3283-01, one of the derivatives of NBRC 3283, on YPGD medium without ethanol. Consequently, an adapted strain (3283-01/42C strain) able to grow at 42ºC under non-fermentation (YPGD medium) condition was acquired (Azuma et al., 2009), but the adapted strain could not ferment well at temperatures over 37ºC. A similar high-temperature adaptation was carried out using *A. pasteurianus* SKU1108 under the acetic acid fermentation conditions on YPGD medium with 4% (v/v) ethanol. As a result, two thermotolerant strains, TI and TH-3, were independently obtained. The TH-3 strain was able to successfully carry out acetic acid fermentation at 40ºC (Matsutani et al., 2013). In this study, the thermal adaptation of *A. pasteurianus* IFO 3283-32, a derivative of NBRC 3283, was conducted under acetic acid fermentation conditions. The adapted strain thus obtained had a total 12 mutations including a 64-kbp deletion, and exhibited a higher growth and fermentation ability at 40ºC while did a decreased ability at lower temperatures. This phenotypic change of the adapted strain is discussed by comparing several different thermally-adapted strains obtained in previous studies.

2.2 MATERIALS AND METHODS

2.2.1 Bacterial strains and culture conditions

A. pasteurianus IFO 3283-32, a derivative of *A. pasteurianus* NBRC 3283 (Azuma et al., 2009), was used for thermal adaptation. Six thermally-adapted strains (NM-1 to NM-6) were obtained and used in this study. The thermally-adapted strains 3283-01/42C obtained from *A. pasteurianus* IFO 3283-01 (Azuma et al., 2009) and TH-3 obtained from a thermotolerant *A. pasteurianus* SKU1108 (Matsutani et al., 2013) were also used for comparison with the strains obtained in this study.

The strains were first inoculated in potato medium (20 g of glycerol, 5 g of glucose, 10 g of yeast extract (Oriental Yeast, Tokyo, Japan), 10 g of polypepton (Nihon Pharmaceuticals Co. Ltd., Osaka, Japan), and 100 mL of potato extract (Matsushita et al., 1982) per 1 L distilled water) on plates from glycerol stock, then incubated at either 30ºC or 37ºC (for adapted strains) for 2–3 days. The resulting colonies were inoculated into 5 mL of potato medium and cultivated at 30ºC and 120 rpm for 12–24 hours. The seed-culture was then transferred to 5 mL of fresh potato medium and cultivated at same conditions until a turbidity of 150 Klett units, to be used as a pre-culture. The main culture was carried out by inoculating 5 mL of the pre-culture into 100 mL of YPGD medium (5 g of yeast extract, 5 g of polypepton, 5 g of glycerol, and 5 g of D-glucose per 1 L distilled water) containing 4% (v/v) ethanol (YPGDE medium) at various temperatures with shaking at 200 rpm. The bacterial growth was measured with Klett-Summerson photoelectric colorimeter. Acidity of culture medium at several growth phases was measured by alkali-titration with 1 mL of culture and 0.8 N NaOH using 10 µL of 0.025% phenolphthalein (tansition pH range: 8.3-10.0) as a pH indicator.

2.2.2 Thermal adaptation

The thermal adaptation of *A. pasteurianus* IFO 3283-32 (growth-limiting temperature of 37ºC) was conducted by repeating passages of the culture at exponential phase under growth-limiting temperatures. Repetitive cultivations were carried out by 5% inoculation once the previous culture had reached the early log phase (acidity 1.0 to 1.5% [w/v]). After the growth rate of each culture had increased and stabilized, the cultivating solution of the final culture was spread onto a potato agar plate. The plate was incubated at the indicated temperature, where the respective adaptation was carried out, to obtain single colonies. The growth of the colonies obtained were compared at the respective high temperatures to a liquid culture in YPGDE medium. The fastest growing strain was then selected as the adapted strain and was used for the subsequent adaptation steps.

2.2.3 Genome sequencing of *A. pasteurianus* NM-6

Chromosomal DNA was isolated from NM-6 cells grown on 5 mL of potato medium at 30ºC for 24 h. After harvesting the cells, chromosomal DNA was isolated using the DNeasy Blood & Tissue Kit (Qiagen, Tokyo, Japan), following the manufacturer's instructions. The DNA concentration was measured and adjusted by Nanodrop (Nanodrop Technologies, Wilmington, DE) before further use.

The draft genome sequence of the NM-6 strain was sequenced using the next-generation sequencing (NGS) platform Illumina Hiseq 2000 (Hokkaido System Science Co., Ltd., Hokkaido, Japan). The sequence data were assembled using Velvet 1.2.08 (Zerbino and Birney, 2008) with 484× genome coverage, resulting in a final assembly of 3,044,391 bp with 52.79% G+C content and a N_{50} length of 78,750 bp. The draft genome sequence of NM-6 contained 241 contigs including, 145 large contigs (>1,000 bp), generating 8,093,642 paired-end reads. The resulting draft genome assembly was used to construct the genome map.

2.2.4 Sequence retrieval of wild type strain and mapping analysis of NM-6 strain

The previously published genome sequences of *A. pasteurianus* IFO 3283-32 (GenBank accession numbers: NC_017102, NC_017103, NC_017111, NC_017112, NC_017134, NC_017135, and NC_017149) (Azuma et al., 2009) were used as the reference sequences for our genome mapping analysis. The Illumina sequence reads of NM-6 were mapped to the reference sequences using Bowtie2 and BWA with default parameters (Li and Durbin, 2009; Langmead et al., 2009). All single nucleotide polymorphisms (SNPs) and indels were detected using SAMtools (ver. 0.1.18) (Ramirez-Gonzalez et al., 2012) and Genome Analysis Toolkit (GATK) (McKenna et al., 2010; DePristo et al., 2011). To confirm the nucleotide mutations detected in the adapted strain, PCR was performed using the genomic DNA of the wild type and the adapted strain as a template. The PCR products were purified using a MagExractor kit (Toyobo, Tokyo, Japan), then directly sequenced using a capillary sequencer using a BigDye® Terminator Cycle sequencing kit (Applied Biosystems, USA).

2.2.5 Intracellular reactive oxygen species (ROS) measurement

Cells were grown on YPGDE medium containing 2 μM H_2DCFDA as the fluorescence probe at 37ºC. The growth temperature was then increased to 39ºC after incubating for 11 h. After a further 0 (11 h), 13 (24 h), and 24 (35 h) hours, the cells were harvested by centrifuging 1 mL of culture at 9000 rpm for 5 min at 4ºC. The resulting

pellet was washed twice with 50 mM potassium phosphate buffer (pH 6.5) before resuspending in 200 μL of the same buffer, followed by sonication. After a second round of centrifugation (12000 rpm, 5 min, 4ºC), the fluorescence of the supernatant was measured. The ROS levels were determined by measuring the fluorescence intensity with excitation at 504 nm and emission at 524 nm at a temperature of 25ºC. The fluorescence intensity was normalized against the protein concentration. The protein contents were measured using the Lowry method with some modifications (Dulley and Grieve, 1975).

2.3 RESULTS

2.3.1 Adaptation of *A. pasteurianus* to high temperature acetic acid fermentation

A thermally-adapted strain (01/42C) previously obtained (Azuma et al., 2009) did not ferment well at temperatures over 37ºC, despite of growing well at 42ºC under non-fermentation (YPGD medium) conditions (Fig. 2.1 and Fig. 2.5(a)). In this study, to obtain a strain able to produce acetic acid at higher temperatures, *A. pasteurianus* IFO 3283-32 was adapted at the growth-limiting high temperatures in flask culture with YPGDE medium (acetic acid fermentation conditions). Due to the stable characteristics of IFO 3283-32 under acetic acid fermentation conditions, wherein the acetic acid is barely overoxidized, this strain was selected for adaptation instead of IFO 3283-01.

The thermal adaptation procedure was carried out by gradually increasing the cultivation temperature from 37ºC to 40ºC. The cultivation was first repeated at 37ºC by inoculating each preculture from the early log phase (acidity 1.0 to 1.5% [w/v]) into the subsequent batch. The first culture exhibited some lag time before entering a rapid growth phase. After repeating the cultivation 7 times, at which point the culture had virtually no lag time, the culture was spread onto agar plates to obtain single colonies. The growth of several colonies was compared in YPGDE liquid medium, whereby the fastest-growing strain, NM-1, was selected as an adapted strain to 37ºC. This strain was used for the subsequent adaptation step at 38ºC. The same thermal adaptation culturing was repeated at 38.5ºC, 39ºC, 39.5ºC, and 40ºC (Fig. 2.2(a)). Fig. 1B and C show an example of the final thermal adaptation of NM-5 carried out at 40ºC. It used to be observed for the growth of the second cultivation to be much slower than that of the first batch, resulting in a lower production rate of acetic acid. However, the growth and acetic acid production rate were found to gradually increase after repeated cultivations. The last culture after 14 passages was plated, from which the fastest-growing colony was isolated, and denoted NM-6. Overall, each of the six adapted strains (NM-1 to NM-6) were obtained step-by-step at each adaptation process from 37ºC to 40ºC, respectively (Fig. 2.2(a)).

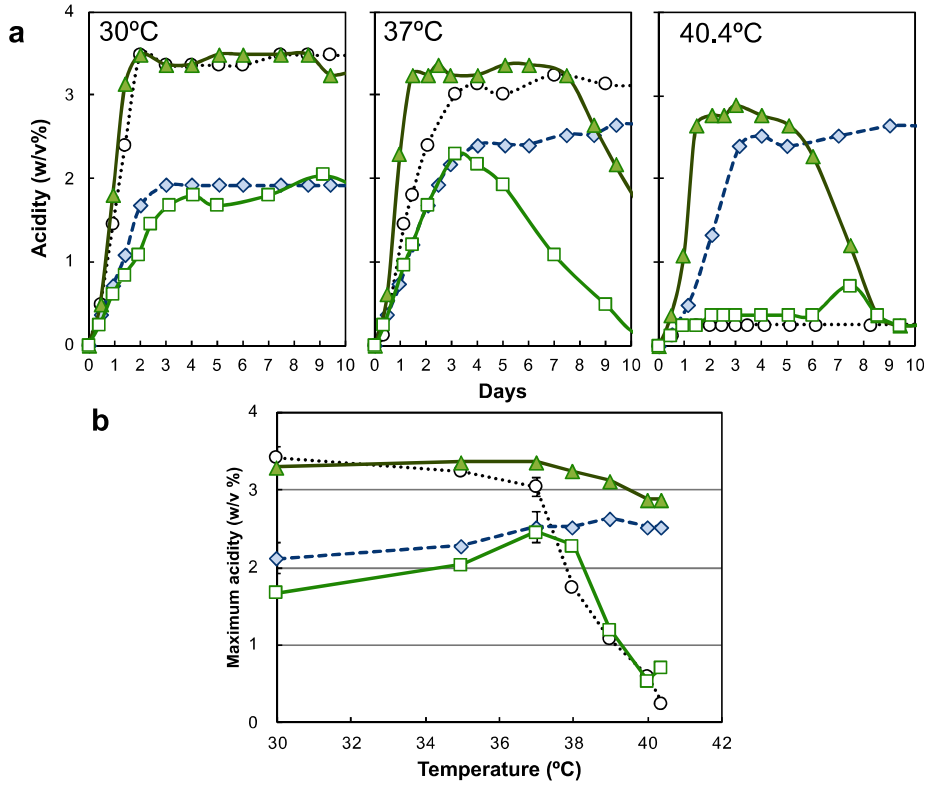

Fig. 2.1. Comparison of growth and maximum acidity at 30. 37, and 40.4°C among *A. pasteurianus* IFO3283-32, NM-6, 01/42C and TH-3 strains. IFO 3283-32 (○), NM-6 (◆), 3283-01/42C (□) and TH-3 (▲) were pre-cultured in potato medium until its turbidity reached to 150 Klett unit. 5 mL of the pre-culture was transferred to 100 mL YPGD with 4% (v/v) ethanol in 500-mL Erlenmeyer flask, and cultured at 30, 37 and 40.4˚C at 200 rpm. (a) Acidity during the growth of each strains is shown. (b) The maximum acidity of each strain at 30, 37, and 40.4°C is shown.

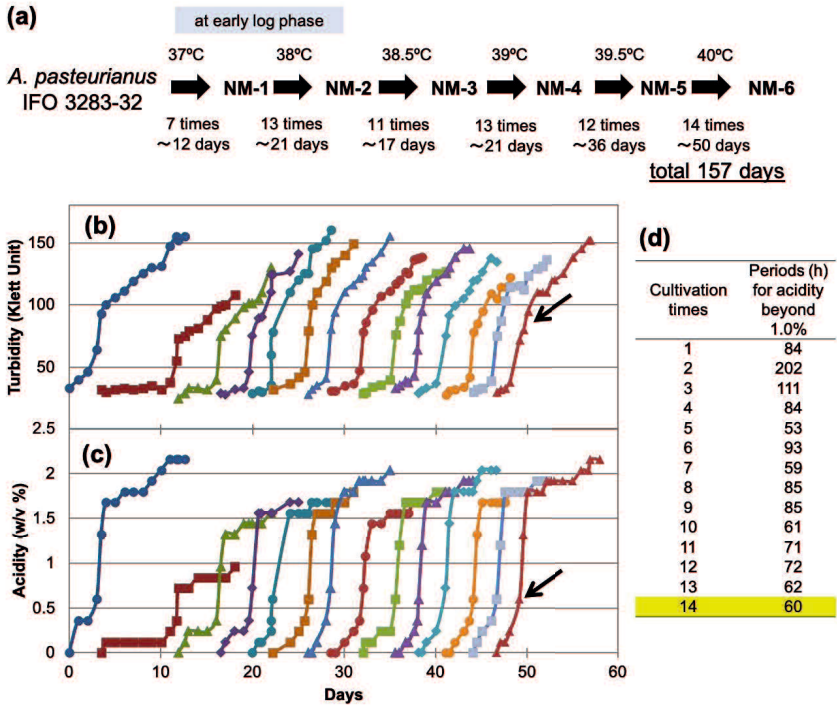

Fig. 2.2. Adaptation process to have 6 adapted strains, NM-1 to NM-6, from *Acetobacter pasuteurianus* IFO 3283-32. (a) Adaptation process of NM strains. (b) (c)Thermal adaptation process of NM-5 strain at 40ºC. NM-5 strain was cultivated in YPGDE (4%) repeatedly total 14 times. The growth (b) and acidity (c) of each culture were monitored. When its acidity reached to 1.0% (w/v), of which the timing is shown in (d), the culture was transferred to a fresh medium. Arrows indicate an isolation point where the culture was spread on potato agar plate to isolate NM-6 strain.

2.3.2 Characterization of the adapted strains

In order to characterize the adapted strains, the growth of these strains was compared at various temperatures under acetic acid fermentation conditions (Fig. 2.3). At 30ºC, the NM strains showed strikingly low turbidity and acetic acid productivity compared with the parental strain IFO 3283-32. The maximum acidity of IFO 3283-32 was 3.5% (w/v), while that of the NM strains did not even reach 3% (w/v). Of the NM strains, NM-1 exhibited a slightly higher growth and acidity than the other NM strains at 30ºC. On the other hand, at 37ºC, the acetic acid production of the parent strain decreased compared to production at 30ºC, while all the NM strains showed increased levels of acetic acid production. Although the turbidity and maximum acidity of IFO 3283-32 were a slightly higher than the other strains at 37ºC, after increasing the temperature to 40.4ºC, the parental strain was unable to grow, while all the NM strains grew well. Nevertheless,

the growth level was different from strain to strain. NM-1 and NM-2 grew after a lag time of 5 days. NM-3 and NM-4 grew after a lag time of 4 and 2 days, respectively. NM-5 and NM-6 grew without a lag time and showed a higher turbidity than the other strains. It should be noted that the growth of these last two strains was similar, however, the acidity of NM-6 was higher than that of NM-5.

Fig. 2.4 summarizes the comparison of maximum acidity, defined as the highest acidity within 3 days, among the IFO 3283-32 and NM strains. The maximum acidity of the parental strain decreased sharply at temperatures over 37ºC, while that of the NM strains either gradually increased or decreased slightly at higher temperatures (Fig. 2.4(a)). The highest maximum acidity of all the NM strains was obtained at 37ºC or over. The maximum acidity at 30ºC was decreased, in order, from the parental strain to NM-6 (Fig. 2.4(b)), while that over 40ºC was increased in the opposite order. These results suggested that optimum temperature for acetic acid fermentation was increased to a higher temperature in the NM strains and consequently, the NM strains acquire the fermentation ability at higher temperature.

In order to confirm whether the thermotolerance of the adapted strains is dependent on the fermentation condition or not, the growth of the parental strain and the NM strains was compared on YPGD and YPGDE (containing 4% [v/v] ethanol) agar plates. The NM strains grew on both YPGD and YPGDE media up to 40ºC, whereas the parental IFO 3283-32 strain failed to grow at this temperature (Fig. 2.5(a, b)). On the YPGDE agar plate (Fig. 2.5(b)), IFO 3283-32 grew poorly at 30ºC and 37ºC compared with YPGD medium. This result is at a contrast to those obtained for the NM strains, which were found to grow on both the YPGDE and YPGD media in a similar manner. These results suggest that the NM strains acquired thermotolerance independent of the fermentation conditions during the course of adaptation.

It has been previously shown that the generation of ROS is increased when microbes are grown at high temperatures (CHAPTER 1; Davidson et al., 1996; Chang et al., 2017; Nantapong et al., 2019). In order to investigate the relationship between thermotolerance and ROS generation in NM-6 strain, the intracellular ROS levels were compared among the parental and NM-6 strains. The strains were first cultivated for 11 h at 37ºC, after which the growth temperature was increased to 39ºC (Figure 2.6). The ROS levels of NM-6 were lower than those of IFO 3283-32, even at 37ºC (11 h). After increasing the temperature to 39ºC, the ROS levels increased in both strains, however, NM-6 showed lower ROS levels than IFO 3283-32 in all growth phases.

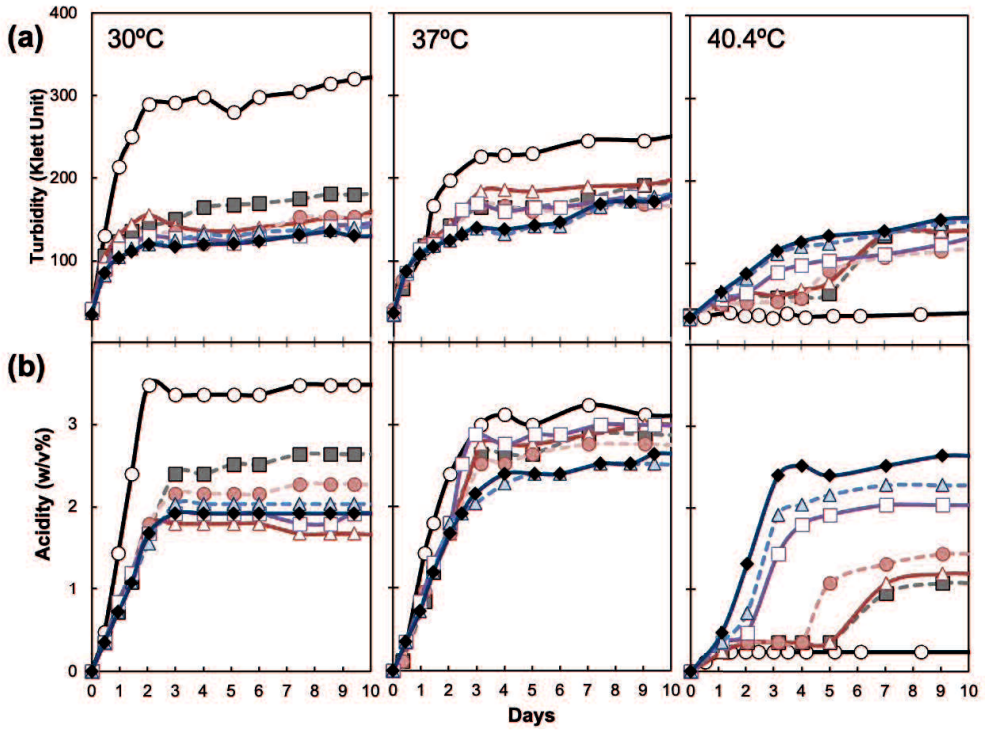

Fig. 2.3. Comparison of acetic acid fermentation among parental and adapted strains at 30, 37 and 40.4ºC. IFO 3283-32 and NM strains were pre-cultured in potato medium until its turbidity reached to 150 Klett unit. 5 mL of the pre-culture was transferred to 100 mL YPGD medium with 4% (v/v) ethanol in 500-mL Erlenmeyer flask, and cultured at 30, 37 and 40.4ºC at 200 rpm. The growth (a) and acidity (b) of the parent (○), NM-1 (■), NM-2 (△), NM-3 (●), NM-4 (□), NM-5 (▲), and NM-6 (◆).

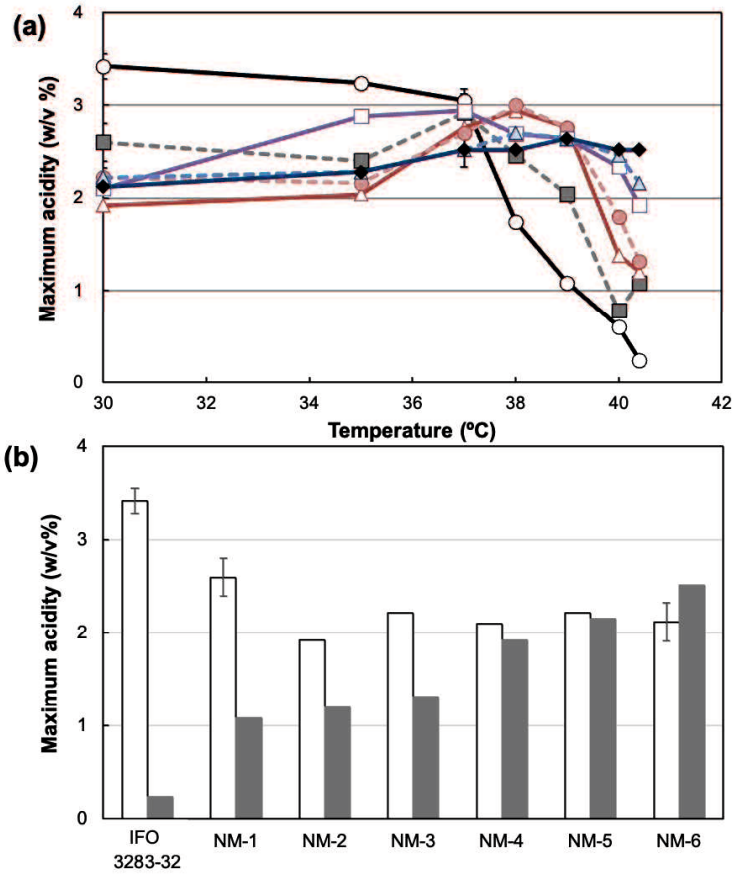

Fig. 2.4. Relation between maximum acidity and growth temperatures among parental and adapted strains. (a) The maximum acidity, defined as the highest acidity within 3 days, of the parent (○), NM-1 (■), NM-2 (△), NM-3 (●), NM-4 (□), NM-5 (▲), and NM-6 (◆) were determined at different temperatures. (b) Comparison of the maximum acidity of each strain determined at 30 (white column) and 40.4°C (grey column). Vertical error bars show SD calculated at least three independent experiment.

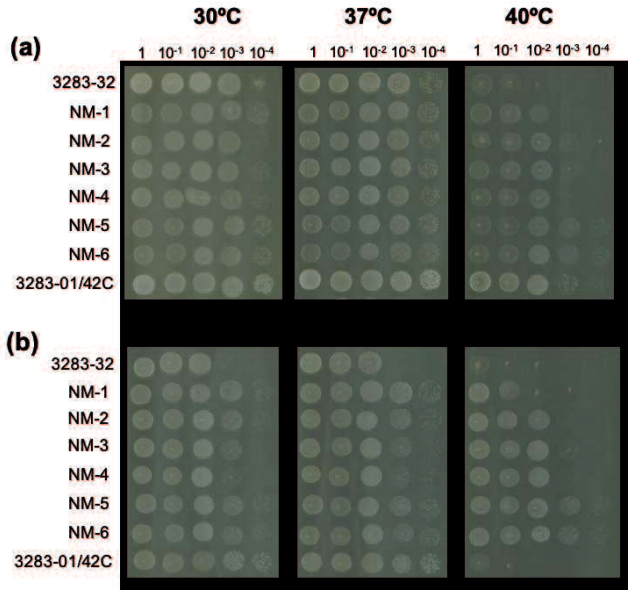

Fig. 2.5. Comparison of plate-culture growth of each strain at 30, 37, and 40°C. *A. pasteurianus* IFO 3283-32 and the adapted NM-1 to NM-6 strains were diluted with 0.85% (w/v) NaCl and spotted on YPGD (a) and YPGDE containing 4% (v/v) ethanol (b) media solidified with 1.5% (w/v) agar to be incubated for 48 h. 3283-01/42C strain was also dotted for the comparison.

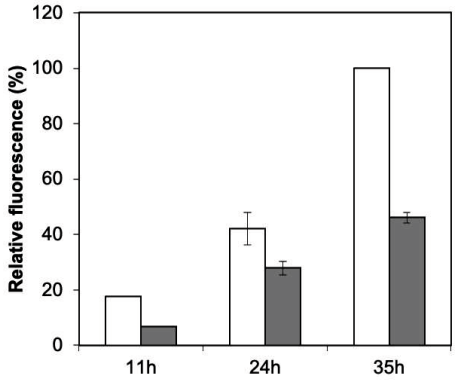

Fig. 2.6. Comparison of ROS levels between *A. pasteurianus* IFO 3283-32 and NM-6 strains. IFO 3283-32 and NM-6 were pre-cultured in potato medium until its turbidity reached to 150 Klett unit. 5 mL of the pre-culture was transferred to 100 mL YPGD with 4% (v/v) ethanol containing 2 μM H_2DCFDA in 500-mL Erlenmeyer flask, and cultured at 37ºC at 200 rpm. Growth temperature was shifted to 39ºC after incubation for 11 h. The fluorescent intensity of IFO 3283-32 (white column) and NM-6 (grey column) strains was measured at 11h (before shifting), 24h, and 35h. Vertical error bars show SD calculated at least three independent experiment.

2.3.3 Genome-wide analysis of thermally-adapted strains

Since *A. pasteurianus* was previously demonstrated to be genetically unstable via genome analysis (Azuma et al., 2009), we postulated that this was the result of SNPs or transposon insertions occurring during short-term thermal adaptation. Therefore, in order to identify the sites of mutations during thermal adaptation, the genome of NM-6 was analyzed using genome mapping for comparison against the genome of the IFO 3283-32 strain. As a result, 19 nucleotide substitutions and 2 plasmid deletions were detected in the NM-6 strain (Table 2.1). The mutation sites in NM-6 were confirmed using PCR sequencing, with the exception of two intergenic regions, which were not read by PCR. In the confirmed 17 mutation sites, 10 mutations were single nucleotide substitutions, three were indels (3-bp insertion, 1-bp deletion, and a large deletion), and four were transposon insertions (Tn). The large deletion was 64-kb long (2.2% of the whole genome size) and contained the genes for APA32-14210 to APA32-14740. This region largely overlapped with the large deletion region previously found in the 3283-01/42C thermally-adapted strain (Azuma et al., 2009) (Table 2.2). In order to determine when the mutations occurred at each adaptation step, all the mutation sites detected in NM-6 were examined by PCR sequencing against other NM strains and the parental strain. The results showed that, of the mutations occurring in NM-6, 5 mutations (3 Tn and 2 nucleotide substitutions) and 1 plasmid (NC_017102) deletion were found in the IFO 3283-32 strain used in this study (Table 2.3). Thus, it was estimated that a total 13 genomic changes, 11 mutations (8 nucleotide substitutions, 2 indels, and 1 Tn), 64-kbp genome deletion, and 1 plasmid lost, occurred in the strain NM-6, obtained after the thermal adaptation of the parental IFO 3283-32 strain. Of these NM-6 mutations (13 items), 1, 4, 6, 7, and 10 mutations were found in NM-1 to NM-5, respectively, as well as a single plasmid deletion in NM-3 to NM-5 (Table 2.3).

NM-1 showed clear phenotypic differences from IFO 3283-32 (the parental strain used in this study), i.e. the growth and acetic acid productivity of NM-1 was lower than that of IFO 3283-32 at under 37ºC (Fig. 2.3), and the growth-limiting temperature of NM-1 was higher than that of IFO 3283-32 (Fig. 2.4). Since the only mutation in NM-1 was a single large deletion in the genome, this mutation may account for the increased acetic acid productivity at over 40ºC and the decreased productivity at under 37ºC. This large deletion region contained 54 genes, some of which may play important roles in thermotolerance, as will be discussed later.

The NM-2 strain had 3 mutations, including three nucleotide substitutions. As described above, the growth rate of NM-2 was lower than that of NM-1 at 30ºC (Fig. 2.3), whereas the growth limiting temperature was slightly higher than that of NM-1 (Fig. 2.4).

Therefore, some of these mutations could be related to thermotolerance in NM-2.

Although there were two mutations and a 1.8-kb plasmid (NC_017112) deletion in NM-3, these may not be related to thermotolerance as the maximum acidity and growth temperature (Fig. 2.4) did not vary greatly between NM-2 and NM-3. On the other hand, the DNA polymerase III subunit alpha, a mutation found in NM-4, may be responsible for the thermotolerance of NM-4, as this strain showed clearly higher acetic acid productivity than NM-3 at 40.4ºC (Fig. 2.3). Although a further 3 mutations were found in NM-5, there was only a slight difference in the thermotolerance between NM-4 and NM-5 (Fig. 2.3 and 2.4). Meanwhile, NM-6 exhibited a higher acetic acid productivity at 40.4ºC than NM-5 (Fig. 2.3 and 2.4). Therefore, either of the two mutations, alanyl-tRNA synthetase or murein transglycosylase, found in NM-6 may contribute thermotolerance.

Table 2.1. Mutation in NM-6.

					in silico prediction form NGA data		in vitro experiment	
product	orf number	Ref. length	CHROM	POS	REF	ALT	validated mutation	mutational pattern
glutamate synthase small subunit	APA32_14740	2904642	NC_017111	1583812-1583823	TT	TTTCCGCGTT	64kb large gap	large deletion
(intergenic region)	-	2904642	NC_017111	637436	G	A	G->A	-
glycerol kinase	APA32_12550	2904642	NC_017111	1314447	TATA	TATAATA	ATA->ATAATA	342L
tRNA delta(2)-isopentenylpyrophosphate transferase	APA32_19280	2904642	NC_017111	2101588	C	A	C->A	E325*
transcriptional regulator LysR	APA32_21040	2904642	NC_017111	2288819-2288822	A	AGTGCTA	transposon	282 (split)
transcriptional regulator TraR/DksA	APA32_25740	2904642	NC_017111	2784137	G	T	G->T	R67L
DNA polymerase III subunit alpha	APA32_19490	2904642	NC_017111	2126361	A	T	A->T	L278Q
hypothetical protein	APA32_01670	2904642	NC_017111	185772	C	T	C->T	P115S
30S ribosomal protein S6	APA32_09930	2904642	NC_017111	1039762	G	A	G->A	G108D
D-methionine transporter substrate-binding periplasmic protein	APA32_21920	2904642	NC_017111	2382964	TA	T	TA->T	112 (split)
alanyl-tRNA synthetase	APA32_07840	2904642	NC_017111	817203	G	A	G->A	A710V
murein transglycosylase	APA32_23030	2904642	NC_017111	2498006	G	A	G->A	P119S
(intergenic region)	-	2904642	NC_017111	594115	C	G		-
(intergenic region)	-	182940	NC_017149	83013-83021	T	A		-
transcriptional regulator	APA32_03030	2904642	NC_017111	315925	TA	TACA	transposon	158 (split)
(intergenic region)	-	2904642	NC_017111	1097243-1097248	G	GCACTAC	transposon	-
glycerol kinase	APA32_12550	2904642	NC_017111	1315060	C	G	C->G	A138P
aspartate:alanine antiporter	APA32_15500	2904642	NC_017111	1672667	C	T	C->T	G333D
(intergenic region)	-	191443	NC_017134	596-606	T	A	transposon	-
plasmid	pAPA32_040	3204	NC_017102	plasmid deletion			plasmid deletion	
plasmid	pAPA32_060	1815	NC_017112	plasmid deletion			plasmid deletion	

Table 2.2. List of deletion genes.

Location	Length	Synonym	Product	Deletion NM strain	Deletion 01/42 C
1456325..		APA32_			
1457194	289	13760	TonB-dependent receptor	-	+
1457534..		APA32_			
1458889	451	13770	transporter	-	+
1458955..		APA32_			
1460391	478	13780	hypothetical protein	-	+
1460651..		APA32_			
1462036	461	13790	transposase	-	+
1462555..		APA32_			
1463382	275	13800	D-galactonate transporter	-	+
1463426..		APA32_			
1464865	479	13810	transposase	-	+
1465031..		APA32_			
1465591	186	13820	D-galactonate transporter	-	+
1465746..		APA32_			
1466654	302	13830	transcriptional regulator LysR	-	+
1466782..		APA32_			
1468569	595	13840	dihydroxy-acid dehydratase	-	+
1468622..		APA32_			
1469446	274	13850	2,4-dihydroxyhept-2-ene-1,7-dioic acid aldolase	-	+
1469676..		APA32_			
1470125	149	13860	N-acyl-D-glutamate deacylase	-	+
1470160..		APA32_			
1471134	324	13870	transposase	-	+
1471068..		APA32_			
1472582	504	13880	N-acyl-D-glutamate deacylase	-	+
1472588..		APA32_			
1473484	298	13890	transcriptional regulator LysR	-	+
1473649..		APA32_			
1474806	385	13900	alcohol dehydrogenase iron-containing	-	+
1474852..		APA32_			
1476213	453	13910	sugar transporter	-	+
1476240..		APA32_			
1477733	497	13920	aldehyde/methylmalonate-semialdehyde dehydrogenase	-	+
1478038..		APA32_	nitrate/sulfonate/bicarbonate transporter substrate-binding		
1479030	330	13930	periplasmic protein	-	+
1479051..		APA32_			
1480013	320	13940	nitrate/sulfonate/bicarbonate transporter permease protein	-	+
1480013..		APA32_	nitrate/sulfonate/bicarbonate transporter ATP-binding		
1480927	304	13950	protein	-	+
1480939..		APA32_			
1481418	159	13960	transcriptional regulator CopG	-	+
1481460..		APA32_			
1482263	267	13970	hypothetical protein	-	+
1482280..		APA32_			
1482924	214	13980	hypothetical protein	-	+
1482943..		APA32_			
1486482	1179	13990	urea amidolyase	-	+
1486488..		APA32_			
1488323	611	14000	amidase	-	+
1488559..		APA32_			
1489503	314	14010	arylesterase	-	+
1489808..		APA32_			
1495834	2008	14020	DNA helicase	-	+
1496173..		APA32_			
1497324	383	14030	acyl-CoA dehydrogenase	-	+
1497515..		APA32_			
1499149	544	14040	outer membrane protein	-	+

1499410..		APA32_			
1500732	440	14050	transposase	-	+
1500749..		APA32_			
1501492	247	14060	outer membrane protein	-	+
1501652..		APA32_			
1501954	100	14070	heme oxygenase	-	+
1501969..		APA32_			
1503219	416	14080	transposase	-	+
1503399..		APA32_			
1503845	148	14090	transposase	-	+
1504209..		APA32_			
1505513	434	14100	sugar transporter	-	+
1505963..		APA32_			
1507309	448	14110	monooxygenase	-	+
1507342..		APA32_			
1509615	757	14120	outer membrane siderophore receptor	-	+
1509738..		APA32_			
1510277	179	14130	flavin mononucleotide (FMN) reductase	-	+
1510284..		APA32_			
1511774	496	14140	sugar transporter	-	+
1511780..		APA32_			
1513228	482	14150	hypothetical protein	-	+
1513236..		APA32_			
1514399	387	14160	alkanesulfonate monooxygenase	-	+
1514402..		APA32_			
1515832	476	14170	monooxygenase	-	+
1515829..		APA32_			
1517109	426	14180	acyl-CoA dehydrogenase	-	+
1517535..		APA32_			
1518083	182	14190	acyl-CoA dehydrogenase	-	+
1518080..		APA32_			
1518700	206	14200	nitroreductase	-	+
1519658..		APA32_			
1520701	347	14210	transposase	+	+
1520680..		APA32_			
1521096	138	14220	transposase	+	+
1521169..		APA32_			
1521261	30	14230	type I DNA methyltransferase M subunit	+	+
1521728..		APA32_			
1523113	461	14240	transposase	+	+
1523493..		APA32_			
1524077	194	14250	type I DNA specificity S subunit	+	+
1524107..		APA32_			
1525906	599	14260	type I/III endonuclease/restriction R subunit	+	+
1526049..		APA32_			
1527434	461	14270	transposase	+	+
1527537..		APA32_			
1529072	511	14280	type I endonuclease/restriction R subunit	+	+
1529075..		APA32_			
1529812	245	14290	metal-dependent hydrolase	+	+
1530008..		APA32_			
1531318	436	14300	hypothetical protein	+	+
1531360..		APA32_			
1531797	145	14310	hypothetical protein	+	+
1531794..		APA32_			
1532141	115	14320	transposase	+	+
1532207..		APA32_			
1533157	316	14330	transposase	+	+
1533161..		APA32_			
1534600	479	14340	transposase	+	+
1535142..		APA32_			
1535969	275	14350	transposase	+	+

1535966..		APA32_			
1536229	87	14360	transposase	+	+
1536390..		APA32_			
1536466	77	14370	Met tRNA	+	+
1536520..		APA32_			
1536638	119	14380	5S ribosomal RNA of rrnE operon	+	+
1536866..		APA32_			
1539475	2610	14390	23S ribosomal RNA of rrnE operon	+	+
1539820..		APA32_			
1539895	76	14400	Ala tRNA	+	+
1539920..		APA32_			
1539996	77	14410	Ile tRNA	+	+
1540233..		APA32_			
1541672	1440	14420	16S ribosomal RNA of rrnE operon	+	+
1542062..		APA32_			
1544575	837	14430	excinuclease UvrABC subunit A UvrA	+	+
1544697..		APA32_			
1545953	418	14440	C4-dicarboxylate transporter	+	+
1546126..		APA32_			
1546767	213	14450	thiopurine S-methyltransferase	+	+
1546892..		APA32_			
1547536	214	14460	glutaredoxin	+	+
1548054..		APA32_			
1549583	509	14470	alpha-ketoglutarate transporter	+	+
1549685..		APA32_	cobalamin(vitamin B12) biosynthesis protein cobalt-		
1550758	357	14480	precorrin-6A biosynthesis protein CbiD	+	-
1550763..		APA32_			
1551521	252	14490	precorrin-4 C(11)-methyltransferase	+	-
1551522..		APA32_			
1551896	124	14500	cobalamin(vitamin B12) biosynthesis protein CbiG	+	-
1551893..		APA32_	cobalamin(vitamin B12) biosynthesis protein Precorrin-6Y		
1553137	414	14510	C5,15-methyltransferase	+	-
1553226..		APA32_			
1554029	267	14520	precorrin 6x reductase	+	-
1553999..		APA32_			
1554757	252	14530	precorrin-3B C(17)-methyltransferase	+	-
1554754..		APA32_			
1555479	241	14540	precorrin-2 C(20)-methyltransferase	+	-
1555480..		APA32_	cobalamin(vitamin B12) biosynthesis protein Precorrin-8X		
1556109	209	14550	methylmutase CobH	+	-
1556096..		APA32_	cobalamin(vitamin B12) biosynthesis protein Precorrin-3B		
1557328	410	14560	biosynthesis protein CobG	+	-
1557498..		APA32_			
1558037	179	14570	hypothetical protein	+	-
1558079..		APA32_			
1559527	482	14580	fumarate hydratase	+	-
1559856..		APA32_			
1561790	644	14590	hypothetical protein	+	-
1561797..		APA32_			
1562765	322	14600	transcriptional regulator Fis	+	-
1562891..		APA32_			
1563784	297	14610	hypothetical protein	+	-
1563872..		APA32_			
1566328	818	14620	glucose dehydrogenase	+	-
1566669..		APA32_			
1568165	498	14630	hypothetical protein	+	-
1568616..		APA32_			
1569959	447	14640	Na+/H+ antiporter	+	-
1570052..		APA32_			
1571503	483	14650	hypothetical protein	+	-
1571500..		APA32_			
1571847	115	14660	hypothetical protein	+	-

1572420..		APA32_			
1572797	125	14670	hypothetical protein	+	-
1572871..		APA32_			
1573953	360	14680	transporter	+	-
1573953..		APA32_			
1575827	624	14690	hypothetical protein	+	-
1575927..		APA32_			
1577129	400	14700	acetate kinase	+	-
1577160..		APA32_			
1578176	338	14710	phosphate acetyl/butaryl transferase	+	-
1578185..		APA32_			
1579195	336	14720	dihydroorotate dehydrogenase	+	-
1579213..		APA32_			
1582800	1195	14730	pyruvate ferredoxin/flavodoxin oxidoreductase	+	-
1582802..		APA32_			
1584556	584	14740	glutamate synthase small subunit	+	-

Table 2.3. Mutation history of adapted strains.

Product	ORF No.	Mutational pattern		IFO 3283-32	NM-1	NM-2	NM-3	NM-4	NM-5	NM-6
Large deletion	APA32_14740	large deletion		-	+	+	+	+	+	+
(intergenic region)	-	NS*	-	-	-	+	+	+	+	+
Glycerol kinase	APA32_12550	3-bp insertion	342L	-	-	+	+	+	+	+
tRNA delta(2)-isopentenyl pyrophosphate	APA32_19280	NS	E325 (FS**)	-	-	+	+	+	+	+
Transcriptional regulator LysR	APA32_21040	Tn***	282 split (FS)	-	-	-	+	+	+	+
Transcriptional regulator TraR/DksA	APA32_25740	NS	R67L	-	-	-	+	+	+	+
DNA polymerase III subunit alpha	APA32_19490	NS	L278Q	-	-	-	-	+	+	+
Hypothetical protein	APA32_01670	NS	P115S	-	-	-	-	-	+	+
30S ribosomal protein S6	APA32_09930	NS	G108D	-	-	-	-	-	+	+
D-methionine transporter substrate-binding periplasmic protein	APA32_21920	1-bp deletion	112 split (FS)	-	-	-	-	-	+	+
Alanyl-tRNA synthetase	APA32_07840	NS	A710V	-	-	-	-	-	-	+
Murein transglycosylase	APA32_23030	NS	P119S	-	-	-	-	-	-	+
(intergenic region)	-	NR****	-							
(intergenic region)	-	NR	-							
Transcriptional regulator	APA32_03030	Tn	158 split (FS)	+	+	+	+	+	+	+
(intergenic region)	-	Tn	-	+	+	+	+	+	+	+
Glycerol kinase	APA32_12550	NS	A138P	+	+	+	+	+	+	+
Aspartate:alanine antiporter	APA32_15500	NS	G333D	+	+	+	+	+	+	+
(intergenic region)	-	Tn	-	+	+	+	+	+	+	+
Plasmid	pAPA32_040	plasmid deletion		+	+	+	+	+	+	+
Plasmid	pAPA32_060	plasmid deletion		-	-	-	+	+	+	+

+ denote mutations.

*NS: Single nucleotide substitution; **FS: Frameshift mutation; ***Tn: Transposon insertion, ****NR: not read by PCR sequencing.

2.4 DISCUSSION

In this study, six thermally-adapted strains were obtained by the gradual thermo-adaptation of *A. pasuteurianus* IFO 3283-32 under acetic acid fermentation conditions. These strains were found to grow well at high temperatures, resulting in increased optimum fermentation temperatures (Fig. 2.3 and 2.4). However, the maximum cell growth and acetic acid production of the adapted NM strains decreased at lower temperatures, such as at 30ºC and 35ºC (Figures 2 and 3). This trade-off of the growth rate between lower and higher temperatures has been previously reported in *Escherichia coli* (Rudolph et al., 2010) and *Saccharomyces cerevisiae* (Caspeta et al., 2015). The 3283-01/42C strain, a thermally-adapted strain from *A. pasteurianus* IFO 3283-01 under non-fermentation conditions (Azuma et al., 2009), also showed decreased acetic acid fermentation at lower temperatures (30–35ºC) (Fig. 2.1), similar to NM-6. However, differences in the NM-6 and 3283-01/42C strains were observed in terms of their fermentation ability at much higher temperatures, around 40ºC; NM-6 exhibited almost the same fermentation ability around 40ºC as at 37ºC. On the other hand, the fermentation ability of 3283-01/42C decreased considerably at 40ºC compared to 37ºC (Fig. 2.1). This may result from the difference in the adaptation conditions, i.e. fermentation vs. non-fermentation. The NM strains have many additional mutations compared with the mutations in 3283-01/42C (Azuma et al., 2009), as described below. In contrast, the TH-3 strain thermally-adapted from *A. pasuteurianus* SKU1108 under fermentation conditions (Matsutani et al., 2013), similar to the adaptation performed for the NM strains, did not show any trade-off phenomena; the acetic acid fermentation ability was the same at 30–37ºC, and was relatively high at temperatures as high as 40ºC (Fig. 2.1). The differences between the NM strains and the TH-3 strain may be due to the difference in the mutations occurring in these strains, which will be described later.

Comparative genome and PCR analysis indicated that the NM-6 strain experienced eleven mutations, a 64-kbp genome deletion, and a plasmid deletion during the thermal adaptation process. The large 64-kbp deletion (54 genes) occurred at the early adaptation step, in NM-1, and overlapped the large deletion (72 genes) in 3283-01/42C. This overlap region was made up of 27 genes containing 3 tRNAs and a ribosomal RNA operon, in addition to several metabolic genes (Table 2.2). The large deletion, the only genomic change in NM-1, could be related to the increased thermotolerance, as well as the decreased growth at lower temperatures, of the strain, most likely via loss of the tRNA and rRNA genes (Table 2.2 and Table 2.3). Such the trade-off phenotype was observed in 3283-01/42C, which has this same gene deletion in the overlap region. In addition, the large deletion also includes C_4-dicarboxylate transporter gene (Matsutani et al., 2013),

the defects of which have been shown to play important roles in the thermotolerance of the TH-3 strain (unpublished data). Furthermore, besides the NM-1 strain, NM-4 and NM-6 showed a clearly increased thermotolerance compared to the pre-adapted strains, NM-3, and NM-5, respectively. The mutation of the DNA polymerase III alpha subunit (in NM-4), as well as alanyl-tRNA synthetase or murein transglycosylase (in NM-6), could contribute to thermotolerance since only the genes corresponding to these enzymes were mutated by the thermal adaptation process. It should be noted that DNA polymerase III alpha subunit has a mutation, L278Q, which was found to be near the active sites, D399, D401, and D555, in the modeled structure (Fig. 2.7), and thus expected to induce some functional change.

Thus far, most of the mutation sites in the NM strains have been expected to be related to replication and translation, the former of which includes the mutation of DNA polymerase (NM-4), while the latter include 3 tRNAs and 3 rRNAs found in a large deletion region (NM-1), as well as mutations in ribosomal protein S6 (NM-5) and alanyl-tRNA synthetase (NM-6). It has been reported that decreasing the rRNA operon copy induces a lower transcription/translation level in *E. coli* (Condon et al., 1995; Gyorfy et al., 2015), and that bacteria with low rRNA operon copies exhibit a high carbon use efficiency such that the utilized carbon source is being efficiently converted to biomass C (Roller et al., 2016). Thus, the NM strains are expected to have decreased abilities for replication and translation, and also have an energy conservation due to the depressed but efficient metabolic activity. This could be also related to the reduced ROS generation observed in the NM-6 strain by compared with the parental strain (Fig. 2.6). Similar results have been recently found in thermally-adapted strains of *E. coli* and *Zymomonas mobilis* (Kosaka et al., 2019), where decreased RNA and/or DNA level and reduced ROS generation are observed in *E. coli* and *Z. mobilis*, respectively. The large genome deletions found in the NM strains and in the 3283-01/42C strain are also expected to lead a direct replication in energy saving due to the decreased genome size (2.2% and 3.2% decrease, respectively). This large genome deletion was not found in the thermally-adapted TH-3 strains. Thermotolerant SKU1108 (parental strain of TH-3) isolated in a tropical area is naturally thermotolerant (Saeki et al., 1997), while mesophilic NBRC 3283 (parental strain for NM strains or 3283-01/42C) suffers from more stress during high temperature thermal adaptation than SKU1108, such that NBRC 3283 may require drastic changes, such as a large genome deletion. Thus, via energy conservation and reduced ROS generation, the adapted strains may enhance their survival under conditions of stress, which may enable acetic acid fermentation stable even at higher temperatures.

Above findings suggest that the decreased replication and translation ability of

the adapted strains may result in decreased cell growth but also energy saving, which may lead to an increased survival ability under stress conditions, such as high temperature and the presence of acetic acid. At the same time, the ability for cells to grow more slowly is part of a trade-off response, i.e. decreased cell growth at lower temperatures. This type of trade-off phenotype is observed in the thermally-adapted strain of mesophilic AAB, *Komagataeibacter medellinensis* NBRC3288 (unpublished results). However, in the case of the TH-3 strain of *A. pasteurianus* SKU1108, where the cells grow well at both lower and higher temperatures, this strain exhibits a higher acetic acid fermentation ability at any temperatures compared to the parental strains (Matsutani et al., 2013). The TH-3 strain has 11 mutations, none of which were replication or translation-related mutations. Instead, this strain had three important mutations in relation to thermotolerance, two of which were defective mutations in the amino acid transporter (Matsutani et al., 2013) and in the dicarboxylate transporter (unpublished results). These mutations were also found in the NM-6 genome; methionine transporter binding protein (flame shift mutation) and dicarboxylate transporter in the large deletion region. Thus, the NM-6 strain may exert both a trade-off response and a thermotolerant response to become thermotolerant.

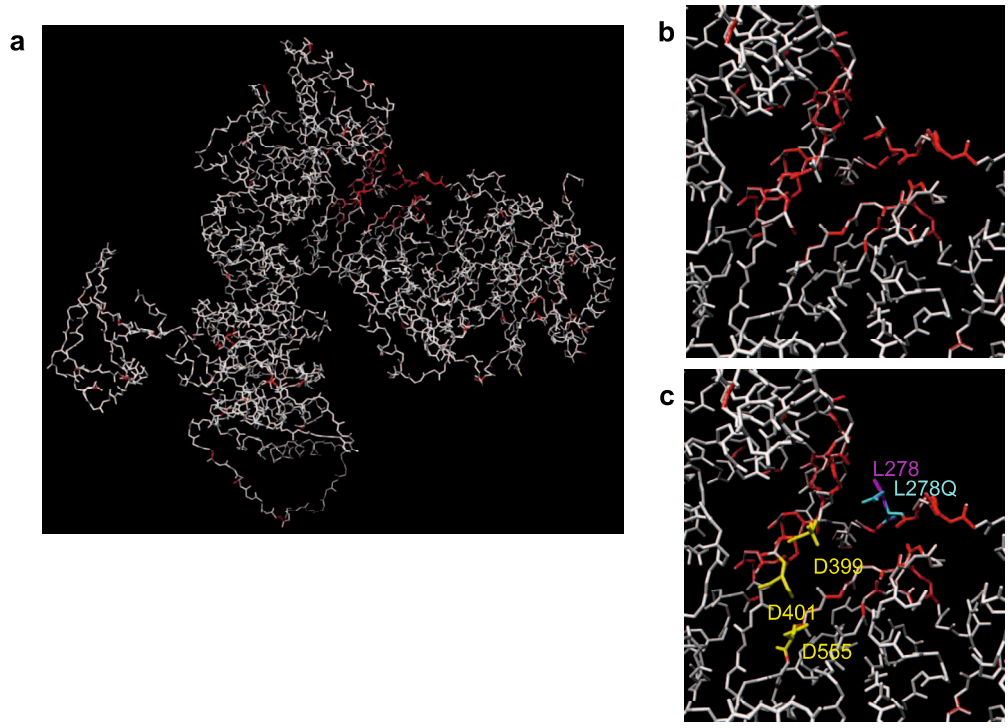

Fig. 2.7. Comparative-modeling structure of DNA polymerase PolIIIα. In *E. coli*, DNA polymerase III is replicative DNA polymerase constituted of a ten-subunit complex with an alpha subunit as the catalytic subunit [1]. Using Protein BLAST to investigate the *A. pasteurianus* enzyme using APA32_19490 as the query sequence, a homologous protein with 41% identity was found in the PDB data (PDB code: 5FKU) [2]. 5FKU is a crystal structure of the DNA polymerase III alpha, beta, epsilon, and tau complex of *E. coli*. It was investigated that the relationship between the active sites and mutation site in the 3D structure generated based on the crystal structure of DNA polymerase III alpha. (a) The superimposed comparative modeling structure of APA32_19490 and PolIIIα mutant (L278Q). The comparative modeling was performed by SWISS-MODEL server [3] and resulting two models were superimposed using MaxCluster base on their Ca-carbon coordinate [4, 5]. The red color show conformation change of mutant PolIIIα. The crystal structure of PolIIIα from *E. coli* K-12 (PDB code:5FKU) was used as template structure. (b) and (c) A close-up of the active site (D399, D401, D555) of PolIIIα and putative mutation site (L278) of NM-6. Active sites of PolIIIα are colored in yellow. Mutation site of NM-6 is colored in cyan.

[1] Lamers MH, Georgescu RE, Lee SG, O'Donnell M, Kuriyan J. Crystal structure of the catalytic alpha subunit of *E. coli* replicative DNA polymerase III. Cell. 2006;126:881-892.

[2] Fernandez-Leiro R, Conrad J, Scheres SH, Lamers MH. cryo-EM structures of the *E. coli* replicative DNA polymerase reveal its dynamic interactions with the DNA sliding clamp, exonuclease and τ. Elife. 2015;4. pii: e11134.

[3] Waterhouse A, Bertoni M, Bienert S, Studer G, Tauriello G, Gumienny R, Heer FT, de Beer TAP, Rempfer C, Bordoli L, Lepore R, Schwede T. SWISS-MODEL: homology modelling of protein structures and complexes. Nucleic Acids Res. 2018;46:W296-W303.

[4] Siew N, Elofsson A, Rychlewski L, Fischer D. MaxSub: an automated measure for the assessment of protein structure prediction quality. Bioinformatics. 2000;16:776-785.

[5] Ortiz AR, Strauss CE, Olmea O. MAMMOTH (matching molecular models obtained from theory): an automated method for model comparison. Protein Sci. 2002;11:2606-2621.

CHAPTER 3

Thermal adaptation of acetic acid bacteria for practical high-temperature vinegar fermentation

ABSTRACT

Thermotolerant microorganisms are useful for high-temperature fermentation. Several thermally adapted strains were previously obtained from *Acetobacter pasteurianus* in a nutrient-rich culture medium, while these adapted strains could not grow well at high temperature in the nutrient-poor practical culture medium, 'rice moromi'. In this study, *A. pasteurianus* K-1034 originally capable of performing acetic acid fermentation in rice moromi, was thermally adapted by experimental evolution using a 'pseudo' rice moromi culture. The adapted strains thus obtained were confirmed to grow well in such the nutrient-poor media in flask or jar-fermentor culture up to 40°C or 39°C; the mutation sites of the strains were also determined. The high-temperature fermentation ability was also shown to be comparable with a low-nutrient adapted strain previously obtained. Using the practical fermentation system, 'Acetofermenter', acetic acid production was compared in the moromi culture; the results showed that the adapted strains efficiently perform practical vinegar production under high-temperature conditions.

3.1 INTRODUCTION

Acetic acid bacteria (AAB) are capable of oxidizing sugar, alcohol, and sugar alcohol, and are thus used for vinegar production or acetic acid fermentation, where ethanol is oxidized to acetic acid via acetaldehyde. Acetic acid fermentation is generally carried out at around 30°C, but the culture temperature increases by the fermentation heat generated in the submerged culture. Thus, strict temperature control is needed to perform good fermentation over 5% acidity. Thermotolerant microorganisms are beneficial for industrial fermentation because they facilitate stable fermentation with reduced cooling costs. Experimental evolution is an efficient approach to obtain mutants that are highly tolerant to stressors, with high productivity, or grow at higher rates (Sandberg et al., 2019). We have succeeded in obtaining many strains adapted to higher temperatures from several fermentative bacteria, including both mesophilic and thermotolerant species; all these

thermally adapted strains have been shown to acquire 2–3°C higher growth temperatures (Matsushita et al., 2016). In a previous study, we obtained thermotolerant strains from AAB by experimental evolution and tried to clarify their thermotolerance mechanism (Matsushita et al., 2016; Matsutani et al., 2013). These thermally adapted strains from *Acetobacter pasteurianus* and *Komagataeibacter oboediens* could produce acetic acid at temperatures over 39°C under acetic acid fermentation conditions (Matsutani et al., 2013; Taweecheep et al., 2019; CHAPTER 2). These “experimental evolution” experiments to obtain thermotolerant AAB had been carried out in a nutrient-rich medium including yeast extract (YE) and peptone for the acetic acid fermentation conditions. However, industrial acetic acid fermentation is performed in a nutrient-poor medium. Rice vinegar, popular vinegar in East and Southeast Asia, is produced from rice, koji, yeast, and water, performing a simultaneous saccharification and alcohol fermentation followed by acetic acid fermentation. The fermentation mash generated from the alcohol fermentation is called as "rice moromi", in which the nutrients are consumed during alcoholic fermentation. Therefore, acetic acid fermentation is performed under relatively nutrient-poor condition, and thus improved by nutrient supplementation. The cell growth was increased by several amino acids, especially proline in *Acetobacter malorum* (Qi et al., 2017), and also the acetic acid production as well as the cell growth was done by aspartate or glutamate in *A. pasteurianus* (Yin et al., 2017). The stress tolerance of bacteria is also reported to be weakened in nutrient-poor conditions or inversely increased by the addition of some nutrients. Addition of magnesium ions was reported to increase thermotolerance in *Lactobacillus* (Yang et al., 2017) and also to repress the heat shock response and ethanol stress in *Saccharomyces cerevisiae* (Birch and Walker, 2000). In *S. cerevisiae*, ethanol tolerance was shown to be enhanced by increased potassium ion concentrations in the culture medium (Lam et al., 2014). Furthermore, in an *Acetobacter aceti* WK strain, the acetification ability reduced at higher temperatures was suppressed by the addition of calcium ions (Krusong et al., 2015). Thus, nutrient conditions are important for acetic acid fermentation under stressful conditions, including high temperatures.

To achieve stable and practical acetic acid fermentation (vinegar production) in rice moromi at high temperatures, a thermotolerant strain that is also able to grow well in nutrient-poor conditions needs to be developed. Recently, experimental adaptation of a thermally adapted strain from *A. pasteurianus* SKU1108 performed using jasmine rice wine culture, and a G-40 strain adapted to nutrient-poor medium was obtained to produce significantly high acetic acid production in jasmine rice wine (Phathanathavorn et al., 2019). In this study, we tried another approach for practical high-temperature acetic acid fermentation with rice moromi; thermal adaptation of *Acetobacter pasteurianus* K-1034,

a strain originally adapted to moromi, was performed by experimental evolution under nutrient-poor conditions.

3.2 MATERIALS AND METHODS

3.2.1 Bacterial strains and culture conditions

Acetobacter pasteurianus K-1034, a laboratory stock strain of *A. pasteurianus* NBRC 3284, was used in this study for the thermal adaptation experiments. NBRC 3284 strain was obtained from Institute of Fermentation Osaka 35 years before, and then preserved using a freeze-drying method for the first 22 years and then a liquid-drying method for another 13 years. The freeze-dried culture was revived in PGY medium (10 g of polypepton (Nihon Pharmaceutical Co., Tokyo, Japan), 10 g of glucose, 10 g of BBL Yeast extract (Becton, Dickinson and Co., Erembodegem, Belgium), 10 g of acetic acid, and 30 mL of ethanol per liter distilled water), and then preserved again by freeze-drying. This procedure was continued every other year for 22 years. For the next 13 years, a liquid-drying method was used instead of the freeze-drying method, which was carried out every 1 to 3 years. This strain was recognized as *A. pasteurianus* K-1034 (Table 1). Thermally adapted strains, RH and SY, were obtained, as described below, from K-1034 strain and used as the adapted strains (Table 1). *A. pasteurianus* NBRC 3284 (stored at -80°C) was also used as the control for culture characterization as well as genome analysis. *A. pasteurianus* TH-3 strain thermally adapted from *A. pasteurianus* SKU1108 (NBRC 101655) in YPGD (5 g each of yeast extract, polypepton, glycerol, and glucose in 1 L distilled water) containing 4% (v/v) ethanol (YPGDE) (Matsutani et al., 2013), *A. pasteurianus* 7E-13, an ethanol-adapted strain of TH-3 strain in YPGD containing 7% ethanol at 37˚C, and *A. pasteurianus* G-40, a low nutrient-adapted strain of the 7E-13 strain in jasmine rice wine at 37˚C (Phathanathavorn et al., 2019) (Table 3.1) were also used for comparison with the K-1034 strain and their adapted strains.

These strains were cultured in YDAE medium (5 g of yeast extract (Oriental Yeast, Tokyo, Japan), 5 g of glucose, 6 mL of acetic acid, and 50 mL of ethanol per liter of distilled water), which was used as ‘pseudo’ moromi, as described below. The seed culture was cultivated in 5 mL of Y3D medium (5 g of yeast extract and 30 g of glucose per liter of distilled water) in a test tube with shaking at 120 rpm at 30°C, or shaking at 200 rpm at 37°C (for the adapted strain). Pre-culture was carried out by inoculating 5 mL of the seed culture into 50 mL of Y3D containing 0.6% (v/v) acetic acid and 5% (v/v) ethanol in a 500-mL baffled Erlenmeyer flask followed by cultivating at 37°C with shaking at 200 rpm until the acidity reached 1.2%. Five milliliters of the pre-culture was

transferred to 100 mL of YDAE, YPGDE (containing 4% (v/v) ethanol), or YPGD1A3E (containing 1% (v/v) and 3% (v/v) ethanol) medium in a 500-mL Erlenmeyer flask and cultivated at various temperatures with shaking at 200 rpm. In case of a baffled flask culture, 2.5 mL of the pre-culture was transferred to 50 mL of rice moromi medium, prepared as described below, in a 500 mL-baffled flask with shaking at 200 rpm. In a jar fermentor, 15 mL of the same pre-culture was transferred to 300 mL of rice moromi medium in 500-mL jar fermentor. The jar fermentor was operated at an agitation rate of 500 rpm and aeration rate of 0.5 vvm. For the ethanol feeding test, the same jar fermentor experiment was carried out with 300 mL of YDAE medium. Ethanol (6 mL) was fed when the acidity reached 2%.

Table 3.1. Bacterial strains used in this study.

Strain	Relevant properties	Source or reference
Acetobacter pasteurianus		
NBRC 3284	Wild type	NBRC
K-1034	Laboratory stock strain of *A. pasteurianus* NBRC 3284	This study
RH	Thermo-adapted strain of *A. pasteurianus* K-1034	This study
SY	Thermo-adapted strain of *A. pasteurianus* K-1034	This study
SKU1108	Natural isolate from fruits of Thailand (NBRC 101655)	NBRC
TH-3	Thermo-adapted strain of *A. pasteurianus* SKU1108	Matsutani et al, 2013
7E-13	Ethanol-adapted strain of *A. pasteurianus* TH-3	Theeragool et al., unpublished data
G-40	Low nutrient-adapted strain of *A. pasteurianus* 7E-13 strain	Phathanathavorn et al., 2019

3.2.2 Rice moromi medium preparation

Rice moromi (fermentation mash) in which some vinegar was added was kindly supplied by Kewpie Jyozo Co., Ltd. The rice moromi with added vinegar (7.6% (v/v) ethanol and 0.9% (v/v) acetic acid) was filtrated to remove solids, and diluted with sterile distilled water to obtain 'rice moromi medium' which contained a final concentration of 5.1% (v/v) ethanol, 0.6% (v/v) acetic acid, 0.01% (v/v) reducing sugar and 0.05% (v/v) nitrogen content (see Table 3.2).

3.2.3 Acetofermenter

The Acetofermenter is an original vinegar fermentor equipped with an aerator based on the technology of Frings Acetator® (Heinrich Frings, Germany) (Heinrich Frings GmbH & Co. KG. “Gas/Liquid Mixing Turbines” https://www.frings.com/Gas-Liquid-Mixing-Turbines.29+M52087573ab0.0.html, 17 Aug 2020). Colonies were picked up from a YDAE agar plate and inoculated in 100 mL of Y3D medium (3 g of glucose and 5 g of BBL Yeast Extract per liter of distilled water containing 1% (v/v) acetic acid and 4% (v/v) ethanol) in a 300-mL Erlenmeyer flask as seed culture. The seed culture was incubated at 30°C and 160 rpm for 24-30 h, after which 1 mL of the seed culture was transferred to 100 mL of pre-culture medium composed of rice moromi medium (containing 5.1% (v/v) ethanol and 0.6% (w/v) acetic acid) in a 300-mL Erlenmeyer flask. The pre-culture was carried out at 37°C and 160 rpm for 24 h. Then, 90 mL of the pre-culture was transferred to 6 L of rice moromi medium in an Acetofermentor (9-L fermentor). The Acetofermenter was operated at various temperatures, with an agitation rate of 50 Hz (2650 rpm) and an aeration rate of 0.6 L/min.

3.2.4 Thermal adaptation

The K-1034 strain was cultivated with 5 mL of potato medium (20 g of glycerol, 5 g of glucose, 10 g of yeast extract (Oriental Yeast, Tokyo, Japan), 10 g of polypepton (Nihon Pharmaceuticals Co. Ltd., Osaka, Japan), and 100 mL of potato extract (Matsushita and Ameyama, 1982) per liter of distilled water) in a test-tube at 30°C with shaking at 120 rpm until the turbidity reached 150–200 Klett units as the seed culture. The seed culture was centrifuged for 5 min at 8000 x g and washed with YD medium (5 g of yeast extract and 5 g of D-glucose per liter of distilled water). The pellet was resuspended in 1 mL YD medium and then inoculated into 100 mL of YDAE medium in a 500-mL Erlenmeyer flask. The culture was cultivated at 37°C with shaking at 200 rpm. When the acidity reached 1.5–2.0% (w/v), 5 mL of the culture was transferred to another 100 mL of fresh YDAE medium in an Erlenmeyer flask. Cultivation was repeated several times (4 to 15 times) until a stable fermentation rate was obtained, and then, the next cultivation was started by raising the temperature by 0.5°C. Thermal adaptation was continued until the strain grew well at 39°C. To isolate a thermally adapted strain, the adaptation culture was spread on YPGD and YDAE agar plates and incubated at 39°C. Several large colonies were picked up and their growth was compared with that of the liquid culture in YDAE medium at 39°C. Two colonies (K-1034 RH and SY) were selected as thermal-adapted strains.

3.2.5 The cell growth and acetic acid production measurements

Cell growth was measured by Klett-Summerson photoelectric colorimeter or measured at an optical density at 610 nm. Acetic acid production was determined by measuring acidity as follows. The acidity of the culture medium at several growth phases was measured by alkali-titration using 1 mL of culture and 0.8 N NaOH with 10 μL of 0.025% phenolphthalein (transition pH range: 8.3–10.0) as a pH indicator.

3.2.6 Other analytical methods

Amino nitrogen and total nitrogen were measured according to AOAC official methods (Official Methods of Analysis of AOAC International, ed. George W. Latimer, Jr., 19th Ed., 2012, AOAC International). Total nitrogen was measured using the Kjeldahl method (AOAC 930.035 Vinegars (1)) using a Distillation Unit K-355 (BUCHI, Switzerland), and amino nitrogen was measured using the formol titration method (AOAC 920.04 Nitrogen (Ammoniacal)).

3.2.7 Genome sequencing and mapping analysis of K-1034, RH, and SY strains

Chromosomal DNA was isolated from K-1034, RH, and SY strains grown on 5 mL of YDAE medium at 30°C or 37°C for 24–48 h. After harvesting the cells, the chromosomal DNA was isolated as described previously (Kawai et al., 2013). Genome sequencing of the two strains, RH and SY, was performed using the Illumina MiSeq at Macrogen Inc. (Seoul,Korea), and also that of K-1034 with the Illumina HiSeq 2500 at Hokkaido System Science Co., Ltd. (Sapporo, Japan). The previously published genome sequence of *A. pasteurianus* IFO 3283-01, which is one of six clones isolated from *Acetobacter pasteurianus* NBRC 3283 stored in 1974, (National Center for Biotechnology Information [NCBI] Reference Sequence accession number: NC_013209.1–NC_013215.1) (Ameyama et al., 2009) was used as the reference sequence for our genome mapping analysis. The Illumina sequence reads of these strains and previously reported NBRC 3284 (DRA accession number: DRR040592) were mapped to the reference sequences using BWA with default parameters (Li and Durbin, 2010). All single nucleotide polymorphisms (SNPs) and indels were detected using the Genome Analysis Toolkit (GATK) (McKenna et al., 2010; DePristo et al., 2011). The data for NBRC 3284 and K-1034 were extracted to detect the strain-specific mutations. Since IFO 3283-01 and NBRC 3284 have only several tens of mutations each other, we used IFO 3283-01 genome as the reference one (Matsutani et al., 2020). Common mutations occurred in all four genomes, NBRC 3284, K-1034, RH, and SY, which indicate the mutations between IFO 3283-01 and NBRC 3284, were excluded from analysis. To

identify the mutations in the two adapted strains, all mutations detected in K-1034, RH, and SY were collected and compared. All mutations not detected in the wild-type strain were considered as adapted strain-specific mutations. To confirm the nucleotide mutations detected in the adapted strain, PCR was performed using the genomic DNA of these three strains as a template. PCR products were purified using a MagExractor kit (Toyobo, Tokyo, Japan) and then directly sequenced on a capillary sequencer using a BigDye® Terminator Cycle sequencing kit (Applied Biosystems, USA).

3.2.8 Sequence data deposition

Illumina sequence reads of the K-1034, K-1034 RH, and K-1034 SY strains were deposited in the DNA Data Bank of Japan [DDBJ] Sequence Read Archive (DRA). The DRA accession numbers for K-1034, K-1034 RH, and K-1034 SY are DRR235002, DRR235003, and DRR235004, respectively.

3.3 RESULTS AND DISCUSSION

3.3.1 Relationship between thermal adaptation and nutritional condition

Previously, we performed thermal adaptation in a relatively rich YPGD medium containing 4% (v/v) ethanol (YPGDE) (Matsutani et al., 2013). The resultant, thermally adapted, TH-3 strain was confirmed to maintain higher acetic acid fermentation ability in YPGDE medium as well as in YPGD medium containing 1% acetic acid and 3% ethanol (YPGD1A3E) at 40°C (3°C higher than the upper limit temperature, 37°C, of the parental strain SKU1108) (Fig. 3.1A). However, it was previously shown that G-40 strain, adapted from 7E-13 to the nutrient-poor medium (Table 3.1), could exhibit a higher acetic acid fermentation ability in a nutrient-poor jasmine rice wine (rice moromi) at 37°C than 7E-13 strain, derived from TH-3 strain (Table 3.1) did (Phathanathavorn et al., 2019). The acetic acid fermentation ability of 7E-13 strain was examined with nutrient-poor ‘pseudo-moromi’ YDAE medium, of which the total and formol nitrogen contents are 2.2 and 1.7 times, respectively, lower than those of YPGD medium but similar to those of ‘rice moromi’ (Table 3.2). In the YDAE medium, compared with YPGDE medium, the 7E-13 strain exhibited a delayed acetic acid production at higher temperature (39°C) (Fig. 3.1B). Thus, experimental evolution including thermal adaptation, could be affected or reflected by the nutritional condition of the culture in which the adaptation is conducted.

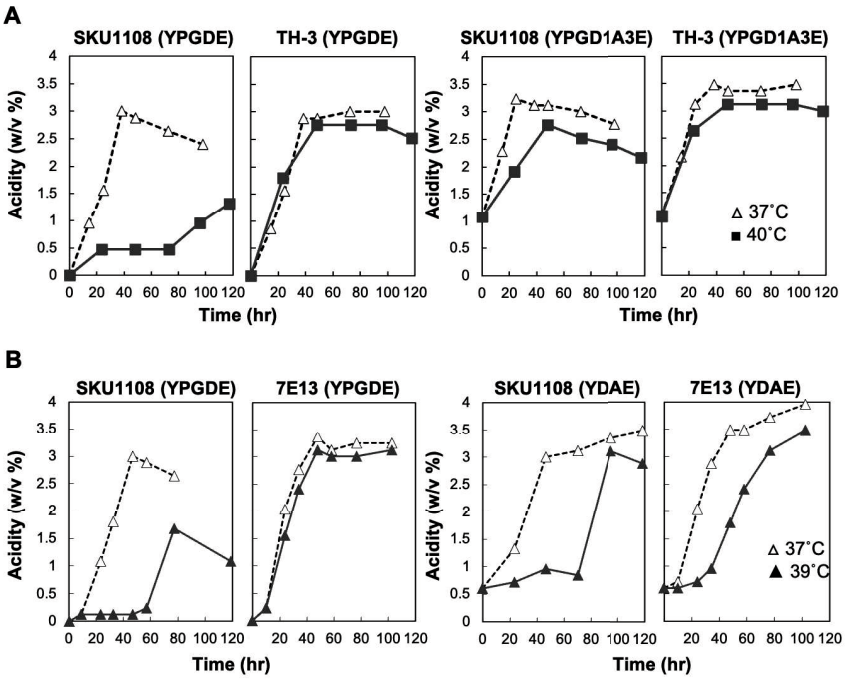

Fig. 3.1. Comparison of acetic acid fermentation with (A) *A. pasteurianus* SKU1108 and TH-3 between YPGDE medium and YPGDAE medium, and with (B) *A. pasteurianus* SKU1108 and 7E-13 between YPGDE medium and YDAE medium. The parent strain SKU1108 and the adapted strains, TH-3 or 7E-13, were cultivated in 50 mL of Y3D medium containing 0.6% acetic acid and 5% ethanol in a 500-mL baffled flask at 37°C until the acidity reached 1.2%, as the pre-culture. The pre-culture (5 mL) was transferred to 100 mL of the main culture medium, YPGDE (containing 4% ethanol), YPGD1A3E (containing 1% acetic acid and 3% ethanol), or YDAE (containing 0.6% acetic acid and 5% ethanol), in a 500-mL Erlenmeyer flask, and cultivated at 37°C (open triangle), 39°C (closed triangle), and 40°C (closed square) with shaking at 200 rpm.

Table 3.2. Sugar and nitrogen concentration in medium.

	Diluted denature rice moromi	Y3DAE medium*	YPGD medium
Reducing sugar (g/100mL) Bertrand method	0.01	2.59	0.40
Total nitrogen (mg/100mL) Kjeldahl method	53.52	57.20	125.3
Formol titration nitrogen (mg/100mL)	19.56	18.65	32.32
pH	3.70	3.78	6.68

*Y3DAE medium containing 3% (w/v) glucose and 0.5% (w/v) BBL Yeast Extract, 0.6% (v/v) acetic acid, and 4.3% (v/v) ethanol.

3.3.2 *A. pasteurianus* K-1034 for practical acetic acid fermentation

To obtain a strain for practical acetic acid fermentation (vinegar production) at higher temperatures, a laboratory stock strain of *A. pasteurianus* NBRC 3284, named K-1034, was selected as the starting strain. As *A. pasteurianus* NBRC 3284 was originally isolated from vinegar, and K-1034 has been utilized for a long time in acetic acid fermentation using 'moromi' (vinegar production), it was suitable for adaptation to nutrition-poor conditions. Thus, the fermentation ability of NBRC 3284 and K-1034 was compared in the nutrient-poor medium YDAE; both strains exhibited a reasonably high acetic acid fermentation ability at 30°C and 35°C, but not at all at 38.5°C (Fig. 3.2). However, at 37°C and 38°C, both strains showed delayed acetic acid production, whereas the K-1034 strain showed better growth than the original strain (Fig. 3.2). To determine the phenotypic differences, the genome sequence of the K-1034 laboratory stock strain was determined and compared with that of the original NBRC 3284 (Matsutani et al., 2020). Four and three differences were found in the genome and plasmid, respectively (Table 3.3), and one of the differences in the genome was in the *nhak2* gene. The original NBRC 3284 strain is reported to demonstrate a thermo-sensitive phenotype due to mutation (12 bp insertion) in the *nhak2* gene compared with that of *A. pasteurianus* NBRC 3283, which exhibits a relatively thermotolerant phenotype (Matsutani et al., 2020). However, the *nhak2* gene of K-1034 had no such 12 bp insertion, similar to the gene of *A. pasteurianus* NBRC 3283, and thus it was reasonable that K-1034 is some kind of revertant, and exhibits higher thermotolerance than NBRC 3284. Thus, NBRC 3284 and K-1034 strains were shown to be useful for acetic acid fermentation in a relatively poor medium like 'moromi' at lower temperatures (30°C to 35°C), but not at higher temperatures over 37°C. Between the both strains, K-1034 strain exhibiting a slightly higher thermotolerance was regarded as a better strain for further adaptation to higher temperatures.

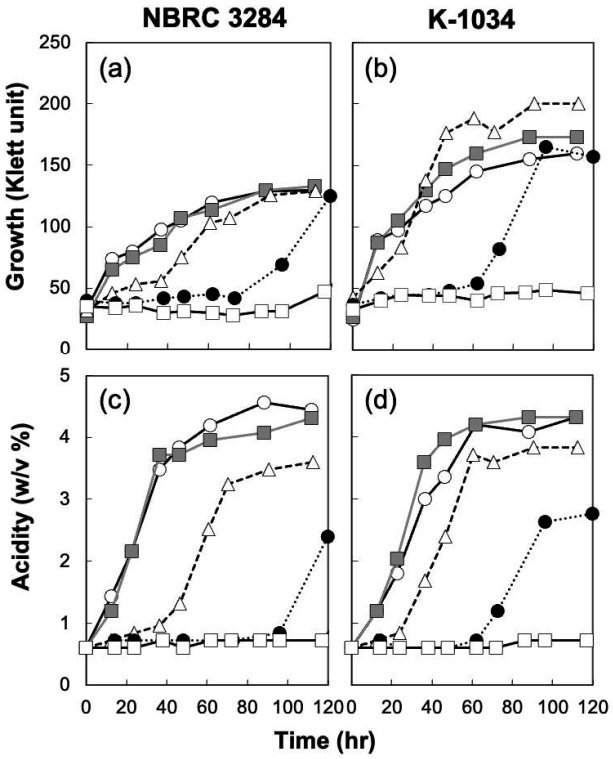

Fig. 3.2. Growth of *A. pasteurianus* NBRC 3284 and K-1034. *A. pasteurianus* NBRC 3284 (a, c) and K-1034 (b, d) were cultivated in 5 mL of potato medium at 30°C until its turbidity reached 150 Klett units. The cultures were collected by centrifugation, washed with YD medium, and resuspended in 1 mL of YD medium. The suspended cells were inoculated in 100 mL of YDAE medium (containing 0.6% acetic acid and 5% ethanol) in a 500-mL Erlenmeyer flask. The main cultures were cultivated at 30°C (open circle), 35°C (gray square), 37°C (open triangle), 38°C (closed circle), and 38.5°C (open square) with shaking at 200 rpm. Their growth (a, b) and acidity (c, d) were measured as described in Materials and Methods.

Table 3.3. List of mutation site of NBRC 3284 and K-1034 against IFO 3283-01 genome.

mutation	NBRC 3284	K-1034	strain	product	orf number	position	Contig length	Reference genome[a)]	pos.[b)]	REF[c)]	ALT[d)]
A392V	-	+	k1034	antiporter of Na+/H+ NhaA/NhaP	APA01_04220	438900..440612	2907495	NC_013209	440074	C	T
frameshift	+	-	nbrc3284	DNA-directed RNA polymerase subunit beta	APA01_09270	964836..969029	2907495	NC_013209	965707	AGCTGCTGGCACC	A
12bp insertion	+	-	nbrc3284	antiporter of Na+/H+	APA01_10370	1089522..1092122	2907495	NC_013209	1090128	A	ATCTCCTTTGTGG
M232P S233C A234P	+	-	nbrc3284	two component response regulator CtrA	APA01_26130	2831584..2832369	2907495	NC_013209	2832270	C	CGA
D11M	-	+	k1034	transposase	APA01_40760	88925..90310	191799	NC_013210	89927	C	G
Y13G	-	+	k1034	transposase	APA01_40760	88925..90310	191799	NC_013210	89941	A	G
R27P	-	+	k1034	transposase	APA01_40760	88925..90310	191799	NC_013210	89960	G	T

[a] GenBank accession numbers used for reference genome

[b] mutated position in reference genome

[c] base sequence of reference genome

[d] base sequence of adapted strain

3.3.3 Thermal adaptation of *A. pasteurianus* K-1034

Thus, to obtain a more thermotolerant strain for practical high-temperature acetic acid fermentation, thermal adaptation of K-1034 was performed in YDAE medium instead of 'rice moromi'. The adaptation was started at 37°C (a temperature the growth is delayed in YDAE medium), and the fermentation temperature was raised from 37°C to 39°C in 5 steps (see Materials and Methods, Fig. 3.3). Finally, the culture was spread on YDAE agar medium and YPGD agar medium to select colonies exhibiting a high growth phenotype in liquid culture. Then, the growth of these colonies was compared with that in YDAE liquid culture at 39°C. Two thermal-adapted strains, RH and SY, were obtained; the former strain was isolated from YPGD agar medium, and the latter was isolated from YDAE agar medium. The adapted strains grew well at 39°C and 40°C (temperatures 2 and 3°C higher than the upper limit temperature of 37°C) in YDAE medium, whereas the parental strain did not (Fig. 3.4). Unlike the K-1034 strain, both adapted strains grew well at 39°C, even in YPGDE medium (data not sown). Thus, two adapted strains were

obtained by experimental adaptive evolution as candidate strains for high-temperature vinegar fermentation.

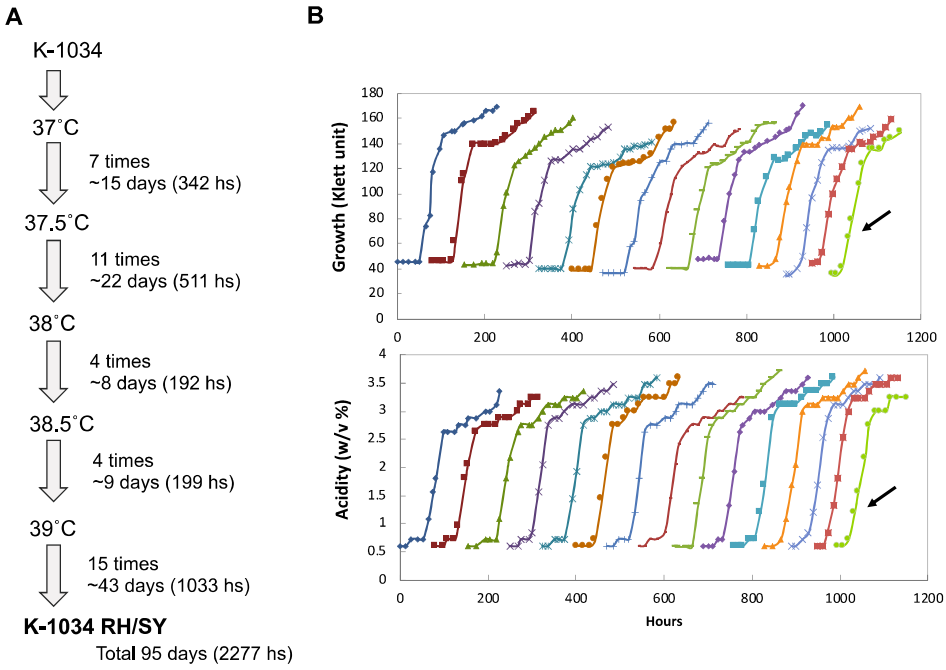

Fig. 3.3. Thermal and low nutrition adaptation of *A. pasteurianus* K-1034. (A) Adaptation flow with stepwise increase of the cultivation temperature from 37°C to 39°C. (B) Growth and acidity changes of the thermal adaptation at 39°C (final adaptation step) is shown as an example. In each cultivation steps, when the acidity reached 1.5–2.0% (w/v), 5 mL of the culture was transferred to another 100 mL of fresh YDAE medium in an Erlenmeyer flask. Cultivation was repeated 15 times. Finally, adapted strains were isolated from sample of arow point culture medium.

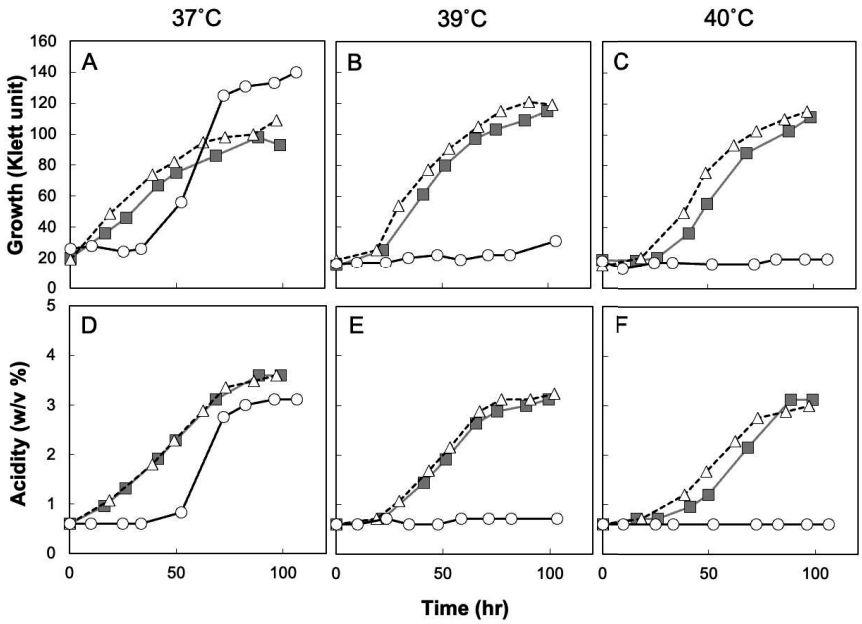

Fig. 3.4. Comparison of growth among *A. pasteurianus* K-1034 and the 2 adapted strains. The K-1034 (open circle), RH (open triangle), and SY (gray square) strains were cultivated in 100 mL of YDAE medium in a 500-mL Erlenmeyer flask at 37°C (A, D), 39°C (B, E), and 40°C (C, F). Growth (A-C) and acidity (D-F) were measured as described in Materials and Methods.

3.3.4 Differences in the genome between K-1034 and the adapted strains, RH and SY

The mutation sites of the RH and SY strains were clarified by genome mapping analysis (Table 3.4). The RH and SY strains had 7 and 6 mutation sites, respectively, of which 5 mutation sites were common to both strains. Of these mutations found in both strains, mutation of 'two component hybrid sensor histidine kinase and regulator' occurred at different positions, T156K in RH and L243R in SY. In a previous study, a mutation in this gene was also reported in a thermal-adapted strain TI from *A. pasteurianus* SKU1108 (Matsutani et al., 2013). The remaining 4 mutations were the same in both strains; of these the mutations in *rpoC* and GTP pyrophosphokinase genes might be candidates for thermotolerance. The mutation in *rpoC* was previously observed in some experimental evolution strains from *Escherichia coli* under high temperature (Tenaillon et al., 2012; Kosaka et al., 2019) and acid stress (Du et al., 2020). In addition, an acetate-adapted strain from *E. coli* was reported to have a mutation in the alpha subunit of RNA polymerase and to have an increased growth rate (Rajaraman et al, 2016). The

rpoE gene (RNA polymerase sigma E factor) was reported as a thermotolerance gene in *Acetobacter tropicalis* SKU1100 (Soemphol et al., 2011). Thus, mutation in some subunits of RNA polymerase is frequently observed in experimental evolution strains, and this could be important for stress response or adaptation. In addition, some thermally adapted strains of *E. coli* have been shown to have mutations in *spoT* (Kosaka et al., 2019; Kishimoto et al., 2010; Blaby et al., 2012). The *spoT* gene encodes GTP pyrophosphokinase (bifunctional (p)ppGpp synthetase/guanosine-3',5'-bis(diphosphate) 3'-pyrophosphohydrolase), which is involved in the synthesis and hydrolysis of (p)ppGpp. The (p)ppGpp is called a 'magic spot' and induces a stringent response by interaction with RNA polymerase and transcriptional factors (Ross et al., 2013; Ross et al., 2016). In a thermally-adapted strain NM-6 from *A. pasteurianus* NBRC 3283 (Chapter 2), large numbers of the mutations are related to replication and translation such as DNA polymerase, ribosomal protein S6, and alanyl-tRNA synthetase including deletion of 3 tRNAs and 3 rRNAs; these mutations suggesting reduced cell growth and/or cell division leading the stress tolerance. Thus, as the mutations of *spoT* and *rpoC* in the RH and SY strains may also lead stress tolerance by reducing the cell growth, these mutations are also candidates that contribute to increased thermotolerance in both strains. G-40 strain, adapted to low-nutrient condition, has no mutations overlapped with RH/SY strains. However, an originally thermo-adapted 7E-13 or TH-3 strain that is a parental strain of G-40 has a 4-bp deletion mutation in *mucR* transcriptional regulator (APT_01785), of which a homologous *mucR* (APA01_16920) was also mutated in RH strain. The MucR of *Sinorhizobium melitoti* (53% identity of the RH strains' homolog) has been shown to be a regulator for exopolysaccharide synthesis (Martín et al., 2000). *Acetobacter aceti* IFO 3284 (now renamed as *A. pasteurianus* NBRC 3284) has been shown to produce an exopolysaccharide consisting of glucose and rhamnose (Moonmangmee et al., 2002), and also such an exopolysaccharide of *A. pasteurianus* SKU1108 or NBRC 3283 has been shown to be related to the acetic acid tolerance (Kanchanarach et al., 2010). Thus, *mucR* mutation may be involved in thermotolerance via production of the exopolysaccharide.

Table 3.4. Mutation sites of RH and SY strains.[a)]

locus_tag	gene	product	reference genome[b)]	pos.[c)]	REF[d)]	ALT[e)]	K-1034	RH	SY
APA01_00810	-	two component hybrid sensor histidine kinase and regulator	NC_013209	85063	C	A	-	T156K	-
APA01_00810	-	two component hybrid sensor histidine kinase and regulator	NC_013209	85324	T	G	-	-	L243R
APA01_01170	-	ATP synthase F1 subunit delta	NC_013209	126481	C	T	-	A16V	A16V
APA01_06450	-	GTP pyrophosphokinase	NC_013209	671982	C	T	-	A652V	A652V
APA01_09280	*rpoC*	DNA-directed RNA polymerase subunit beta'	NC_013209	969975	G	A	-	E285K	E285K
APA01_12130	-	hypothetical protein	NC_013209	1268779	C	T	-	E124K	E124K
APA01_16920	*mucR*	MucR family transcriptional regulator	NC_013209	1836011	A	G	-	M96V	-
APA01_43920	*parA*	plasmid partitioning family protein ParA/MinD	NC_013212	27021	T	G	-	upstream	upstream

[a] Complete genome sequence of NBRC 3283 strain was used for the reference of mapping analysis.
[b] GenBank accession numbers used for reference genome
[c] mutated position in reference genome
[d] base sequence of reference genome
[e] base sequence of adapted strain

3.3.5 Fermentation in moromi medium and scale up fermentation.

Acetic acid fermentation was then performed with these thermally adapted strains, RH and SY strains, in rice moromi, which has been used for industrial rice vinegar production. Fig. 3.5 shows the acetic acid fermentation in 'moromi' medium cultivated in a baffled flask and 500 mL jar fermentor. In a baffled flask culture, both the adapted strains showed acetic acid production at 37°C and 39°C, whereas K-1034 did a weak production at 37°C but not any at 39°C (Fig. 3.5A and C). When compared with YDAE medium in Erlenmeyer flask (Fig. 3.4), the acetic acid fermentation ability of K-1034 was largely decreased at 37°C. This is probably due to the high aeration condition in baffled flask, beside the difference in medium, as described below. In a jar fermentor (Fig. 3.5B

and D), K-1034 produced acetic acid in a short time as with the adapted strains at 37°C, but did not produce any acetic acid at 39°C. However, in both baffled flask and jar fermentor, ethanol seemed to be vaporized, especially in the later phase, by air bubbling to repress the final acetic acid production level. To solve this problem, ethanol was fed in a jar fermentor experiment, where YDAE medium was used instead of the 'moromi' medium. This ethanol feeding experiments were carried out with RH and SY strains, by comparing with G-40 strain (Fig. 3.6). Ethanol feeding actually increased the production of acetic acid in both the strains, RH being better than SY (Fig. 3.6A and C). Thus, the adapted strains could perform acetic acid production as high as standard vinegar fermentation at 39°C in a jar fermentor even with nutrient-poor medium. As described previously, the G-40 strain was obtained from the 7E-13 strain (further adapted from the TH-3 strain) by adapting to low nutrient conditions with jasmine rice wine (Phathanathavorn et al., 2019). The G-40 strain, which exhibited high acetic acid production with jasmine rice wine medium in a jar fermentor at 37°C, was also examined in YDAE medium with ethanol-feeding conditions (Fig. 3.6B and D). The G-40 strain showed relatively high acetic acid production at 39°C, unlike the parental 7E-13 strain, which showed a large delay in fermentation. The results indicated that either thermal adaptation of the strain originally adapted to the low-nutrient (like RH or SY strain) or low-nutrient adaptation of the strain originally adapted to high temperature (like G-40 strain) could lead high temperature acetic acid fermentation in low-nutrient culture.

Finally, we performed a scale-up fermentation with a practical vinegar fermentor, Acetofermenter. In this system (9 L scale), using 6 L of rice moromi medium, acetic acid production was examined with the adapted strains, compared with the parental strain. The K-1034 strain showed sufficient acetic acid production at 32°C or 35°C, but none at 37°C, whereas RH and SY strains showed reasonably high acetic acid production at 37°C or 38°C (2°C or 3°C higher temperature than the upper limit temperature of 35°C) (Fig. 3.7). However, unlike the flask and jar fermentor cultures, these adapted strains showed no acetic acid fermentation at 39°C (data not shown). The Acetofermenter differs from usual bioreactors in using a special turbine (aerator) at the bottom of the bioreactor. The aerator can create both extremely fine bubbles and shear stress during agitation. Therefore, although efficient mass transfer of oxygen can be provided to the fermentation liquid by fine bubbles, the shear stress may cause some level of mechanical cell damage. This may be the reason why the cells could not produce any acetic acid at the high temperature (39°C) in the Acetofermenter different form the usual jar fermentor. The G-40 strain described above was also shown to have a high fermentation ability similar to the RH or SY strains at 37°C in the Acetofermenter (Fig. 3.7).

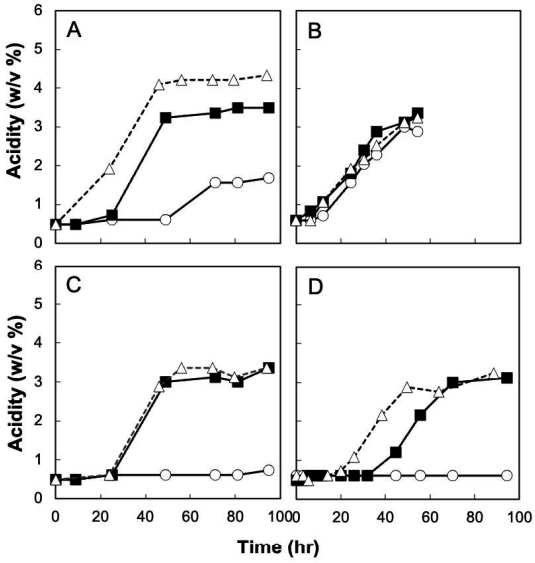

Fig. 3.5. Comparison of acetic acid production by *A. pasteurianus* K-1034 and the adapted strains in rice moromi under different culture conditions. The K-1034 (open circles), RH (open triangles), and SY (closed squares) were cultivated in 50 mL of rice moromi medium in a 500 mL-baffled flask at 37°C (A) and 39°C (C) with shaking at 200 rpm. The same strains were cultivated in 300 mL of rice moromi medium in a 500-mL jar fermentor at 37°C (B) and 39°C (D).

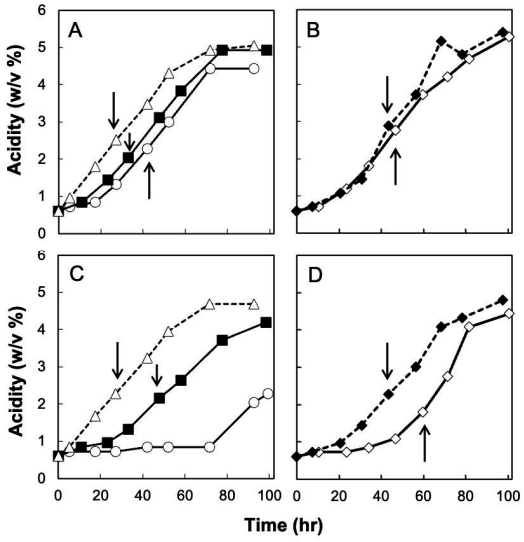

Fig. 3.6. Acetic acid fermentation of the *A. pasteurianus* K-1034, RH, SY, 7E-13, and G-40 in a jar fermentor under ethanol feeding condition. Strains were cultivated in a 300 mL of YDAE medium in a 500 mL-jar fermentor at 37 (A, B) and 39°C (C, D) at 500 rpm and 0.5 vvm. Panels (A) and (C) show *A. pasteurianus* K-1034 (open circles), RH (open triangles), and SY (closed squares). Panels (B) and (D) show *A. pasteurianus* 7E-13 (open diamond) and G-40 (closed diamond). Arrows indicate the feeding of 6 mL ethanol.

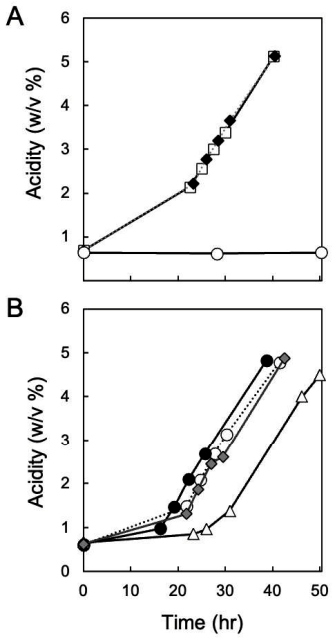

Fig. 3.7. Growth comparison of *A. pasteurianus* K-1034 and the adapted strains in an Acetofermenter. The Acetofermenter was operated at various temperatures with an agitation rate of 50 Hz (2650 rpm) and with an aeration rate of 0.6 L/min. (A) Acetic acid production by K-1034 at 32°C (open square), 35°C (closed diamond), and 37°C (open circle). (B) Acetic acid production by RH at 37°C (closed circle) and by SY at 37°C (open circle) and 38°C (open triangle). The gray diamond shows acetic acid production by G-40 at 37°C.

3.4 CONCLUSION

In this study, thermal adaptation (experimental evolution at higher growth temperature) was applied to a practically useful *Acetobacter pasteurianus* strain. The adapted RH or SY strains were found to be useful for high-temperature acetic acid fermentation in a typical jar fermentor. These adapted strains could ferment acetic acid even at 39°C, and over 40°C, as shown with the G-40 strain, where acetic acid production could be accomplished in the jar fermentor without any temperature control where the temperature raised up to 40°C. (Fig. 3.8). In this study, we further found that the adapted RH or SY strains (and the G-40 strain) are useful for high temperature fermentation in an Acetofermenter (a specific bioreactor for practical acetic acid fermentation), wherein fermentation could be performed even at 37°C. We then estimated the power consumption of 2,000 L-scale fermentation based on the results in Fig. 3.7. The heat balance during fermentation was assumed by the sum of ΔrH for acetic acid fermentation, heat of

agitation, cooling by airflow, and heat dissipation. The estimated heat balance of K-1034 at 30°C was +857 MJ, whereas that of RH and SY strains at 37°C was +784 MJ and +796 MJ, respectively. Thus, it is possible to decrease the electricity consumption required for cooling by 8.5% and 7.0%, respectively. In conclusion, such thermal adapted strains could be useful for practical vinegar fermentation, with reduced cooling costs.

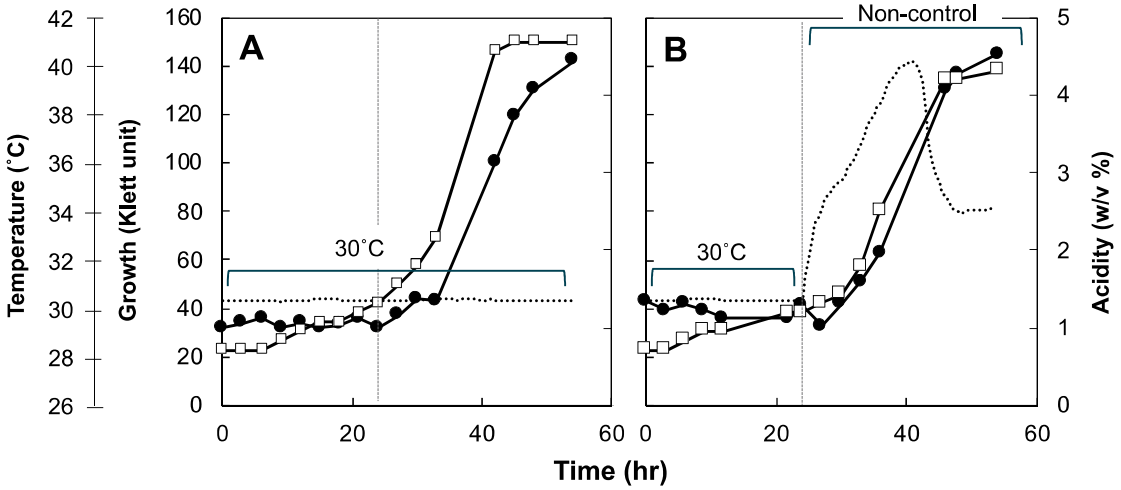

Fig. 3.8. Acetic acid fermentation of the *A. pasteurianus* G-40 in a jar fermentor with and without temperature control. (A, B) *A. pasteurianus* G-40 was cultivated in 2 L of YDAE medium in a 5-L jar fermentor at 500 rpm and 0.5 vvm. The pre-culture (Y3D containing 0.6% acetic acid and 5% ethanol medium culture; 100 mL) was inoculated and cultivated at 30˚C for the first 24 h in both the fermentors. Then, the temperature of the fermentor was maintained at 30˚C in A, whereas the temperature control was shut off in B. Fermentation was then continued for another 24 h. Symbols show the growth, closed circle; acidity, open square, and temperature, dot line.

REFERENCE

Altschul SF, Madden TL, Schäffer AA, Zhang J, Zhang Z, Miller W, Lipman DJ. 1997. Gapped BLAST and PSI-BLAST: a new generation of protein database search programs. Nucleic Acids Res 25:3389-3402.

Auton M, Bolen DW. 2004. Additive transfer free energies of the peptide backbone unit that are independent of the model compound and the choice of concentration scale. Biochemistry 43:1329-1342.

Azuma Y, Hosoyama A, Matsutani M, Furuya N, Horikawa H, Harada T, Hirakawa H, Kuhara S, Matsushita K Fujita N, Shirai M. 2009. Whole-genome analyses reveal genetic instability of *Acetobacter pasteurianus*. Nucleic Acids Research 37:5768-5783.

Bankapalli K, Saladi S, Awadia SS, Goswami AV, Samaddar M, D'Silva P. 2015. Robust glyoxalase activity of Hsp31, a ThiJ/DJ-1/PfpI family member protein, is critical for oxidative stress resistance in *Saccharomyces cerevisiae*. J Biol Chem 290:26491-26507.

Benaroudj N, Lee DH, Goldberg AL. 2001. Trehalose accumulation during cellular stress protects cells and cellular proteins from damage by oxygen radicals. J Biol Chem 276:24261-24267.

Birch RM, Walker GM. 2000. Influence of magnesium ions on heat shock and ethanol stress responses of *Saccharomyces cerevisiae*. Enzyme Microb Technol 26:678-687.

Blaby IK, Lyons BJ, Wroclawska-Hughes E, Phillips GC, Pyle TP, Chamberlin SG, Benner SA, Lyons TJ, Crécy-Lagard Vd, Crécy Ed. 2012. Experimental evolution of a facultative thermophile from a mesophilic ancestor. Appl Environ Microbiol 78:144-155.

Bligh EG, Dyer WJ. 1959. A rapid method of total lipid extraction and purification. Can J Biochem Physiol 37:911-917.

Bringer S, Bott M. 2016. "Central Carbon Metabolism and Respiration in *Gluconobacter oxydans*", p 235-253. *In* Matsushita K. TH, Tonouchi N. & Okamoto-Kainuma A. (ed), Acetic Acid Bacteria -Ecology and Physiology-. Springer Japan, Tokyo.

Carlberg I, Mannervik B. 1975. Purification and characterization of the flavoenzyme glutathione reductase from rat liver. J Biol Chem 250:5475-5480.

Caspeta L, Chen Y, Ghiaci P, Feizi A, Buskov S, Hallstrom BM, Petranovic D, Nielsen J. 2014. Biofuels. Altered sterol composition renders yeast thermotolerant. Science 346:75-78.

Caspeta L, Nielsen J. 2015. Thermotolerant Yeast Strains Adapted by Laboratory Evolution Show Trade-Off at Ancestral Temperatures and Preadaptation to Other Stresses. MBio 6:e00431.

Chang R, Lv B, Li B. 2017. Quantitative proteomics analysis by iTRAQ revealed underlying changes in thermotolerance of *Arthrospira platensis*. J Proteomics 165:119-131.

Condon C, Liveris D, Squires C, Schwartz I, Squires CL. 1995. rRNA operon multiplicity in *Escherichia coli* and the physiological implications of *rrn* inactivation. J Bacteriol 177:4152-4156.

Darling AE, Mau B, Perna NT. 2010. progressiveMauve: multiple genome alignment with gene gain, loss and rearrangement. PLoS One 5:e11147.

Davidson JF, Schiestl RH. 2001. Mitochondrial respiratory electron carriers are involved in oxidative stress during heat stress in *Saccharomyces cerevisiae*. Mol Cell Biol 21:8483-8489.

Davidson JF, Whyte B, Bissinger PH, Schiestl RH. 1996. Oxidative stress is involved in heat-induced cell death in *Saccharomyces cerevisiae*. Proc Natl Acad Sci U S A 93:5116-5121.

De Virgilio C, Hottiger T, Dominguez J, Boller T, Wiemken A. 1994. The role of trehalose synthesis for the acquisition of thermotolerance in yeast. I. Genetic evidence that trehalose is a thermoprotectant. Eur J Biochem 219:179-186.

DePristo MA, Banks E, Poplin R, Garimella KV, Maguire JR, Hartl C, Philippakis AA, del Angel G, Rivas MA, Hanna M, McKenna A, Fennell TJ, Kernytsky AM, Sivachenko AY, Cibulskis K, Gabriel SB, Altshuler D, Daly MJ. 2011. A framework for variation discovery and genotyping using next-generation DNA sequencing data. Nat Genet 43:491-498.

Du B, Olson CA, Sastry AV, Fang X, Phaneuf PV, Chen K, Wu M, Szubin R, Xu S, Gao Y, Hefner Y, Feist AM, Palsson BO. 2020. Adaptive laboratory evolution of *Escherichia coli* under acid stress. Microbiology 166:141-148.

Dulley JR, Grieve PA. 1975. A simple technique for eliminating interference by detergents in the Lowry method of protein determination. Anal Biochem 64:136-141.

Gibney PA, Schieler A, Chen JC, Rabinowitz JD, Botstein D. 2015. Characterizing the in vivo role of trehalose in *Saccharomyces cerevisiae* using the AGT1 transporter. Proc Natl Acad Sci U S A 112:6116-6121.

Grant SG, Jessee J, Bloom FR, Hanahan D. 1990. Differential plasmid rescue from transgenic mouse DNAs into *Escherichia coli* methylation-restriction mutants. Proc Natl Acad Sci USA 87:4645-4649.

Guzman LM, Belin D, Carson MJ, Beckwith J. 1995. Tight regulation, modulation, and high-level expression by vectors containing the arabinose P_{BAD} promoter. J Bacteriol 177:4121-4130.

Gyorfy Z, Draskovits G, Vernyik V, Blattner FF, Gaal T, Posfai G. 2015. Engineered ribosomal RNA operon copy-number variants of *E. coli* reveal the evolutionary trade-offs shaping rRNA operon number. Nucleic Acids Res 43:1783-1794.

Hattori H, Yakushi T, Matsutani M, Moonmangmee D, Toyama H, Adachi O, Matsushita K. 2012. High-temperature sorbose fermentation with thermotolerant *Gluconobacter frateurii* CHM43 and its mutant strain adapted to higher temperature. Appl Microbiol Biotechnol 95:1531-1540.

Hottiger T, De Virgilio C, Hall MN, Boller T, Wiemken A. 1994. The role of trehalose synthesis for the acquisition of thermotolerance in yeast. II. Physiological concentrations of trehalose increase the thermal stability of proteins *in vitro*. Eur J Biochem 219:187-193.

Hyatt D, Chen GL, Locascio PF, Land ML, Larimer FW, Hauser LJ. 2010. Prodigal: prokaryotic gene recognition and translation initiation site identification. BMC Bioinformatics 11:119.

Kallnik V, Meyer M, Deppenmeier U, Schweiger P. 2010. Construction of expression vectors for protein production in *Gluconobacter oxydans*. J Biotechnol 150:460-465.

Kanchanarach W, Theeragool G, Inoue T, Yakushi T, Adachi O, Matsushita K. 2010. Acetic

Acid Fermentation of *Acetobacter pasteurianus*: Relationship between Acetic Acid Resistance and Pellicle Polysaccharide Formation. Biosci Biotechnol Biochem 74:1591-1597.

Katzen F, Becker A, Ielmini MV, Oddo CG, Ielpi L. 1999. New mobilizable vectors suitable for gene replacement in gram-negative bacteria and their use in mapping of the 3' end of the *Xanthomonas campestris* pv. campestris gum operon. Appl Environ Microbiol 65:278-282.

Kawai S, Goda-Tsutsumi M, Yakushi T, Kano K, Matsushita K. 2013. Heterologous overexpression and characterization of a flavoprotein-cytochrome c complex fructose dehydrogenase of *Gluconobacter japonicus* NBRC 3260. Appl Environ Microbiol 79:1654-60.

Kishimoto T, Iijima L, Tatsumi M, Ono N, Oyake A, Hashimoto T, Matsuo M, Okubo M, Suzuki S, Mori K, Kashiwagi A, Furusawa C, Ying BW, Yomo T. 2010. Transition from positive to neutral in mutation fixation along with continuing rising fitness in thermal adaptive evolution. PLoS Genet 6:e1001164.

Kosaka T, Nakajima Y, Ishii A, Yamashita M, Yoshida S, Murata M, Kato K, Shiromaru Y, Kato S, Kanasaki Y, Yoshikawa H, Matsutani M, Thanonkeo P, Yamada M. 2019. Capacity for survival in global warming: Adaptation of mesophiles to the temperature upper limit. PLoS One 14: e0215614.

Kostner D, Peters B, Mientus M, Liebl W, Ehrenreich A. 2013. Importance of *codB* for new *codA*-based markerless gene deletion in *Gluconobacter* strains. Appl Microbiol Biotechnol 97:8341-8349.

Kovach ME, Elzer PH, Hill DS, Robertson GT, Farris MA, Roop RM, Peterson KM. 1995. Four new derivatives of the broad-host-range cloning vector pBBR1MCS, carrying different antibiotic-resistance cassettes. Gene 166:175-176.

Krusong W, Kerdpiboon S, Jindaprasert A, Yaiyen S, Pornpukdeewatana S, Tantratian S.J. 2015. Influence of calcium chloride in the high temperature acetification by strain *Acetobacter aceti* WK for Vinegar. Appl Microbiol 119:1291-300.

Kuczyńska-Wiśnik D, Stojowska K, Matuszewska E, Leszczyńska D, Algara MM, Augustynowicz M, Laskowska E. 2015. Lack of intracellular trehalose affects formation of *Escherichia coli* persister cells. Microbiology 161:786-796.

Lam FH, Ghaderi A, Fink GR, Stephanopoulos G. 2014. Engineering alcohol tolerance in yeast. Science 346:71-75.

Langmead B, Salzberg SL. 2012. Fast gapped-read alignment with Bowtie 2. Nat Methods 9:357-359.

Langmead B, Trapnell C, Pop M, Salzberg SL. 2009. Ultrafast and memory-efficient alignment of short DNA sequences to the human genome. Genome Biol 10:R25.

Laslett D, Canback B. 2004. ARAGORN, a program to detect tRNA genes and tmRNA genes in nucleotide sequences. Nucleic Acids Res 32:11-16.

Lee JN, Shin HD, Lee YH. 2003. Metabolic engineering of pentose phosphate pathway in *Ralstoniaeutropha* for enhanced biosynthesis of poly-beta-hydroxybutyrate. Biotechnol Prog 19:1444-1449.

Lee S, Lee HJ, Jung JH, Park CM. 2015. The *Arabidopsis thaliana* RNA-binding protein FCA

regulates thermotolerance by modulating the detoxification of reactive oxygen species. New Phytol 205:555-569.

Li H, Durbin R. 2009. Fast and accurate short read alignment with Burrows-Wheeler transform. Bioinformatics 25:1754-1760.

Li H, Durbin R. 2010. Fast and accurate long-read alignment with Burrows-Wheeler transform. Bioinformatics 26:589-595.

Lim SJ, Jung YM, Shin HD, Lee YH. 2002. Amplification of the NADPH-related genes *zwf* and *gnd* for the oddball biosynthesis of PHB in an *E. coli* transformant harboring a cloned *phbCAB* operon. J Biosci Bioeng 93:543-549.

Martín M, Lloret J, Sánchez-Contreras M, Bonilla I, R Rivilla R. 2000. MucR is necessary for galactoglucan production in *Sinorhizobium meliloti* EFB1. Mol Plant Microbe Interact 13:129-135.

Matsushita K, Ameyama M. 1982. D-Glucose dehydrogenase from *Pseudomonas fluorescens*, membrane-bound. Methods Enzymol 89:149-154.

Matsushita K, Azuma Y, Kosaka T, Yakushi T, Hoshida H, Akada R, Yamada M. 2016. Genomic analyses of thermotolerant microorganisms used for high-temperature fermentations. Biosci Biotechnol Biochem 80:655-668.

Matsushita K, Fujii Y, Ano Y, Toyama H, Shinjoh M, Tomiyama N, Miyazaki T, Sugisawa T, Hoshino T, Adachi O. 2003. 5-keto-D-gluconate production is catalyzed by a quinoprotein glycerol dehydrogenase, major polyol dehydrogenase, in *Gluconobacter* species. Appl Environ Microbiol 69:1959-1966.

Matsushita K, Toyama H, Adachi O. 1994. Respiratory chains and bioenergetics of acetic acid bacteria. Adv Microb Physiol 36:247-301.

Matsushita K, Yamamoto T, Toyama H, Adachi O. 1998. NADPH Oxidase System as a Superoxide-generating Cyanide-Resistant Pathway in the Respiratory Chain of *Corynebacterium glutamicum*. Biosci Biotechnol Biochem 62:1968-1977.

Matsutani M, Ito K, Azuma Y, Ogino H, Shirai M, Yakushi T, Matsushita K. 2015. Adaptive mutation related to cellulose producibility in *Komagataeibacter medellinensis* (*Gluconacetobacter xylinus*) NBRC 3288. Appl Microbiol Biotechnol 99:7229-7240.

Matsutani M, Matsumoto N, Hirakawa H, Shiwa Y, Yoshikawa H, Okamoto-Kainuma A, Ishikawa M, Kataoka N, Yakushi T, Matsushita K. 2020. Comparative genomic analysis of closely related *Acetobacter pasteurianus* strains provides evidence of horizontal gene transfer and reveals factors necessary for thermotolerance. J Bacteriol 202:e00553-19.

Matsutani M, Nishikura M, Saichana N, Hatano T, Masud-Tippayasak U, Theergool G, Yakushi T, Matsushita K. 2013. Adaptive mutation of *Acetobacter pasteurianus* SKU1108 enhances acetic acid fermentation ability at high temperature. J Biotechnol 165:109-119.

Matsutani M, Suzuki H, Yakushi T, Matsushita K. 2014. Draft genome sequence of *Gluconobacter thailandicus* NBRC 3257. Stand Genomic Sci 9:614-623.

McKenna A, Hanna M, Banks E, Sivachenko A, Cibulskis K, Kernytsky A, Garimella K, Altshuler D, Gabriel S, Daly M, DePristo MA. 2010. The Genome Analysis Toolkit: a

MapReduce framework for analyzing next-generation DNA sequencing data. Genome Res 20:1297-1303.

Messner KR, Imlay JA. 1999. The identification of primary sites of superoxide and hydrogen peroxide formation in the aerobic respiratory chain and sulfite reductase complex of *Escherichia coli.* J Biol Chem 274:10119-10128.

Messner KR, Imlay JA. 2002. Mechanism of superoxide and hydrogen peroxide formation by fumarate reductase, succinate dehydrogenase, and aspartate oxidase. J Biol Chem 277:42563-42571.

Moonmangmee D, Adachi O, Ano Y, Shinagawa E, Toyama H, Theeragool G, Lotong N, Matsushita K. 2000. Isolation and characterization of thermotolerant *Gluconobacter* strains catalyzing oxidative fermentation at higher temperatures. Biosci Biotechnol Biochem 64:2306-2315.

Moonmangmee S, Kawabata K, Tanaka S, Toyama H, Adachi O, Matsushita K. 2002. A novel polysaccharide involved in the pellicle formation of *Acetobacter aceti*. J. Biosci. Bioeng 93:192-200.

Murata M, Fujimoto H, Nishimura K, Charoensuk K, Nagamitsu H, Raina S, Kosaka T, Oshima T, Ogasawara N, Yamada M. 2011. Molecular strategy for survival at a critical high temperature in *Eschierichia coli*. PLoS One 6:e20063.

Murphy TA, Wyatt GR. 1965. The enzymes of glycogen and trehalose synthesis in silk moth fat body. J Biol Chem 240:1500-1508.

Nantapong N, Murata R, Trakulnaleamsai S, Kataoka N, Yakushi T, Matsushita K. 2019. The effect of reactive oxygen species (ROS) and ROS-scavenging enzymes, superoxide dismutase and catalase, on the thermotolerant ability of *Corynebacterium glutamicum*. Appl Microbiol Biotechnol 103:5355-5366.

Nantapong N, Otofuji A, Migita CT, Adachi O, Toyama H, Matsushita K. 2005. Electron transfer ability from NADH to menaquinone and from NADPH to oxygen of type II NADH dehydrogenase of *Corynebacterium glutamicum*. Biosci Biotechnol Biochem 69:149-159.

Oide S, Gunji W, Moteki Y, Yamamoto S, Suda M, Jojima T, Yukawa H, Inui M. 2015. Thermal and solvent stress cross-tolerance conferred to *Corynebacterium glutamicum* by adaptive laboratory evolution. Appl Environ Microbiol 81:2284-2298.

Oide S, Inui M. 2017. Trehalose acts as a uridine 5'-diphosphoglucose-competitive inhibitor of trehalose 6-phosphate synthase in *Corynebacterium glutamicum*. FEBS J 284:4298-4313.

Phathanathavorn T, Naloka K, Matsutani M, Yakushi T, Matsushita K, Theeragool G. 2019. Mutated *fabG* gene encoding oxidoreductase enhances the cost-effective fermentation of jasmine rice vinegar in the adapted strain of *Acetobacter pasteurianus* SKU1108. J Biosci Bioeng 127:690-697.

Purvis JE, Yomano LP, Ingram LO. 2005. Enhanced trehalose production improves growth of *Escherichia coli* under osmotic stress. Appl Environ Microbiol 71:3761-3769.

Qi Z, Dong D, Yang H, Xia X. 2017. Improving fermented quality of cider vinegar via rational nutrient feeding strategy, Food Chem 224:312-319.

Rajaraman E, Agrawal A, Crigler J, Seipelt-Thiemann R, Altman E, Eiteman MA. 2016. Transcriptional analysis and adaptive evolution of *Escherichia coli* strains growing on acetate. Appl Microbiol Biotechnol 100:7777-7785.

Ramirez-Gonzalez RH, Bonnal R, Caccamo M, Maclean D. 2021. Bio-samtools: Ruby bindings for SAMtools, a library for accessing BAM files containing high-throughput sequence alignments. Source Code Biol Med 7:6.

Richhardt J, Bringer S, Bott M. 2012. Mutational analysis of the pentose phosphate and Entner-Doudoroff pathways in *Gluconobacter oxydans* reveals improved growth of a Δ*edd* Δ*eda* mutant on mannitol. Appl Environ Microbiol 78:6975-6986.

Rodriguez-Verdugo A, Carrillo-Cisneros D, Gonzalez-Gonzalez A, Gaut BS, Bennett AF. 2014. Different tradeoffs result from alternate genetic adaptations to a common environment. Proc Natl Acad Sci U S A 111:12121-12126.

Roller BR, Stoddard SF, Schmidt TM. 2016. Exploiting rRNA operon copy number to investigate bacterial reproductive strategies. Nat Microbiol 1:16160.

Ross W, Sanchez-Vazquez P, Chen AY, Lee JH, Burgos HL, Gourse RL. 2016. ppGpp Binding to a Site at the RNAP-DksA Interface Accounts for Its Dramatic Effects on Transcription Initiation during the Stringent Response. Mol Cell 62:811-823.

Ross W, Vrentas CE, Sanchez-Vazquez P, Gaal T, Gourse RL. 2013. The magic spot: a ppGpp binding site on *E. coli* RNA polymerase responsible for regulation of transcription initiation. Mol Cell 50:420-429.

Rudolph B, Gebendorfer KM, Buchner J, Winter J. 2010. Evolution of *Escherichia coli* for growth at high temperatures. J Biol Chem 285:19029-19034.

Saeki A, Theeragool G, Matsushita K, Toyama H, Lotong N, Adachi O. 1997. Development of thermotolerant acetic acid bacteria useful for vinegar fermentation at higher temperatures. Biosci Biotech Biochem 61:138-145.

Sandberg TE, Salazar MJ, Weng LL, Palsson BO, Feist AM. 2019. The emergence of adaptive laboratory evolution as an efficient tool for biological discovery and industrial biotechnology. Metab Eng 56:1-16.

Satomura A, Katsuyama Y, Miura N, Kuroda K, Tomio A, Bamba T, Fukusaki E, Ueda M. 2013. Acquisition of thermotolerant yeast *Saccharomyces cerevisiae* by breeding via stepwise adaptation. Biotechnol Prog 29:1116-1123.

Satomura A, Miura N, Kuroda K, Ueda M. 2016. Reconstruction of thermotolerant yeast by one-point mutation identified through whole-genome analyses of adaptively-evolved strains. Sci Rep 6:23157.

Seemann T. 2014. Prokka: rapid prokaryotic genome annotation. Bioinformatics 30:2068-2069.

Sjödin A, Svensson K, Lindgren M, Forsman M, Larsson P. 2010. Whole-genome sequencing reveals distinct mutational patterns in closely related laboratory and naturally propagated *Francisella tularensis* strains. PLoS One 5:e11556.

Soemphol W, Deeraksa A, Matsutani M, Yakushi T, Toyama H, Adachi O, Yamada M, Matsushita K. 2011. Global analysis of the genes involved in the thermotolerance mechanism of

thermotolerant *Acetobacter tropicalis* SKU1100. Biosci Biotechnol Biochem 75:1921-1928

Soemphol W, Saichana N, Yakushi T, Adachi O, Matsushita K, Toyama H. 2012. Characterization of genes involved in D-sorbitol oxidation in thermotolerant *Gluconobacter frateurii*. Biosci Biotechnol Biochem 76:1497-1505.

Street TO, Bolen DW, Rose GD. 2006. A molecular mechanism for osmolyte-induced protein stability. Proc Natl Acad Sci U S A 103:13997-14002.

Sánchez-Riego AM, Mata-Cabana A, Galmozzi CV, Florencio FJ. 2016. NADPH-Thioredoxin Reductase C Mediates the Response to Oxidative Stress and Thermotolerance in the *Cyanobacterium Anabaena* sp. PCC7120. Front Microbiol 7:1283.

Tapia H, Young L, Fox D, Bertozzi CR, Koshland D. 2015. Increasing intracellular trehalose is sufficient to confer desiccation tolerance to *Saccharomyces cerevisiae*. Proc Natl Acad Sci U S A 112:6122-6127.

Taweecheep P, Naloka K, Matsutani M, Yakushi T, Matsushita K, Theeragool G. 2019. In Vitro Thermal and Ethanol Adaptations to Improve Vinegar Fermentation at High Temperature of *Komagataeibacter oboediens* MSKU 3. Appl Biochem Biotechnol 189:144-159.

Tenaillon O, Rodríguez-Verdugo A, Gaut RL, McDonald P, Bennett AF, Long AD, Gaut BS. 2012. The molecular diversity of adaptive convergence. Science 335:457-461.

Thelander L. 1967. Thioredoxin reductase. Characterization of a homogenous preparation from *Escherichia coli* B. J Biol Chem 242:852-859.

Thevelein JM, Hohmann S. 1995. Trehalose synthase: guard to the gate of glycolysis in yeast? Trends Biochem Sci 20:3-10.

Tonouchi N, Sugiyama M, Yokozeki K. 2003. Coenzyme specificity of enzymes in the oxidative pentose phosphate pathway of *Gluconobacter oxydans*. Biosci Biotechnol Biochem 67:2648-2651.

Wallace-Salinas V, Gorwa-Grauslund MF. 2013. Adaptive evolution of an industrial strain of Saccharomyces cerevisiae for combined tolerance to inhibitors and temperature. Biotechnol Biofuels 6:151.

Wolf A, Krämer R, Morbach S. 2003. Three pathways for trehalose metabolism in *Corynebacterium glutamicum* ATCC13032 and their significance in response to osmotic stress. Mol Microbiol 49:1119-1134.

Wu J, Sun J, Kaback HR. 1996. Purification and functional characteriza- tion of the C-terminal half of the lactose permease of *Escherichia coli*. Biochemistry 35:5213–5219.

Yakushi T, Matsushita K. 2010. Alcohol dehydrogenase of acetic acid bacteria: structure, mode of action, and applications in biotechnology. Appl Microbiol Biotechnol 86:1257-1265.

Yang Y, Huang S, Wang J, Jan G, Jeantet R, Chen XD. 2017. Mg^{2+} improves the thermotolerance of probiotic *Lactobacillus rhamnosus* GG, *Lactobacillus casei* Zhang and *Lactobacillus plantarum* P-8. Lett Appl Microbiol 64:283-288.

Yin H, Zhang R, Xia M, Bai X, Mou J, Zheng Y, Wang M. 2017. Effect of aspartic acid and glutamate on metabolism and acid stress resistance of *Acetobacter pasteurianus*. Microb Cell Fact

16:109

Yoshida T, Ayabe Y, Yasunaga M, Usami Y, Habe H, Nojiri H, Omori T. 2003. Genes involved in the synthesis of the exopolysaccharide methanolan by the obligate methylotroph *Methylobacillus sp* strain 12S. Microbiology 149:431-444.

Zahid N, Schweiger P, Galinski E, Deppenmeier U. 2015. Identification of mannitol as compatible solute in *Gluconobacter oxydans*. Appl Microbiol Biotechnol 99:5511-5521.

Zang X, Geng X, Wang F, Liu Z, Zhang L, Zhao Y, Tian X, Ni Z, Yao Y, Xin M, Hu Z, Sun Q, Peng H. 2017. Overexpression of wheat ferritin gene TaFER-5B enhances tolerance to heat stress and other abiotic stresses associated with the ROS scavenging. BMC Plant Biol 17:14.

Zerbino DR, Birney E. 2008. Velvet: algorithms for de novo short read assembly using de Bruijn graphs. Genome Res 18:821-829.

Zerbino DR, McEwen GK, Margulies EH, Birney E. 2009. Pebble and rock band: heuristic resolution of repeats and scaffolding in the velvet short-read de novo assembler. PLoS One 4:e8407.

ACKNOWLEDGEMENT

I would like to express my deep and sincere thanks to my supervisor Prof. Dr. Kazunobu Matsushita and Prof. Dr. Toshiharu Yakushi for their continuous support, discussion, suggestion throughout the course of my study. I am deeply grateful to Asst. Prof. Dr. Naoya Kataoka for his kindly support, comments and suggestion on my work.

I would like to express my gratitude to Dr. Minenosuke Matsutani from NODAI Genome Research Center, Tokyo University of Agriculture, for his bioinformatic analysis, kindly comments and discussions on my study.

I am deeply grateful to Ms. Hiromi Hattori from the Laboratory of Applied Microbiology at Yamaguchi University for her technical support and kindly discussion on my study.

I would like to express my sincere thanks to Prof. Dr. Hirohide Toyama from Department of Bioscience and Biotechnology, Faculty of Agriculture, University of the Ryukyus for his kindly advices and discussions on my study. I would also like to thank Ms. Chihiro Matayoshi, from Department of Bioscience and Biotechnology Faculty of Agriculture, University of the Ryukyus for her helpful experiment on my work.

I would like to express my deep thanks Prof. Dr. Yoshinao Azuma, from Biology-oriented Science and Technology, Kinki University, who provided a strain and helped discussion.

I am deeply grateful to Mr. Yasushi Shiraishi and Mr. Naoki Osumi from Kewpie Jyozo Co., Ltd for their kindly provided a strain, experiment and discussions on this study.

I would like to express my sincere thanks Assoc. Prof. Dr. Gunjana Theeragool, Ms. Theerisara Phathanathavorn and Ms. Uraiwan Masud-Tippayasak from Department of Microbiology, Faculty of Science, Kasetsart University for their kindly provided a strain and discussion.

I am deeply grateful to Ms. Riho Sueyoshi from the Laboratory of Applied Microbiology at Yamaguchi University. She performed thermal adaptation of *A. pasteurianus* K-1034 and helped experiment on my study.

I would like to deeply thank the member of Applied Microbiology (Obi) Laboratory, Yamaguchi University for support on my study and laboratory life. Also, I would like to thank the member of Information Biochemistry (Josei) Laboratory for support on this study.

This study was funded by the Advanced Low Carbon Technology Research and Development Program (ALCA) of the Japan Science and Technology Agency (JST;

JPMJAL1106).

Finally, I would like to deeply thank to my family and friends for support my study and life. I really appreciate to the people who relate to me among my study.

Nami Matsumoto

要旨

耐熱化育種酢酸菌の耐熱化機構に関する研究

Study on thermotolerant mechanisms of thermotolerant acetic acid bacteria by experimental evolution

酢酸菌は、グラム陰性の絶対好気性菌で、自然界では植物の花や果物に生息し、果実の腐敗に関連して様々な（自然）発酵にも関与している。酢酸菌は、細胞膜表層にある酵素によって糖やアルコールを酸化する酸化発酵を行う特徴を持ち、酢酸発酵やソルボース発酵等の産業的な発酵にも用いられている。しかし、大規模な発酵装置を用いた発酵では、機械熱や発酵によって生じる熱が、菌の生育や発酵能力を阻害するため、厳密な温度コントロールが必要となっている。そこで、耐熱性を有する微生物を用いて厳密な温度制御を必要としない発酵を行うことが出来れば、エネルギーやコストを削減でき、脱炭素社会の実現に貢献しうる新しい発酵技術となることが期待できる。そのため、常温性の発酵微生物を耐熱化する育種技術の開発と得られた耐熱化株の耐熱化機構の解明が望まれている。

本研究では、耐熱化機構を解明するために、いくつかの酢酸菌を実験室進化の手法を用いて高温発酵条件下で耐熱性を示す耐熱化育種株を得て、その耐熱化機構を解析した。CHAPTER 1 では、*Gluconobacter* 属、CHAPTER 2、3 では *Acetobacter* 属の酢酸菌を用い、さらに CHAPTER 3 では、実用的な発酵条件と菌株を用いて、高温酢酸発酵能を持つ実用株の取得とその実用化発酵試験を行った。

CHAPTER 1 では、ソルボース発酵性酢酸菌 *Gluconobacter frateurii* CHM43 株の耐熱化育種株の耐熱化機構について解析した。この耐熱化株は、ゲノム上の多剤耐性輸送体の一塩基挿入によるフレームシフト変異が唯一の変異であった。そこで、人工的に多剤耐性輸送体に一塩基を挿入した株（Wild-G）を作製し、その耐熱性が向上することを確認した。同時に、細胞内でトレハロースの蓄積が観察されたことから、多剤耐性輸送体はトレハロースの排出に関与しており、トレハロースの菌体内蓄積が耐熱性を導くと予想した。そこで、トレハロース合成経路破壊株（Δ*otsAB*）を作製したが、予想に反してトレハロースを生成しないにも拘らず、耐熱化株よりも高温での生育能が向上した。Δ*otsAB* は、野生株や Wild-G 株に比べ、より多くの酢酸を最終代謝産物として生成するようになったことから、トレハロースの細胞内蓄積は、代謝フラックスを変動させ、ペントースリン酸経路への炭素の流入を増加させたと予想した。予想通り、Wild-G の NADPH/$NADP^+$比は野生株よりも高く、Δ*otsAB* では、さらに大幅に増加していた。加えて、NADPH/$NADP^+$比の上昇に比例して、細胞内 ROS レベルが低下することも明らかとなった。これら結果より、耐熱化株では、輸送体の変異によって NADPH 生成を増加させる代謝変動が引き起こされ、そのことによって耐熱性が向上したと結論づけた。

CHAPTER 2 では、酢酸発酵菌株である *Acetobacter pasteurianus* IFO 3283-32 の耐熱化

育種を酢酸発酵条件下で行い、37°C から 40°C まで段階的に温度を上昇させて 6 株の耐熱化株を取得した。これらの耐熱化株は、高温での酢酸発酵能が上昇している代わりに低温域ではその発酵能が低下するトレードオフの関係を示した。ゲノム解析と PCR シーケンス解析によって、最終適応株では、11 箇所の変異と 64-kb の大規模ゲノム欠失、1 プラスミドの欠失が明らかとなった。耐熱化株の特徴から、大規模領域（多数の ribosomal RNA や tRNA 遺伝子が含まれる）の欠失と DNA polymerase （11 箇所の変異のうちの 1 つ）の変異が耐熱化に大きく寄与していることが示唆された。この耐熱化株の生理学的な特徴と遺伝子変異の関係について他の *A. pasteurianus* 株の耐熱化株の特徴と比較した結果、この株では複製や翻訳を抑え細胞増殖を緩やかにすることで高温ストレスを回避し、引き替えに中温域での生育能が相対的に低下するようになったと考察した。

上述の CHAPTER 1 や 2 では、耐熱化育種を栄養豊富な実験用培地条件で行ったが、このような栄養豊富な培地で耐熱化育種した株は実際の食酢醸造に用いられている低栄養な“米もろみ”培地では、耐熱性が低いことが明らかとなった。そこで、CHAPTER 3 では、“米もろみ”のような実用的な培地で高温発酵できる株を単離するために、実用的酢酸発酵に用いられている株 *A. pasteurianus* K-1034 を用いて擬似“もろみ”培地で耐熱化育種を行い、2 つの耐熱株 RH と SY を取得した。2 つの耐熱化株は、低栄養培地条件下のフラスコ培養では 40°C、jar fermentor 培養では 39°C で酢酸発酵を行うことが可能であった。これらの株の変異箇所を特定したところ、RH と SY 株は、5 ヶ所の重複を含む、それぞれ 7 及び 6 ヶ所の変異を有していた。これらの耐熱化育種株を、先行研究で取得された低栄養適応育種株 G-40 株とともに、実用的な「高通気酢酸」発酵装置である‘Acetofermenter’ を用いて“米もろみ”での高温酢酸発酵を試験したところ、親株が全く発酵できない 37°C において効果的な食酢醸造が行えることが明らかとなった。

LIST OF PUBLICATIONS

1. **Matsumoto N**, Hattori H, Matsutani M, Matayoshi C, Toyama H, Kataoka N, Yakushi T, Matsushita K. A Single-Nucleotide Insertion in a Drug Transporter Gene Induces a Thermotolerance Phenotype in *Gluconobacter frateurii* by Increasing the NADPH/$NADP^+$ Ratio via Metabolic Change.
   Appl Environ Microbiol. 2018;84. pii: e00354-18. (Chapter 1)

2. **Matsumoto N**, Matsutani M, Azuma Y, Kataoka N, Yakushi T, Matsushita K. In vitro thermal adaptation of mesophilic Acetobacter pasteurianus NBRC 3283 generates thermotolerant strains with evolutionary trade-offs.
   Biosci Biotechnol Biochem. 2020;84(4):832-841. (Chapter 2)

3. **Matsumoto N,** Osumi N, Matsutani M, Phathanathavorn T, Kataoka N, Theeragool G, Yakushi T, Shiraishi Y, Matsushita K. Thermal adaptation of acetic acid bacteria for practical high-temperature vinegar fermentation.
   Biosci Biotechnol Biochem. 2021 Mar 4:zbab009. doi: 10.1093/bbb/zbab009. Online ahead of print. PMID: 33686416. (Chapter 3)